DIVERSITY IN SRC-FAMILY KINASE ACTIVATION MECHANISMS: IMPLICATIONS FOR SELECTIVE INHIBITOR DISCOVERY

by

Jamie A. Moroco

Bachelor of Science, Carnegie Mellon University, 2007

Submitted to the Graduate Faculty of

The University of Pittsburgh School of Medicine

in partial fulfillment of the requirements for the degree of

Doctor of Philosophy

University of Pittsburgh

2013

UNIVERSITY OF PITTSBURGH

SCHOOL OF MEDICINE

This dissertation was presented

by

Jamie A. Moroco

It was defended on

October 17, 2013

and approved by

Guillermo A. Calero, MD, Structural Biology

Martin C. Schmidt, PhD, Microbiology and Molecular Genetics

Cary Wu, PhD, Pathology

Qiming Jane Wang, PhD, Thesis Committee Chair, Pharmacology and Chemical Biology

Thomas E. Smithgall, PhD, Thesis Advisor, Microbiology and Molecular Genetics

DIVERSITY IN SRC-FAMILY KINASE ACTIVATION MECHANISMS: IMPLICATIONS FOR SELECTIVE INHIBITOR DISCOVERY

Jamie A. Moroco, PhD

University of Pittsburgh, 2013

The Src kinase family encompasses eight non-receptor protein tyrosine kinases in mammals that regulate signaling pathways in virtually every cell type. Src-family kinases (SFKs) share a common regulatory mechanism that requires two intramolecular interactions to maintain the inactive state. These involve binding of the SH3 domain and a PPII helix in the SH2-kinase linker and interaction of the SH2 domain and a phosphotyrosine residue in the C-terminal tail. To compare the activation dynamics of the individual SFKs, a synthetic SFK SH3 domain-binding peptide (VSL12) was used to probe the sensitivity of SFKs to SH3-based activation. Surface plasmon resonance was used to confirm equivalent binding of the VSL12 peptide to the SH3 domains and near-full-length kinases. SFKs were tested with VSL12 in a kinetic kinase assay to measure the changes in the rate of activity induced by SH3:linker displacement. All SFKs tested were susceptible to activation, but to varying degrees. Further, autophosphorylation of the c-Src and Hck activation loops prior to VSL12-induced activation revealed that c-Src can achieve a higher level of activation if primed before SH3 domain displacement. These results suggest that distinct activation thresholds may exist for individual SFKs. To apply these findings in an inhibitor discovery setting, the interaction of c-Src with focal adhesion kinase (FAK) was studied. FAK activates c-Src by binding to its SH2 and SH3 domains and disrupting their regulatory influence on the kinase domain. The c-Src:FAK complex plays a major role in the migration and invasion of both normal and cancer cells, making it an attractive target for drug

discovery. To test the idea that FAK binding induces allosteric changes in the kinase domain active site, a screening assay was developed to target these changes with small molecule inhibitors. Assay conditions were identified where c-Src activity was dependent on a phosphopeptide encompassing the FAK SH3- and SH2-binding motifs for c-Src. A focused library of kinase-biased inhibitors was screened to identify compounds displaying selectivity for the c-Src:pFAK peptide complex. An aminopyrimidinyl carbamate, WH-4-124-2, was discovered that showed five-fold selectivity for the complex. Molecular docking studies of this inhibitor on the kinase domain of Lck bound to imatinib suggest that WH-4-124-2 is a "Type II" kinase inhibitor that prefers the unphosphorylated, "DFG-out" conformation of the kinase. Selective inhibitors of a specific FAK-induced c-Src conformation may provide a unique approach to selective targeting of this key cancer cell signaling pathway.

TABLE OF CONTENTS

LIST OF TABLES

LIST OF FIGURES

PREFACE

I would like to take this opportunity to thank all those who have made this work possible through your help and support both in and out of the lab.

To my advisor, Dr. Thomas Smithgall, for the many opportunities you have given me over the last five years. Without your guidance and mentorship, I would not have been able to reach this point in my career. I appreciate that you have allowed me to be independent and do the work I needed to do, but also that you were there to "crack the whip" when I needed it most. I have learned so much as a scientist in your laboratory, not limited to techniques at the bench. I have grown as a writer and a thinker and I am very grateful for that. I feel very fortunate to have been a member of the Smithgall Lab and I look forward to our continued collaboration.

To my committee members, Dr. Jane Wang, Dr. Cary Wu, Dr. Martin Schmidt, and Dr. Guillermo Calero, thank you for your guidance and suggestions to make this work its best. I appreciate the time you have contributed to helping me reach my goals.

Thank you to my fellow Smithgall Lab members, past and present, for being there for so many things. Advice and guidance for my experiments, favors in (and out of) the lab, the lunches, the coffees, the gripes, and the laughs. It has been great to work in an environment where we get along and it helped to make most days easier. Special thanks to Dr. Lori Emert-Sedlak for advising me from my first day in the lab, I know you will be helping me until my last. Thank you for being a great friend, especially over these last few months when things have

gotten tougher than I expected. Your encouragement and willingness to listen has helped me more than you know.

Thank you also to all those who have collaborated with us to make this project possible: Jodi Craigo, for your help and guidance with SPR; Thomas Wales, Roxana Iacob, and John Engen, for your mass spectrometry work and expertise; Nathanael Gray and other Gray lab members for the compound library and continued support with follow-up; Matt Baumgartner and Carlos Camacho, for the compound docking models.

Thank you to the Molecular Pharmacology Graduate Program for providing me with a strong foundation for my graduate work. I appreciate the investment of time and energy from Dr. Patrick Pagano, Dr. Guillermo Romero, and Dr. Bruce Freeman to listen the graduate students to make the program serve us as best it can so we can all be successful. Thanks also to Pat Smith, for your friendly face and your help coordinating everything through all my years in the program. Thank you to Cindy Duffy, Jen Walker, and the Graduate Office Staff, as well as Mary Lou Meyer of the MMG department for your assistance along the way.

I would like to thank my family and friends, new and old, for their support and encouragement during my time in graduate school. Thank you to my parents for being there when times were toughest, especially over the last few months. I never thought I would be living back at home but here we are, and it has been great to spend some time there before moving away.

Most of all, thank you to my husband Mark, who is so encouraging and supportive. I could not and would not have finished if it were not for you.

This thesis is dedicated to my Uncle Phil, since he was the reason I got into this business in the first place.

1.0 INTRODUCTION

1.1 SRC FAMILY KINASES

The Src-Family Kinases (SFKs) are a family of eight non-receptor protein tyrosine kinases with multiple members expressed in virtually every cell type in humans. Long before the discovery of c-Src, Sir Peyton Rous discovered in the early 1900s that a virus could cause tumor growth in chickens (*1*). This virus was later identified as the Rous Sarcoma Virus (RSV) and was the first description of cancer caused by a virus. It was not until the 1970s that v-Src was identified as the causative agent of cancer in the RSV genome, followed soon after by the discovery of the cellular homolog, c-Src (*2, 3*). Subsequently, the remaining family members were identified in the human genome. Three family members, c-Src, Fyn, and c-Yes, are ubiquitously expressed, while the rest of the family members, Hck, Lyn, Fgr, Lck, and Blk, show a more restricted expression pattern, mainly in hematopoietic cell lineages (*4*). Three additional kinases, Srm, Brk, and Frk are also considered relatives to the Src-kinase family, but their regulation is not as well defined (*5*). The SFKs are involved in a variety of signaling pathways that control many different cellular processes, including proliferation, cell adhesion and migration, cell survival, and the immune response. The sections below will detail the structure and regulation of the kinase family, the cellular events triggered by kinase activation, and the consequences of deregulation of kinase activation.

1.1.1 Structure and Regulation

The SFKs share a common domain organization and downregulated conformation (Figure 1).

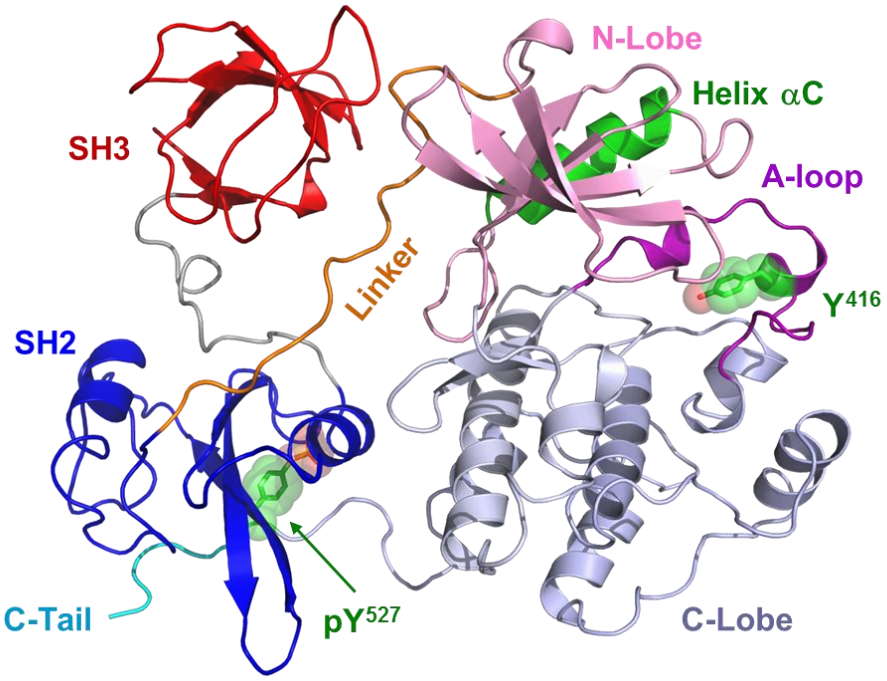

Figure 1. X-ray crystal structure of c-Src in the downregulated conformation

The structure of c-Src in the downregulated conformation is representative of the eight members of this kinase family in mammals. The domain organization is shared by all family members: SH3 domain, red; SH3-SH2 connector, dark gray; SH2 domain, blue; SH2-kinase linker, orange; kinase domain N-lobe, pink; αC helix, green; activation loop, purple; kinase domain C-lobe, light gray; C-terminal tail, cyan. The side-chains of the regulatory tyrosines, Y416 and Y527, chicken Src numbering, are shown, where Y527 is phosphorylated. The SH3 domain interacts with the SH2-kinase linker and the SH2 domain interacts with the phosphotyrosine tail to maintain the downregulated state of the kinase. PDB ID: 2SRC (*6*)

The N-terminus contains lipid modification sequences for myristoylation and, in some cases, palmitoylation (*7*). Lipid modification is necessary for the localization of the SFKs to the cell

membrane for interaction with other proteins. Following these lipid modification sequences is the unique domain, where the sequence homology between family members is lowest. This is followed by the SH3 domain (which binds polyproline sequences), the SH2 domain (which binds phosphotyrosine-containing sequences), a bi-lobed kinase domain, and a regulatory C-terminal tail containing a conserved tyrosine residue important for regulation of kinase activity. This C-terminal tyrosine is phosphorylated by the C-terminal Src kinase (Csk), or the closely related kinase Chk, and can be dephosphorylated by a number of phosphatases, including CD45 (*8–12*). The x-ray crystal structures of c-Src and Hck in the downregulated, inactive conformations have been solved and the structure of c-Src is shown in Figure 1 (*6*). Two intramolecular interactions occur within the kinase to maintain the inactive state; one between the SH3 domain and SH2-kinase linker, and the other between the SH2 domain and C-terminal tail. The SH3 domain binds the polyproline type II (PPII) helix formed in the linker and the SH2 domain binds the conserved tyrosine residue in the tail when it is phosphorylated. Displacement of either one or both of these interactions leads to kinase activation. These interactions will be discussed in more detail in the sections below.

1.1.1.1 Phylogeny

While the Src-kinase family is comprised of eight members in mammals, the phylogenetic tree of all non-receptor protein tyrosine kinases shows that the eight members can be broken down into two distinct subfamilies (Figure 2) (*13*). Subfamily A consists of c-Src, c-Yes, Fyn, and Fgr, while subfamily B consists of Hck, Lyn, Lck, and Blk. Alignment of the full-length or individual domain sequences of all eight kinases results in the same subfamily breakdown. Analysis of the sequence alignment of the eight family members shows the most

obvious divergence between the subfamilies in the SH2-kinase linker and the C-terminal tail (Figure 3).

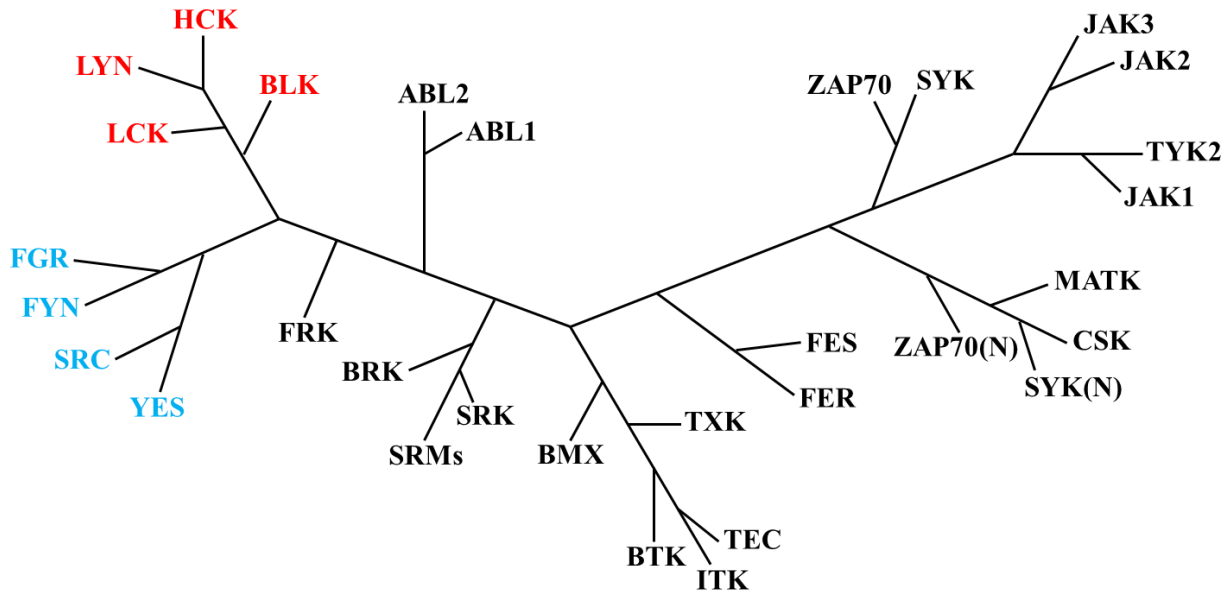

Figure 2. Phylogenetic tree of non-receptor protein tyrosine kinases

Sequence alignment of the SH2 domains of all non-receptor protein tyrosine kinases in the human kinome results in this phylogenetic breakdown. The subfamily A SFKs are shown in blue and the subfamily B SFKs are shown in red. Tree adapted from Filippakopoulos,P., *et al.* (*13*).

There are specific differences that may contribute to the diversity in regulation of not only the subfamilies, but also the individual family members. The most obvious sequence divergence in the linker region is that there is only one proline in the SrcA subfamily member linkers, while all members of the B subfamily have two. Despite this difference, the PPII helix still forms in the c-Src linker and binds to the SH3 domain (Figure 1). Section 1.1.1.2 will explain more about SH3 ligand binding and Section 1.1.1.4 will give more detail regarding the SH2-kinase linkers.

In the C-terminal tail, Y527 (chicken c-Src numbering, used throughout) is conserved among all family members and is essential for downregulation of kinase activity. However, the

sequence following the tyrosine differs between the subfamilies and could have an effect on specificity of ligands that activate the kinases via SH2:tail displacement. More about the kinase regulation by SH3 and SH2 domain interactions will be discussed in the following sections.

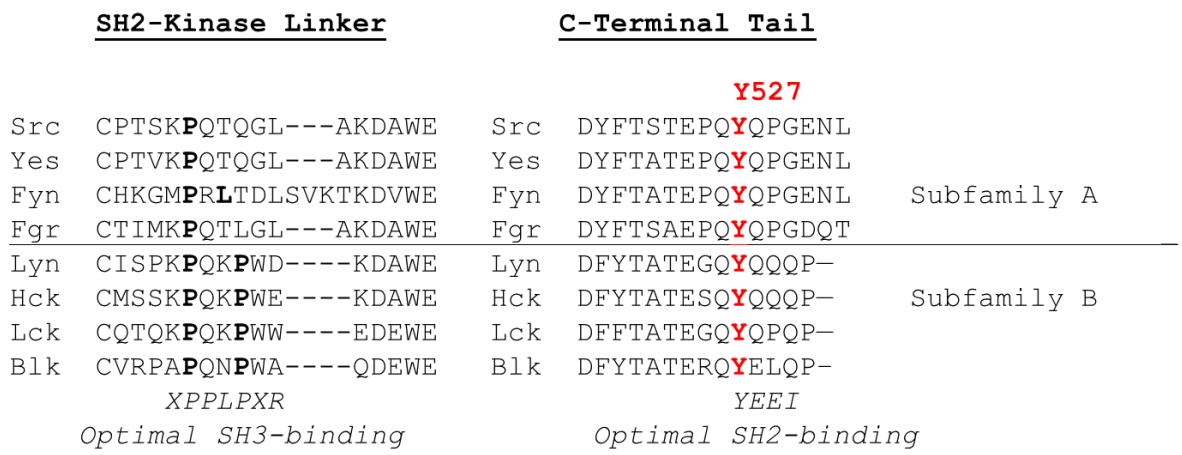

Figure 3. Sequence alignment of SH2-Kinase linker and C-terminal tail regions of SFKs

The sequence alignment of the SFK SH2-kinase linkers and C-terminal tails is shown to highlight the sequence diversity between the SrcA and SrcB subfamilies. The optimal Class II SH3-binding sequence is shown and the linker residues that fit the consensus sequence are indicated in bold. The optimal SH2-binding sequence is shown and the conserved tail tyrosine is indicated in red in the C-terminal tail alignment.

1.1.1.2 SH3 Domain

The Src Homology 3 (SH3) domain is a modular protein domain composed of roughly 60 amino acids and is found in many signaling proteins. The SH3 domain was identified as a conserved protein domain in the late 1980s after the sequences of other proteins were found to be homologous with a region of c-Src, now identified as residues 85-140 (*14*). The three-dimensional structures of the isolated SH3 domains of multiple proteins have been solved by both x-ray crystallography and NMR, including many members of the Src-kinase family (*15,*

16). SH3 domain structures are highly conserved, and in the case of the SFKs, the SH3 domain portion of the near-full length structure does not change from the structure of the isolated SH3 domain.

SH3 domains interact with other signaling molecules through binding to PPII helices. This principle was first discovered in a screen for peptides that bound to the SH3 domain from the non-receptor protein tyrosine kinase c-Abl (*17*). The c-Abl tyrosine kinase has a very similar core structure to the SFKs and shares a similar mechanism of downregulation, such that the SH3:linker interaction is important for maintaining the inactive state of the kinase (*18*). The screen resulted in the discovery of the consensus sequence for Abl SH3 binding, XPXXXPPPFXP, where X is any amino acid. Subsequently, a peptide library was screened to determine the consensus sequences for c-Src and PI3K SH3 binding, which were found to be RXLPPLPRΦ, where Φ represents a hydrophobic residue, and RXLPPRPXX, respectively (*19*). Therefore, while SH3 domains are structurally very similar, their selectivity for polyproline sequences differs based on the sequence of the SH3 domain itself. Further studies showed that despite the similarity between c-Src and c-Abl, peptides selected as high-affinity for the c-Abl SH3 domain did not bind to the c-Src SH3 domain, and vice versa (*19*).

Examination of SH3-binding sequences has led to the division of these sequences into two distinct classes based on their binding orientation: Class I ligands, which share the consensus sequence RXLPPXP, and Class II ligands, which conform to XPPLPXR. Residues flanking these sequences can enhance the affinity for the SH3 domain. Many SH3 domains, including those of the SFKs, can bind proline-rich sequences in either orientation. Figure 4 diagrams the two orientations of ligand binding by SH3 domains, with the c-Src SH3 domain residue numbering.

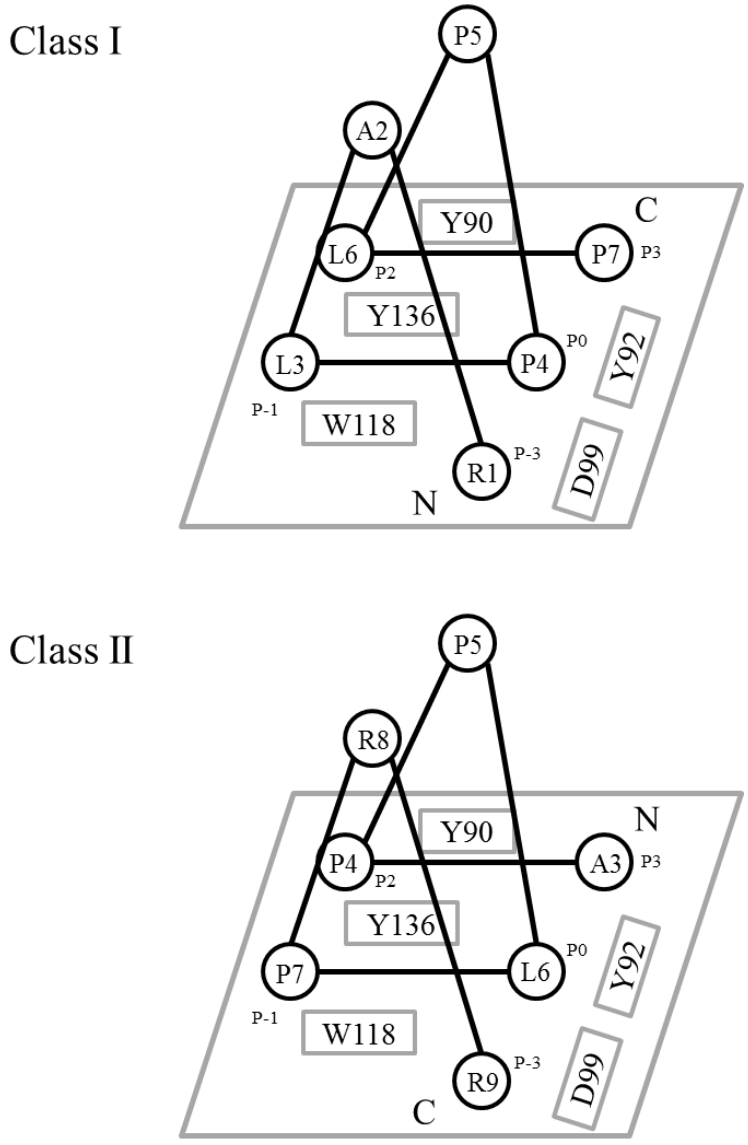

Figure 4. Class I and Class II ligand binding orientations to the c-Src SH3 domain

The c-Src SH3 domain residues Y90, Y92, D99, W118, and Y136 are shown in boxes on the planar surface of each panel. The Class I ligand bound in the top panel has the sequence **R_1**A<u>LPPLP$_7$</u>RY (corresponding to R1-P7), while the Class II ligand bound in the bottom panel has the sequence AF<u>A_3PPLP</u>R**R_9** (A3-R9), with the core sequence, XPPXP, underlined. The designation between Class I and Class II ligands is dependent on the location of the R residue (in bold), which is N-terminal to the consensus sequence in Class I ligands and C-terminal to the consensus sequence in Class II ligands. Residues bound to sites P_{-3}-P_3 are shown in Table 1. Figure adapted from Dalgarno, *et al.* (*20*).

Three hydrophobic sites are formed by conserved SH3 domain residues. Site 1 binds the R residue in the ligand and is formed by D99 and W118 in the SH3 domain, which is considered the P_{-3} position of the SH3 domain. Site 2 is formed by Y92, Y136, and W118 and site 3 is formed by residues Y90 and Y136. Sites 2 and 3 bind the LP repeats of the consensus sequence. In Table 1, the residues that bind to each position in the SH3 domain are listed, summarized from Figure 4.

Table 1. PPII Helix binding sites in the SFK SH3 domain

Position	Class I (Consensus RXLPPLP)	Class II (Consensus XPPLPXR)
P_{-3}	R	R
P_{-2}	X	R
P_{-1}	L	P
P_0	P	L
P_1	P	P
P_2	L	P
P_3	P	X

The Class I and ClassII polyproline ligand residues that bind to specific positions in the SH3 domain are summarized from Figure 4 (*20, 21*).

Class I ligand binding can be visualized in the crystal structure of the c-Src SH3 domain in complex with the high-affinity ligand VSL12 (VSLARRPLPPLP), as shown in Figure 13 (*22*). More about this interaction is discussed in Chapter 2.

As mentioned previously, one interaction that maintains the downregulated state of SFKs involves the SH3 domain and a PPII helix formed in the SH2-kinase linker. The sequences found in the SFK linkers bind in a Class II orientation, but are of rather low affinity for their SH3 domains. Consequently, displacement of the SH3:linker interaction by a high-affinity sequence in another protein can activate the kinase. Shown in Figure 5 is an alignment of the SFK SH3 domains and linker regions.

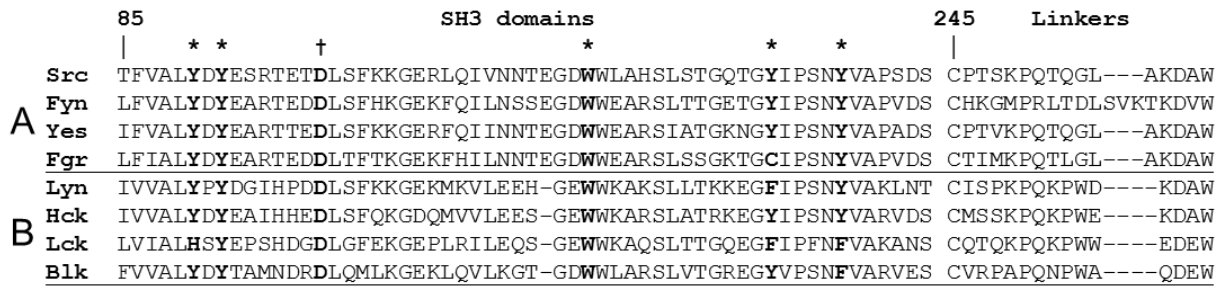

Figure 5. Sequence alignment of Src-family kinase SH3 domains and SH2-kinase linkers.

The Src-kinase family can be divided into two subfamilies based on sequence homology as shown (A and B subgroups). Key hydrophobic residues that contribute to the binding surface are highlighted in bold and marked with an asterisk (their positions in the structure of the Src SH3 domain are modeled in Figure 13). The conserved aspartate residues (D99) that contribute to VSL12 peptide binding are also bolded and marked with a †. SFK linker sequences are more diverse and display suboptimal residues at key positions that face the SH3 domain in the inactive state. The positions of linker residues that contact the SH3 domain in the inactive structure of c-Src are modeled in Figure 13.

The SH3 domain residues that form the hydrophobic binding pockets are strongly conserved among the entire Src-kinase family. The linker sequences are not as conserved and may contribute to the specificity of binding partners that activate the SFKs in cells. The binding of the c-Src linker to the SH3 domain can be seen in the near-full-length crystal structure. Figure 13 shows the details of this interaction, which is discussed in more detail in Sections 1.1.1.4 and 2.1. While contacts are made between the SH3 domain and linker, the interaction is suboptimal relative to high affinity peptide ligands such as VSL12 (Chapter 2).

1.1.1.3 SH2 Domain

Src Homology 2 (SH2) domains are modular protein domains that are a common feature of all non-receptor protein tyrosine kinases, in addition to being present in many other cellular

signaling molecules. SH2 domains were first discovered in the context of v-Fps, the transforming tyrosine kinase present in the Fujinami avian sarcoma virus, as a short stretch of amino acids adjacent to the kinase domain important for regulation of kinase activity and host range (*14*, *23*). Sequence alignment showed that this sequence was conserved in both v-Src and v-Abl, and was subsequently named SH2 for Src homology 2. The structures of isolated SH2 domains are similar among many different protein families (*24-26*).

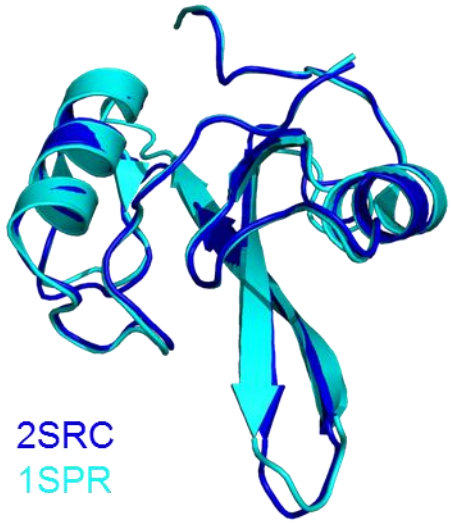

Figure 6. SH2 domains from near-full-length and isolated proteins are structurally identical

The x-ray crystal structure of the isolated c-Src SH2 domain in cyan (PDB ID: 1SPR) (*26*) is shown aligned to the SH2 domain portion of the near-full-length downregulated structure of c-Src in blue (PDB ID: 2SRC).

Figure 6 shows an overlay of the structure of the isolated c-Src SH2 domain with the SH2 domain portion of the near-full-length downregulated structure, illustrating that they are nearly identical and adopt the same three-dimensional structure independently of their overall sequence

context. SH2 domains bind to phosphotyrosine-containing sequences and in the SFKs, the SH2 domain binds to the phosphotyrosine tail to maintain the downregulated state of the kinase. This interaction is essential for downregulation of kinase activity, as evidenced by mutational analysis (further discussed in Section 1.1.1.6).

SH2 domains modulate signaling pathways by binding to phosphotyrosine-containing sequences (*27*). The consensus high-affinity SFK SH2 binding sequence was identified as pYEEI by using recombinant c-Src SH2 domain protein to pull down peptides from a phosphotyrosine-peptide library (*28*). This sequence is found in the hamster polyomavirus middle T antigen, which had already been shown to bind and activate the SFKs (*29*). The consensus sequence for SH2 binding varies depending on the SH2 domain, much like the specificity for polyproline motifs varies by the SH3 domain. While all of the SFK SH2 domains preferentially bind the pYEEI sequence, other families of SH2-containing proteins prefer different phosphotyrosine-containing sequences. In the c-Src SH2 domain, the phosphotyrosine and pY+3 isoleucine residues bind to two hydrophobic pockets in the SH2 domain in a manner that is referred to as a two-pronged plug fitting into a socket (*30*). Many residues in the SH2 domain contribute to the formation of these two hydrophobic pockets as identified in the structure of the c-Src SH2 domain in complex with a pYEEI peptide (*26*). Figure 7 shows this structure in the absence and presence of the peptide with the essential side chains displayed to illustrate the pockets and the binding of the peptide.

The SFK SH2 domains are essential not only for maintaining regulatory control over the enzymes, but also for directing the kinases to their targets in the cell to activate various signaling pathways. The recruitment of SFKs to multiple targets in the cell via their SH2 domains,

including growth factor receptors and focal adhesions, leads to their activation at these sites and their involvement in the stimulation of cell proliferation and cell migration.

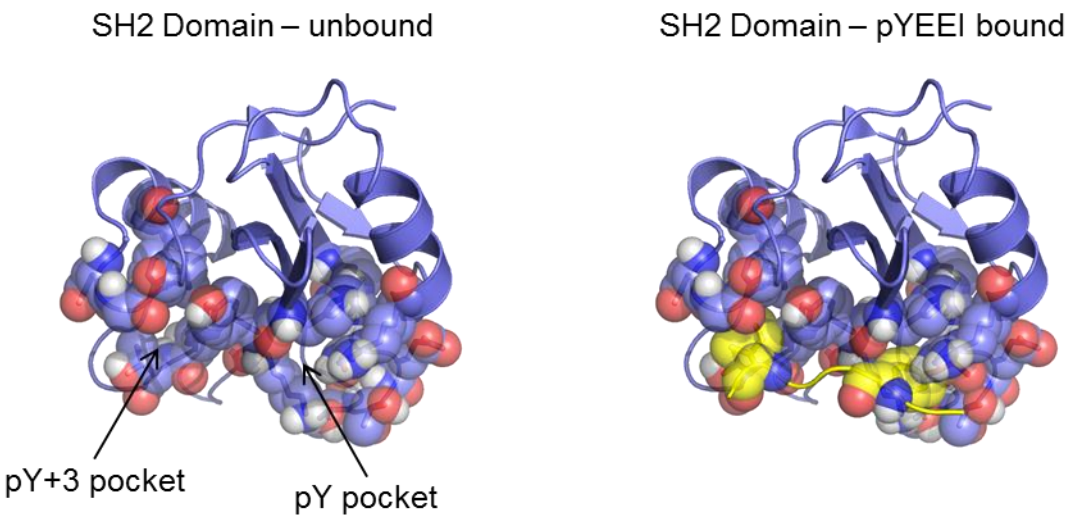

Figure 7. SH2 domain of c-Src unbound and bound to a pYEEI peptide

The x-ray crystal structure of the c-Src SH2 domain was solved in complex with the peptide EPQ**Y**$^{\mathbf{p}}$EEIPIYL (*26*). On the left, the SH2 domain is shown without the peptide present to illustrate the pockets that bind to the pY and pY+3 residues. The essential side chains referenced in the original publication are shown in a spherical space-filled model. On the right, the pYEEI peptide is bound, shown in yellow, with the phosphotyrosine and isoleucine side chains shown bound in the respective hydrophobic pockets.

1.1.1.4 SH2-Kinase Linker

The SH2-Kinase linker is a relatively short sequence that is important in the regulation of SFK activity. The x-ray crystal structures of both c-Src and Hck in their downregulated conformations show that the linker forms a PPII helix and binds to the SH3 domain in a Class II orientation to form one of the necessary intramolecular interactions to maintain the inactive

kinase state. As described in Section 1.1.1.2, the consensus Class II binding sequence is XPPLPXR. The sequence alignment in Figure 3 shows that the SrcA subfamily linkers contain only one proline, while the SrcB subfamily linkers contain two prolines. None of the SFK linkers contain an arginine residue at the consensus position. Despite this, examination of the c-Src crystal structure shows that the linker still forms a PPII helix and interacts with the SH3 domain. This single proline binds to the SH3 domain in the P_2 position, as expected for a Class II ligand (Figure 4, Table 1). The position usually occupied by a proline in the consensus sequence is residue Q253 in the c-Src linker. The side chain of this glutamine residue cannot pack into the P_{-1} position and points away from the SH3 domain (Figure 13). The P_{-3} position normally occupied by arginine in the consensus sequence is L255 in c-Src, which points away from the SH3 domain and contacts the kinase domain between residues Y326 and W286. No other significant contacts between the c-Src linker and the SH3 domain are made, but in the context of the downregulated conformation, the interaction persists.

The Hck linker contains two proline residues and also forms a PPII helix as seen in the crystal structure of Hck in its downregulated conformation (Figure 8), demonstrating that this general aspect of downregulation is conserved across the A and B subfamilies of SFKs. The binding of the linker is different for Hck, which is a subfamily B kinase. This is due to the presence of the two proline residues in the linker, which bind in the P_{-1} and P_2 positions of the SH3 domain (*31*).

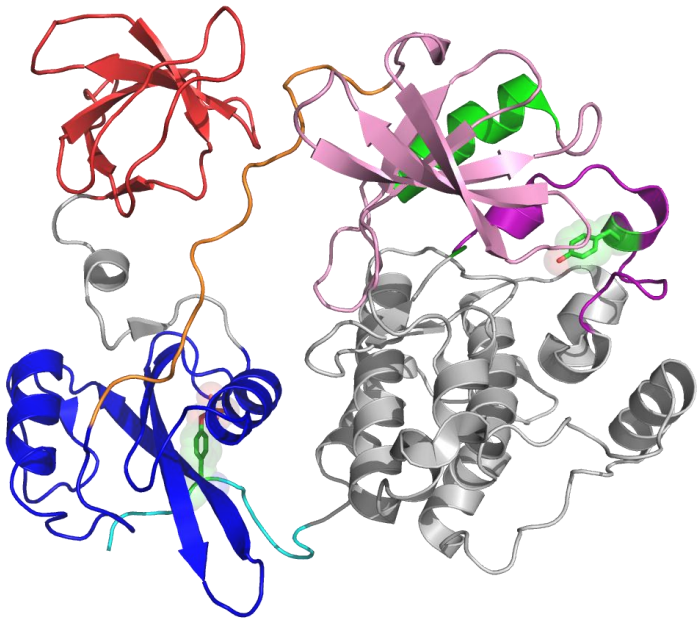

Figure 8. X-ray crystal structure of Hck in the downregulated conformation

The x-ray crystal structure of Hck in the downregulated conformation was solved by Kuriyan and co-workers in 1997 (PDB ID: 1QCF) (*32*). Domain organization and color is the same as in Figure 1 for c-Src. The same intramolecular interactions between the SH3 domain and linker and the SH2 domain and phosphotyrosine tail observed for c-Src are maintained in the downregulated conformation here.

1.1.1.5 Kinase Domain

The kinase domain of SFKs is composed of N-terminal and C-terminal lobes and resembles the conserved bilobed architecture of all protein kinase domains (*33*). The kinase domain, also considered the Src homology 1 (SH1) domain, adopts a conformation incompatible with activity in the downregulated structures of c-Src and Hck. The structure of the active kinase domain has been solved for the T-cell Src-family member, Lck (*34*). To illustrate the differences between the active and inactive forms of the kinase domain, they are shown side by side in Figure 9. The left panel shows the inactive kinase domain conformation of c-Src, taken from the

near-full length downregulated structure where the SH3-SH2 portion of the protein is hidden. The right panel shows the structure of the active Lck kinase domain.

Differences to note in the overall structure in the top panel of Figure 9 are the positions of the activation loop and the αC helix. In the inactive conformation of c-Src on the left, the activation loop physically blocks entry to the substrate binding site. Additionally, Y416 is not phosphorylated and is pointed inward towards the hinge region, making it inaccessible for phosphorylation. This is also considered the "DFG-in" conformation due to the position of the conserved aspartate-phenylalanine-glycine (DFG) motif at the N-terminal end of the activation loop. In the active Lck structure on the right, the Y416 is phosphorylated and the activation loop flips away from the hinge region, allowing substrate access. The DFG motif flips here to the "out" position.

In the bottom left panel of Figure 9, showing the inactive c-Src kinase domain, the K295 and E310 residues are not paired as they would be in an active kinase. Rather, K295 is paired with D404 of the DFG motif and E310 is paired with R409 and Y382. On the bottom right in the active Lck structure, the αC helix rotates inward to position E310 towards K295 so that the K:E ion pair can form, which is critical for kinase activity. Now that Y416 is phosphorylated, it pairs with R409 and R385. The conserved DFG motif undergoes a flip as well, to the DFG-out position. The DFG-in and DFG-out conformations are important in the discussion of kinase inhibitor specificity in Section 1.4.

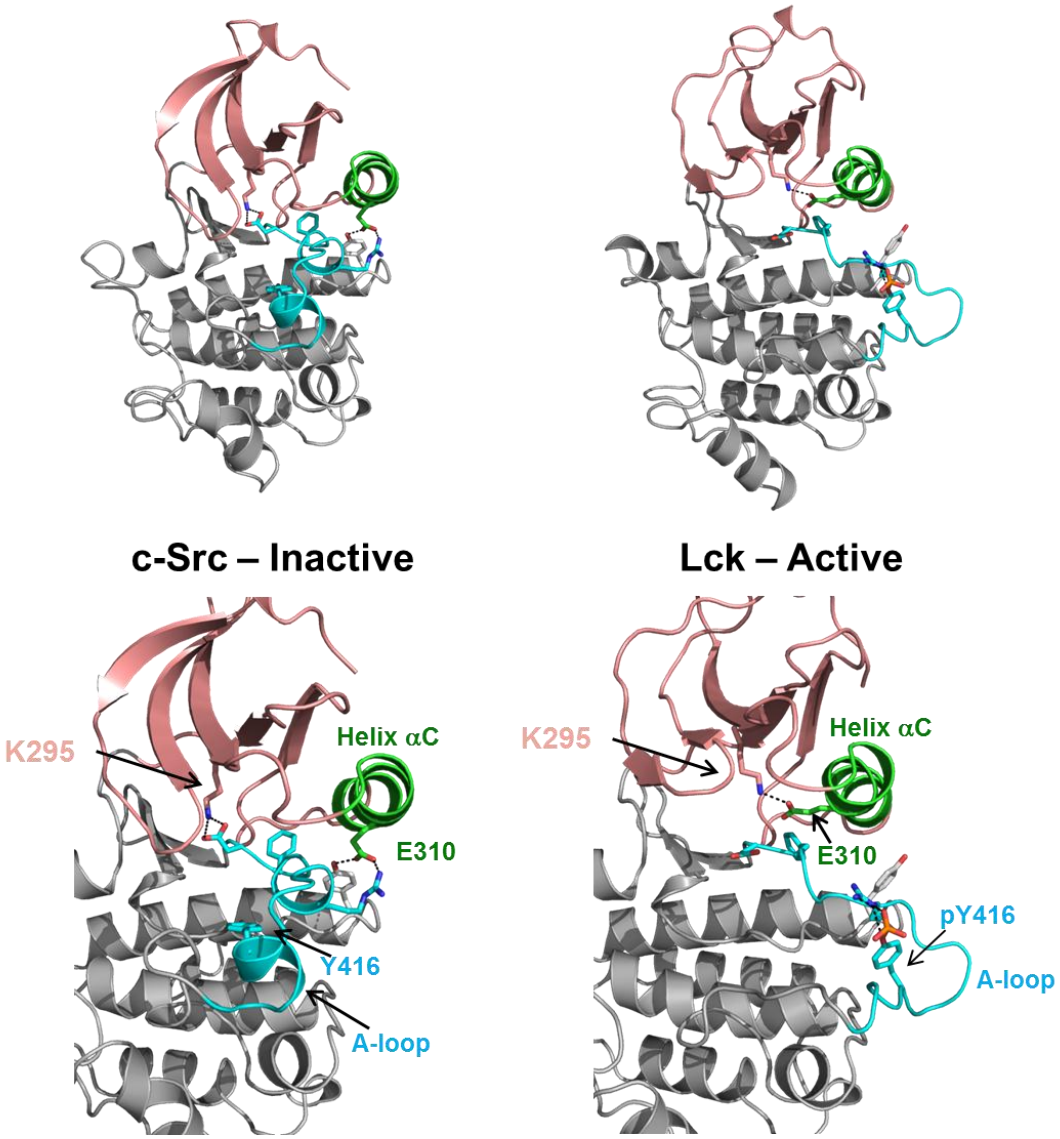

Figure 9. Kinase domains of c-Src and Lck in the inactive and active conformations

The kinase domain portion of downregulated c-Src (PDB ID: 2SRC, left) is shown compared to the active Lck kinase domain (PDB ID: 3LCK, right). The N-lobe is displayed in pink, αC helix in green, activation loop in cyan, and the C-lobe is shown in gray. Critical side chains are displayed to illustrate the changes in specific interactions depending on the activation state of the kinase. The top panel shows a view of the entire kinase domains (where the tandem SH3-SH2 domains would be on the left side) and the bottom panel shows a zoomed-in view of the hinge region with the interactions stabilizing the active or inactive conformation.

1.1.1.6 C-Terminal Tail

The conserved tyrosine residue, Y527, in the C-terminal tail region of the SFKs is essential for the downregulation of kinase activity. Phosphorylation of this residue allows for interaction with the SH2 domain to maintain the downregulated state of the kinase. Dephosphorylation of pTyr-527 by a phosphatase represents one mechanism of kinase activation. The sequence of the SFK C-terminal tail does not fit the consensus of an optimal SH2 ligand, as shown in the sequence alignment in Figure 3, so displacement of the SH2:tail interaction by a ligand with higher affinity can also result in kinase activation. The sequences of the tails differ between SrcA and SrcB subfamilies and this may represent clues towards the specificity of SFK binding and pathway activation. Furthermore, in v-Src, the oncogenic viral homolog of c-Src, the C-terminal end of the kinase is truncated and lacks the C-terminal tyrosine, resulting in constitutive kinase activity (*35, 36*). Similarly, experimental substitution of Y527 with phenylalanine in the SFKs results in hyperactivation of the kinase (*37-41*). In fibroblast transformation assays, the Y527F mutation results in transformation of the cells, while the wild-type c-Src protein does not have this effect.

The C-terminal tyrosine is regulated by phosphorylation by the C-terminal Src kinase (Csk) and the closely related homolog, Chk (*10, 12*). Csk has a similar domain composition and organization as the SFKs with SH3-SH2-kinase. However, there are few similarities in the overall structures and regulation of Csk and the SFKs. Csk does not contain tyrosine residues in the kinase domain and tail that are analogous to the SFKs, and regulation is different. Csk does have a similar activation mechanism, in that it can bind to a number of proteins through its SH2 domain and become activated (*42*). Some of these proteins are known substrates of the SFKs, suggesting that the SFKs and Csk are involved in a negative feedback loop wherein active SFKs

phosphorylate their substrates which then bind and activate Csk. This leads to SFK inactivation as Csk phosphorylates the C-terminal tail. Additionally, Csk has been found in complex with phosphatases like the PEST (proline-glutamine-serine-threonine) domain-enriched protein tyrosine phosphatase (PEP) and PTP-PEST which can dephosphorylate the activation loop of the SFKs (*43*, *44*). This supports a mechanism for total inactivation of the SFKs whereby Csk phosphorylates the tail and the phosphatase dephosphorylates the activation loop. Furthermore, in cases where the SFKs are activated by SH2:tail displacement, these phosphatases may also dephosphorylate the SFK binding partner to disrupt the interaction between it and the SH2 domain. This allows for re-association of the C-terminal tail with the SH2 domain (*45*).

Tail dephosphorylation and subsequent activation of the SFKs is mediated by a number of phosphatases, though the specific phosphatase responsible depends on the cellular context. There is evidence that protein tyrosine phosphatase 1B (PTP1B), receptor protein tyrosine phosphatase α (PTPα), tandem SH2 domain-containing protein tyrosine phosphatase (SHP1), and the transmembrane receptor-like tyrosine phosphatase CD45 each to play a role in tail dephosphorylation to activate the SFKs (*8*, *46-48*). More about this mechanism of activation will be discussed below.

1.1.1.7 Activation Mechanisms

The SFKs can be activated through multiple mechanisms that vary based on the cellular context. For full activation, the activation loop Y416 must be phosphorylated. There are multiple pathways to this level of activation and each can be initiated by a variety of cellular proteins and environments. The fundamentals of each mechanism will be discussed here, and in Section 1.2, examples of kinase activation in various physiological contexts will be given.

One mechanism of kinase activation is by dephosphorylation of the C-terminal tail, as mentioned in the previous section. This leads to the loss of the SH2:tail interaction and results in kinase activity. The tail has been shown to be dephosphorylated by multiple phosphatases, including PTP1B, SHP1, PTPα, and CD45. In Section 1.1.2.2, the role of Lck in the maturation and activation of T cells will be discussed, where CD45 is the phosphatase implicated in Lck activation.

A second mechanism of activation is through displacement of one or both of the intramolecular regulatory interactions by the binding of high-affinity ligands. The SH2 and SH3 domains are modular domains that target the SFKs to many signaling pathways throughout many different cell types. As the SH3 and/or SH2 domains bind to target proteins, the intramolecular interactions that maintain the downregulated state of the kinase are displaced. This relieves the kinase domain of the conformational constraints that stabilize the inactive conformation. The activation of SFKs in this manner by growth factor receptors will be discussed in Section 1.1.2.1. Additionally, the activation of c-Src in this manner by focal adhesion kinase (FAK) will be discussed in Section 1.1.2.3 and the implication of this activation event will be covered in Section 1.3.

The kinases are also activated by phosphorylation of the activation loop. Normally, this is an autophosphorylation event that occurs after one of the previously mentioned mechanisms takes place. Subsequent to regulatory domain displacement as described above, the kinase domain reorients the activation loop to allow for substrate access to the active site with the activation loop tyrosine extended outward for autophosphorylation. The autophosphorylation of the activation loop is thought to be in trans rather than cis, supporting the idea that multiple SFKs cluster at one site of activation (*49, 50*).

1.1.2 Physiological Regulation of Src-Family Kinase Activity

The SFKs have been studied in great detail in knockout mouse models to determine the responsibilities and requirements for each family member. Table 2 shows the phenotypes that result from the genetic ablation of each individual family member. None of the individual SFK knockout mouse models result in an embryonic lethal phenotype indicating that no specific family member is required for embryonic development. Since multiple SFKs are expressed in every cell type, there likely exists functional redundancy leading to compensation by the remaining family members in each knockout model. Individual SFK-null mice were eventually crossed to create the triple knockout of c-Src, c-Yes, and Fyn ($SYF^{-/-}$). This triple-knockout is embryonic lethal at day E9.5 due to failure to turn (*51*).

Table 2. Phenotypes observed in SFK mutant mice

SFK mutant	Phenotype
c-Src	Osteopetrosis
Fyn	Impaired memory, defect in thymocyte signaling
c-Yes	None observed
Fgr	None observed
Hck	None observed
Lyn	Impaired B-cell function, autoimmunity
Lck	Impaired TCR signaling, block in T-cell development
Blk	None observed
Src + Fyn + Yes[a]	Embryonic lethal (E9.5)

[a] Reference (*52*)
Table adapted from Lowell and Soriano, 1996 (*53*).

This required developmental event results in inversion of the germ layers and is essential for the embryo to assume the correct position for continued development. There were also multiple developmental defects seen in the embryos. Mouse embryonic fibroblasts (MEFs) cultured from $SYF^{-/-}$ embryos show a dramatic decrease in migration compared to those from wild type littermates.

1.1.2.1 Growth factor receptor-induced activation of SFKs

Growth factor receptors are transmembrane receptor tyrosine kinases (RTKs) that transmit signals into the cell in response to various growth factors. These signals activate various pathways, including JAK/STAT, MAP kinase, and PI3K, which lead to proliferation and survival (*54-56*). The involvement of SFK activity in response to growth factor stimulation has been shown for multiple growth factor receptors, including the epidermal growth factor receptor (EGFR), fibroblast growth factor receptor (FGFR), platelet-derived growth factor receptor (PDGFR), and colony stimulating factor-1 receptor (CSF-1R). Growth factor stimulation of these receptors results in autophosphorylation on their intracellular domains, creating high-affinity binding sites for the SH2 domains of SFKs, specifically c-Src and Fyn. Activation by these receptors implicates the SFKs in the downstream RTK pathways.

The earliest studies to connect the activation of SFKs with growth factor receptors were in the context of the EGF receptor (*57, 58*). In these studies, DNA synthesis was measured in MEFs in response to EGF. DNA synthesis was increased up to five-fold in cells overexpressing c-Src compared to wild type cells. Additionally, it was observed that individual mutation of the kinase domain, SH2 domain, or myristoylation sequence of c-Src was enough to prevent this increase in DNA synthesis. Mutation of the kinase domain to abolish activity showed that c-Src activity was necessary for the induction of DNA synthesis by EGF stimulation, while the SH2

domain and myristoylation sequence mutations affected c-Src localization to the EGF receptor and cell membrane, respectively. Subsequently, it was shown that the SFKs interact with, and are activated by, the CSF-1R (*59*). This study showed that the SFKs c-Src, c-Yes, and Fyn were all activated in response to stimulation of cells with CSF-1, but not when the CSF-1R was mutated at Y809. This tyrosine residue is part of the SH2 binding site and when mutated to phenylalanine, the binding is prevented and the SFKs cannot associate. This was shown in both co-immunoprecipitation experiments and kinase assays with SFKs immunoprecipitated from CSF-1-activated cell lysates. Using MEFs derived from the $SYF^{-/-}$mouse, a role for c-Src in the FGFR pathway was also established (*60*). Stimulation of $SYF^{-/-}$ cells with FGF-1 resulted in a modest increase in cell proliferation and DNA synthesis. Reintroduction of c-Src in this line significantly increased DNA synthesis and cell proliferation response to FGF-1. Prior to this study, it was reported that c-Src was not essential for FGF-1-induced cell proliferation (*61*). However, those studies were performed by comparing cells isolated from wild type and $c\text{-}Src^{-/-}$ mice, and compensation from c-Yes and Fyn would likely mask the role of c-Src in this pathway.

The role of the SFKs in the PDGFR-induced pathways has remained less clear. Conflicting evidence is presented regarding the involvement of the SFKs in this pathway, namely using the same $SYF^{-/-}$ cells as were used in the FGFR study above. Stimulation of these cells with PDGF did not result in an inhibition of DNA synthesis compared to wild type cells (*51*). However, the $SYF^{-/-}$ cells were immortalized by the addition of the SV40 large T antigen. A subsequent study implicates this in the requirement of the SFKs in the response to PDGF stimulation (*62*). Multiple other studies have since linked the SFKs to PDGFR signaling, supporting their role in this pathway. One study used a SFK inhibitor to show inhibition of DNA

synthesis in response to PDGF (*63*), while another showed that overexpression of catalytically inactive c-Src or Fyn inhibited the increase in DNA synthesis in response to PDGF (*64*).

1.1.2.2 Role of Lck activity in T-cell activation and maturation

The C-terminal tail of the SFKs must be phosphorylated to bind to the SH2 domain and maintain the downregulated state of the kinase. Multiple phosphatases have been implicated in the dephosphorylation of the C-terminal tail to induce kinase activation, as mentioned above in Section 1.1.1.6. A well-studied example is in T-cell activation where Lck activity is regulated by Csk and the receptor-like tyrosine phosphatase CD45 (*65*). T cells are activated upon binding of antigens to the T-cell receptor (TCR). The first event in the signaling cascade upon antigen binding is the activation of SFKs, specifically Lck and Fyn which are the most prevalent family members in T cells. Lck is kept in the downregulated state by phosphorylation of the C-terminal tail by Csk. Upon antigen stimulation, CD45 dephosphorylates the tail to prime the kinase for activation. There is evidence of trans-phosphorylation of the Lck activation loop tyrosine by other Lck molecules at the membrane (*65*). Active Lck phosphorylates the TCR, which creates high affinity binding sites for the SH2 domains of ZAP-70, a critical member of the TCR signaling cascade. ZAP-70 is phosphorylated by Lck and goes on to activate downstream signaling pathways that lead to T cell activation. Lck activity must be tightly regulated in this system, because loss of Lck regulation leads to hyperactivation of T cells while Lck deficiency leads to lack of T cell activation and immunodeficiency. CD45 is also critical in the pathway, as CD45 deficiency results in lower SFK activity and an increase in pY527.

1.1.2.3 Focal adhesion kinase-induced activation of c-Src

Some proteins contain tandem high affinity binding sequences for both the SH3 and SH2 domains of SFKs. Focal adhesion kinase (FAK) contains SH3- and SH2-binding sequences in close proximity and has been shown to bind and activate c-Src (*66*). The activity of c-Src induced by FAK is diminished when one of the FAK binding sites is missing or mutated, showing that dual engagement is required for full FAK-induced activity. As described above in Section 1.1.1.7, the displacement of the intramolecular interactions in c-Src results in the release of the conformational constraints imposed on the kinase domain and exposure of the activation loop tyrosine, allowing for autophosphorylation and maximal kinase activity. Once bound, the c-Src:FAK complex is important in the migration of cells via focal adhesion turnover. This will be discussed in more detail in Section 1.3.

1.1.3 Pathological Roles of Src-Family Kinases

1.1.3.1 Solid tumor malignancies

There is no shortage of evidence for the connection of the SFKs to many types of cancer. SFKs are shown to be overexpressed in many solid tissue malignancies, including tumors of the breast, ovary, and colon (*67-70*). More importantly, increased c-Src activity is reported in these cancers as well. The involvement of SFKs in cell proliferation and survival through activation by growth factor receptors (as discussed in Section 1.1.2.1) implicates them in the initiation and progression of cancer. A common finding in solid tumors overexpressing c-Src is that growth factor receptors are overexpressed as well (*71*, *72*). One example is that of EGFR and c-Src overexpression in breast cancer (*73*). Both EGFR and c-Src are found to be upregulated and hyperactive in tumor cells. Not only does the increased activity of just one of these kinases have

the potential to overstimulate proliferation and survival pathways, but they are found to have a synergistic effect. Since EGFR is overexpressed, the higher density of receptors at the cell surface is postulated to result in trans-autophosphorylation of the intracellular domains, even in the absence of extracellular growth factor stimulation. Even with normal levels of c-Src expression, the increased number of c-Src SH2 binding sites on the EGFR intracellular domains can result in constitutively activated c-Src and downstream signaling pathways.

In addition to the activation of proliferation and survival pathways, c-Src is also implicated in migration and invasion of cancer cells and in cancer metastasis (*74, 75*). These effects are facilitated through the c-Src:FAK complex, which is essential for focal adhesion turnover. Studies in colorectal cancer have shown that c-Src protein levels rise in the early stages of cancer and are then maintained as the tumor progresses (*76*). In contrast, c-Src activity levels continue to rise through each stage of cancer and are highest during metastatic dissemination. This observation supports an important role for c-Src in metastatic disease. More about the role of the c-Src:FAK complex in cancer will be discussed in Section 1.3.2. and is the major focus of Chapter 3.

1.1.3.2 Hematopoietic SFKs in Chronic Myelogenous Leukemia

The expression of certain SFKs is restricted to hematopoetic cells, so their involvement in blood cancers is not surprising. Hck and Lyn have been implicated in the pathogenesis of chronic myelogenous leukemia (CML) (*77, 78*). CML is caused by a reciprocal chromosomal translocation between the breakpoint cluster region (Bcr) locus on chromosome 22 and the c-Abl locus on chromosome 8, resulting in the Bcr-Abl oncoprotein (*79, 80*). The Bcr-Abl protein mainly consists of the c-Abl protein, but the N-terminus is replaced with Bcr, so regulation of kinase activity is disrupted and the kinase is constitutively active. This initially results in a large

expansion in the neutrophil population in the peripheral blood during the chronic phase of the disease. Ultimately, CML patients undergo a transition known as blast crisis, in which differentiation is disrupted and the disease more closely resembles acute myeloid leukemia (AML).

The SFKs were first implicated in CML when Hck and Lyn were shown to be bound and activated by Bcr-Abl (*81*). Subsequently, it was shown that a kinase-dead mutant of Hck suppresses transformation by Bcr-Abl in a myeloid cell line (*82*). Additionally, Hck was linked to Stat5 activation in CML cells (*83*) and both Hck and Lyn were shown to phosphorylate Bcr-Abl (*84*). The absence of these phosphorylation events resulted in lower Bcr-Abl transforming ability. This showed that there is a reciprocal relationship between the SFKs and Bcr-Abl as they were both shown to bind to and activate each other.

CML was the first malignancy for which the causative agent was pinpointed, and this encouraged the discovery of targeted small-molecule kinase inhibitors of Bcr-Abl. The kinase inhibitor imatinib, which was first discovered in a screen for inhibitors of the PDGF receptor tyrosine kinase, was an instant success in the treatment of CML as it is a very effective Bcr-Abl inhibitor in vivo (*85*). Unfortunately, resistance to this drug develops in patients due to mutations in the drug binding pocket in the kinase domain and elsewhere in the protein (*86, 87*). Underscoring the importance of SFKs in CML, the next successful treatment came in the form of dasatinib, a dual SFK/Abl inhibitor (*88*). Dasatinib is also very successful in the clinic against CML by simultaneously inhibiting both Bcr-Abl and the SFKs and can overcome some mechanisms of resistance to imatinib.

1.1.3.3 The Hck:Nef complex in HIV infection

The human immunodeficiency virus-1 (HIV-1) encodes multiple accessory proteins essential for viral pathogenesis. Nef is an accessory protein that has been implicated in multiple aspects of HIV infection and disease (*89*). More importantly, it is thought to elicit its activity through the binding of SFKs (*90-92*). Nef has been implicated in disease progression to acquired immunodeficiency syndrome (AIDS) in animal models of disease and in humans . Expression of the Nef protein in a transgenic mouse model resulted in the development of AIDS-like disease, even in the absence of HIV infection (*93*). This is supported by a study in which a group of patients were identified as long-term non-progressors (LTNPs), as their disease had not progressed to AIDS, even ten years after initial infection (*94, 95*). The sequences of their viral genomes were analyzed and it was discovered that all of them were defective for Nef. These data support the idea that Nef is both necessary and sufficient for progression to AIDS.

Nef itself is an accessory protein that has no catalytic function. It must therefore elicit its function through binding to host proteins to have the effects described above. Nef contains a polyproline motif shown to have a high affinity for the Hck SH3 domain (*90*). It has also been shown to activate Lyn and, to a lesser degree, c-Src (*96*). The interaction between SFKs and Nef has been well studied biochemically, but the role of SFKs in HIV is less clear. Evidence for SFK involvement, however, comes in part from studies of Nef expression in $Hck^{-/-}$ mice. These mice show delayed development of AIDS-like disease in comparison to the Nef-expressing transgenic mice described above (*97*).

Nef has been shown to bind with very high affinity (K_D = 0.25 μM) to the isolated SH3 domain of Hck (*98*). Binding of Nef to Hck can activate the kinase very effectively. The PPII helix formed in Nef binds to the SH3 domain in a Class II orientation (*99*). The specificity of

different SFK SH3 domains has been attributed to a single isoleucine residue in the SH3 domain (*98*). This residue is present in Hck, but not in Fyn, to which Nef normally does not bind. However, mutation of the residue in Fyn from arginine to isoleucine results in a similar binding affinity as Hck SH3 to Nef (K_D = 0.38 μM). This Fyn SH3 R96I mutant was subsequently used in crystallographic studies to solve the structure of Nef in complex with an SFK SH3 domain (Figure 10) (*99*).

The SH3:Nef structure shows the interaction of the PPII helix formed in Nef with the same SH3 domain residues as outlined in Section 1.1.1.2 (Y90, Y92, D99, W118, Y136). Interestingly, when Nef activates Hck by SH3 domain displacement, the pY tail stays bound to the SH2 domain (unpublished data). This is also supported by evidence in yeast growth experiments using Csk to downregulate SFK activity (*96*).

The expression of SFKs is toxic in yeast, providing a simple phenotypic readout for SFK activity. Co-expression with Csk to phosphorylate the C-terminal tail and downregulate the kinase activity reverses this effect. Expression of Nef with Hck leads to higher levels of toxicity in yeast, which can no longer be overcome by expression of Csk. This is in contrast to the same experiment performed with c-Src. Coexpression of Nef and c-Src results in higher toxicity than c-Src expression alone, which is similar to observations with Hck. However, co-expression of Csk reverses the toxic effect induced by Nef activation in yeast, suggesting that SH3 domain displacement in c-Src is not enough to reach maximal activation. This is also supported by evidence of the requirement of both SH3- and SH2-binding sequences for FAK-induced c-Src activation, discussed in Section 1.1.2.3.

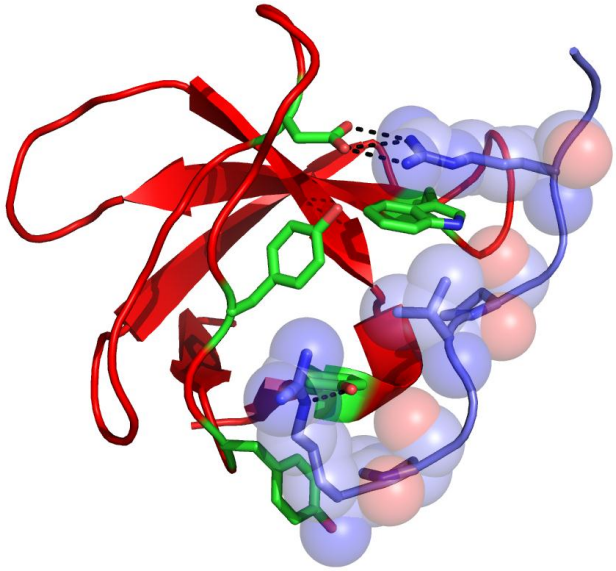

Figure 10. SH3 domain of Fyn R96I mutant in complex with PPII helix of Nef

The x-ray crystal structure of the core domain of Nef was solved in complex with the SH3 domain of Fyn (containing the R96I mutation so that binding could occur). The residues in the SH3 domain (red) that form the hydrophobic pockets necessary for PPII helix binding are shown in green (Y90, Y92, D99, W118, Y136). The PPII helix of Nef is shown and the side chains of the key residues that bind the SH3 domain are shown with spheres to illustrate the fit of the helix into the SH3 domain.

1.2 FOCAL ADHESION KINASE

Focal Adhesion Kinase (FAK) is a 125 kDa non-receptor protein tyrosine kinase that was initially discovered in a pool of tyrosine phosphorylated proteins isolated from RSV-infected cells, that localizes to focal adhesions (*100*). FAK is ubiquitously expressed and deletion in mice results in embryonic lethality due to poorly formed vasculature systems (*101*). The embryos also

exhibit failure to turn, similar to $SYF^{-/-}$ embryos, suggesting that the functions that result from the cooperation of FAK and the SFKs, particularly cell migration, are essential for development (*102*). FAK is a binding partner of c-Src and both have been implicated in cancer, so this section will focus on the functions of FAK that relate to cooperation with SFKs.

1.2.1 Protein Structure

The FAK protein is composed of an N-terminal four-point-one/ezrin/radixin/moesin (FERM) domain, a central kinase domain, and a C-terminal focal adhesion targeting (FAT) domain (Figure 11) (*103*). Between the FERM and kinase domains is a short linker containing high-affinity binding sequences for the c-Src SH3 and SH2 domains. The region between the kinase and FAT domains contains proline-rich sequences that serve as docking sites for the SH3 domains of other signaling proteins. The most complete x-ray crystal structure of FAK is shown in Figure 11 in which the protein is truncated after the kinase domain. The structure of the FAT domain has been solved in isolation (*104*), though it is unclear how that portion of the protein would fit into the structure of the full-length protein.

The structure of the FERM domain in the FERM-Kinase construct (Figure 11, gray) is identical to the structure of the isolated FAK FERM domain (PDB ID: 2AL6, not shown) (*105*). The FERM domain consists of the F1, F2, and F3 lobes, each having its own unique structure, and is important for stabilizing the inactive conformation of FAK (discussed below). The kinase domain of FAK resembles the conserved architecture of protein kinase domains with the classic bilobed structure (*33*). The FERM-Kinase structure models the autoinhibited structure of FAK, yet the kinase domain shows hallmarks of both an inactive structure and an active structure. This will be further discussed in Section 1.2.2.1 regarding the inactive FAK conformation.

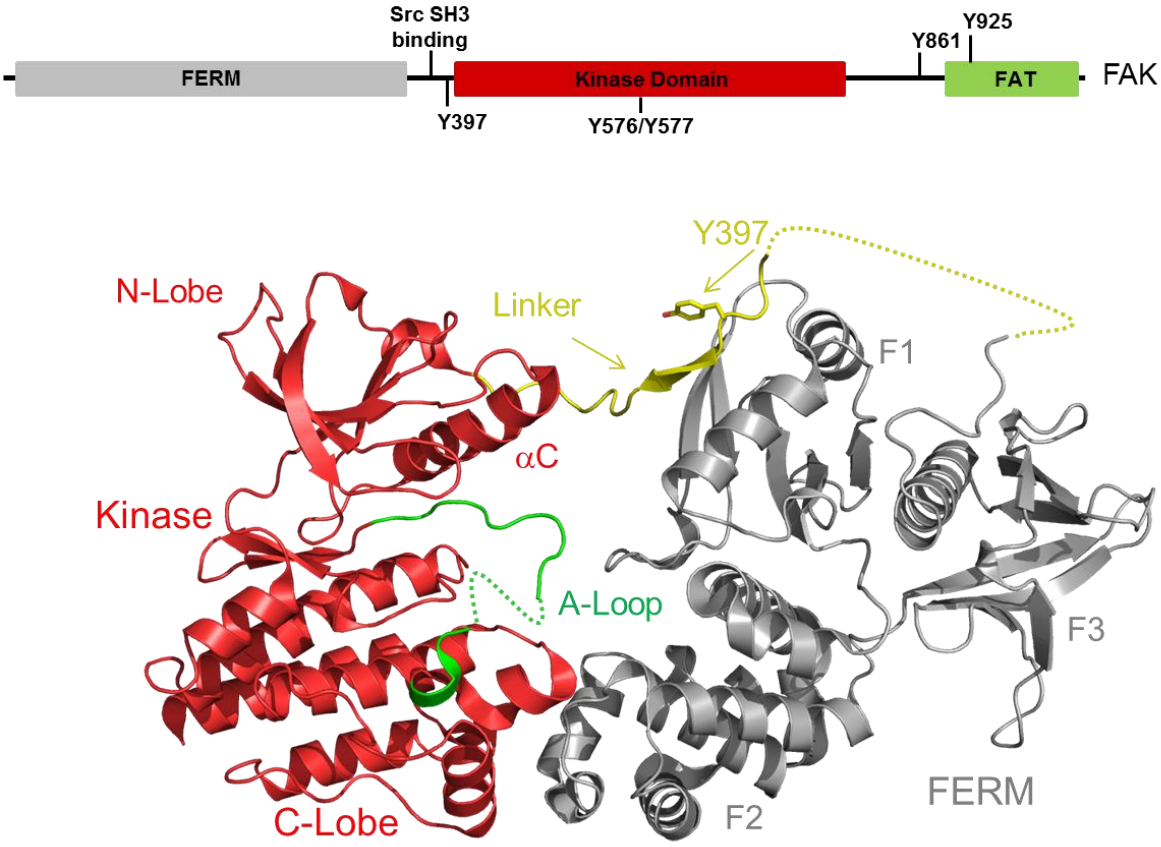

Figure 11. Focal Adhesion Kinase (FAK) structure and domain organization

The domain organization of FAK is shown at the top, with an N-terminal FERM domain, a short linker containing the c-Src SH3 binding site and the autophosphorylation site Y397 (which becomes a high affinity binding site for the c-Src SH2 domain), the bilobed kinase domain, a proline-rich region with binding sites for the SH3 domains of other signaling proteins, and a C-terminal FAT domain, which targets the protein to focal adhesions. The bottom shows the crystal structure of the autoinhibited protein (PDB ID: 2J0J) (*103*). The crystallized protein is truncated after the kinase domain, so does not include the proline-rich region or the FAT domain. In the crystal structure, the kinase domain is shown in red, with the activation loop in green. A short stretch of the activation loop is disordered in the structure and is represented by dashed lines. The FERM domain is shown in gray and the linker is shown in yellow, with the autophosphorylation site indicated with the arrow. A portion of the linker containing the c-Src SH3 binding site was also disordered in the structure and is represented with the dashed line.

Two regions of the protein in the FERM-Kinase structure are unresolved: a portion of the FERM-kinase linker and a portion of the activation loop. The unresolved portion of the FERM-kinase linker contains the c-Src SH3 binding site, though Y397 is present in the structure. This residue is essential for c-Src binding through its SH2 domain (*106*). That Y397 is not phosphorylated in the structure supports an inactive kinase. The disordered activation loop in the kinase domain is not surprising, as many kinase domain structures are missing this region due to its dynamic nature. The missing section includes the activation loop tyrosine residues, Y576 and Y577.

The C-terminal proline-rich segment is not present in any of the structures of other FAK domains. Multiple SH3 binding sites are present in this region which recruit SH3 domain-containing proteins like p130Cas (*107*). The x-ray crystal structure of the isolated FAT domain has been solved alone and in complex with peptides with sequences from the FAK-binding protein, paxillin (*108, 109*). The FAT domain is responsible for targeting FAK to focal adhesions through binding to adapter proteins like talin and paxillin, which bind directly to actin.

1.2.2 Kinase Regulation

1.2.2.1 Inactive conformation

The mechanism of downregulation of FAK kinase activity was determined through extensive biochemical analyses (*110*) and confirmed by the structure of the FAK FERM-Kinase construct (Figure 11). Deletion of the FERM domain results in constitutive kinase activation. This structure supports a role for the binding of the FERM domain to the kinase domain to suppress kinase activity. The main point of contact between the FERM and kinase domains is between the F2 lobe of FERM and the C-lobe of the kinase domain. F596 in the kinase domain

fits into a hydrophobic pocket formed by residues Y180, M183, V196, and L197 in the F2 lobe. Additionally, multiple interdomain hydrogen bonds are formed to stabilize the F2:C-lobe interaction. A second interaction is formed between the linker and the N-lobe of the kinase domain, involving residues D402, E403, and S463. The linker also binds to the surface of the F1 lobe of the FERM domain and this interaction makes Y397 unavailable for phosphorylation.

As mentioned in the previous section, the conformation of the kinase domain does not fit exactly into that of an inactive kinase, namely because the K:E ion pair is present (discussed in Section 1.1.1.5), which is required for kinase activity. That interaction alone does not necessarily drive kinase activity, and other aspects of the kinase structure support an inactive conformation. Due to the position of the FERM domain, substrate access to the kinase domain is blocked. In addition, while the tyrosine residues in the kinase domain are not resolved in the structure, it is likely that they are sequestered within the FERM domain and inaccessible for phosphorylation.

1.2.2.2 Mechanisms of Activation

The process of FAK activation is stimulated by integrin signaling. Integrins are heterodimeric transmembrane receptors with no innate catalytic activity (*111, 112*) . Integrins transduce signals into cells in response to the extracellular environment. When integrins are activated by ECM ligand binding, a conformational change occurs in the intracellular domains of the integrin dimer starting the process of focal adhesion formation. This conformational change can recruit FAK through proteins including talin and paxillin. These actin-binding proteins are recruited to activated integrin receptors and recruit FAK via the FAT domain to the focal adhesion. Once present at the focal adhesion, interaction of the FERM domain with other proteins in the complex leads to release of the autoinhibitory interactions and Y397 undergoes

autophosphorylation, creating a high affinity binding site for the c-Src SH2 domain. Binding of the c-Src SH2 domain results in activation of c-Src, as discussed previously, and c-Src phosphorylates FAK on multiple residues (*113-115*). Two residues, Y576 and Y577, are in the FAK activation loop and phosphorylation of these residues is required for full activation of FAK. Phosphorylation of two other residues, Y861 and Y925, is necessary in the recruitment of other proteins to the focal adhesion complex, including p130Cas and Grb2. Once phosphorylated by the c-Src:FAK complex, p130Cas associates with Crk, while Grb2 binds to SOS, both leading to activation of Rho-family GTPases that control actin polymerization and adhesion (*115-118*).

1.3 C-SRC AND FAK IN NORMAL CELLULAR FUNCTION AND CONSEQUENCES OF KINASE DEREGULATION

1.3.1 Cell Migration

Cell migration is a tightly regulated process involving over fifty different cellular proteins (*119*). Cells attach to each other through adherens junctions and to the extracellular matrix (ECM) via focal adhesions. Regulation of each type of adhesion is achieved through many distinct proteins, but some proteins have a role in both, including c-Src and FAK. The function of c-Src in both cell-cell and cell-ECM adhesions is to facilitate disassembly, which is required for cell migration (*120*). Cells lacking FAK or the three ubiquitously expressed SFKS, c-Src, c-Yes, and Fyn, show a dramatic decrease in the rate of cell migration (*51, 121*). This is due to the decrease in the disassembly of focal adhesions and adherens junctions.

1.3.1.1 Cell-cell adhesion

Adherens junctions are formed between cells through the binding of E-cadherin, a transmembrane glycoprotein (*122*, *123*). Extracellular E-cadherin molecules on neighboring cells bind to each other and are regulated by the intracellular protein complexes that form and are linked to the actin cytoskeleton. The intracellular domain of E-cadherin is linked to the actin cytoskeleton by β-catenin, α-catenin, and p120catenin (*124*). When signaling events trigger the disruption of cell-cell contacts, c-Src is recruited to initiate breakdown of the complex. PTP1B co-localizes with c-Src to adherens junctions and has been shown to activate c-Src by dephosphorylation of the C-terminal tail (*71*). Studies in FAK null cells show that FAK is also required for the disruption of cell-cell contacts.

1.3.1.2 Cell-ECM adhesion

Focal adhesions are formed to facilitate the connection between the extracellular environment and the actin cytoskeleton (*118*). Heterodimeric integrin receptors are transmembrane proteins that transmit extracellular signals into the cell. ECM ligand binding to integrin receptors induces a conformational change in the intracellular domains that leads to the recruitment of actin-binding proteins, including talin and vinculin. FAK is recruited to the focal adhesion through its FAT domain, which binds talin. As described in Section 1.2.2.2, FAK becomes activated in response to binding other focal adhesion proteins through its FERM domain. This leads to subsequent recruitment of c-Src and the formation of the c-Src:FAK complex. The activity of c-Src:FAK is responsible for the disassembly of focal adhesions by phosphorylating paxillin, which leads to the activation of downstream signaling cascades. To prevent disassembly, Csk is also localized to focal adhesions to downregulate c-Src activity until the appropriate time (*125*, *126*).

1.3.2 Cancer

One hallmark of cancer cells is the loss of adhesion to other cells and to the extracellular matrix (*71*). As these processes are regulated by c-Src and FAK activity as described above, it is not surprising that both are found to be overexpressed and hyperactivated in cancer. At adherens junctions, c-Src not only facilitates the disruption of the E-cadherin-catenin-actin complex, but also targets E-cadherin for degradation (*127, 128*). E-cadherin regulates cellular invasion and loss of E-cadherin function results in a more invasive phenotype. Further, as the c-Src:FAK complex facilitates focal adhesion disassembly, it is not surprising that a hyperactive complex results in an increased rate of migration in cancer cells.

1.4 SMALL-MOLECULE INHIBITORS OF SRC-FAMILY KINASES AND FOCAL ADHESION KINASE AS ANTI-CANCER THERAPY

1.4.1 Overview and History of Kinase Inhibitors

The first kinase inhibitor to enter clinical trials was the Bcr-Abl inhibitor, imatinib (Gleevec), for the treatment of CML (*85, 129*). This was the first example of a small molecule inhibitor targeted to the causative agent of a specific cancer (*130*). Imatinib was discovered in a screen for inhibitors of the PDGF receptor, but was found to also have activity against c-Abl and c-Kit. Ultimately, resistance to imatinib develops in patients with advanced CML (*131*). This led to the development of second-generation Bcr-Abl inhibitors like nilotinib and dasatinib, which is also a SFK inhibitor (*88, 132*). The x-ray crystal structures of the Abl kinase domain in complex

with imatinib and dasatinib have been solved and are shown in Figure 12 to illustrate the binding modes of these compounds to the kinase domain (*133-135*) .

Kinase inhibitors can be classified into at least four different types (*136, 137*). Type I inhibitors bind directly to the ATP-binding site in the hinge region of the kinase domain and are directly competitive with ATP. Structures of kinases in complex with Type I inhibitors are generally found in the active, DFG-in conformation. Type II inhibitors make contact with the ATP-binding site, but also with an allosteric pocket in the kinase domain formed when in the DFG-out conformation. As the DFG motif rearranges to create this allosteric site, the phenylalanine residue partially blocks the ATP-binding site. Consequently, the DFG-out conformation is consistent with an inactive kinase. Type III inhibitors only bind to this allosteric site in the kinase domain and make no contact with the ATP-binding site, while Type IV inhibitors bind at a site completely removed from the catalytic region. Type III and Type IV inhibitors will not be discussed here.

Imatinib is a Type II inhibitor that binds to c-Abl/Bcr-Abl when it is in the DFG-out conformation (Figure 12A). While originally thought to only bind to the inactive form of the kinase, the crystal structure shows that the K:E ion pairing is present, which is a feature of the active conformation. However, the activation loop tyrosine is not phosphorylated and the activation loop itself is in a position consistent with an inactive kinase (*138*). The conformation of c-Abl when imatinib is bound likely represents a transition state between inactive and active conformations.

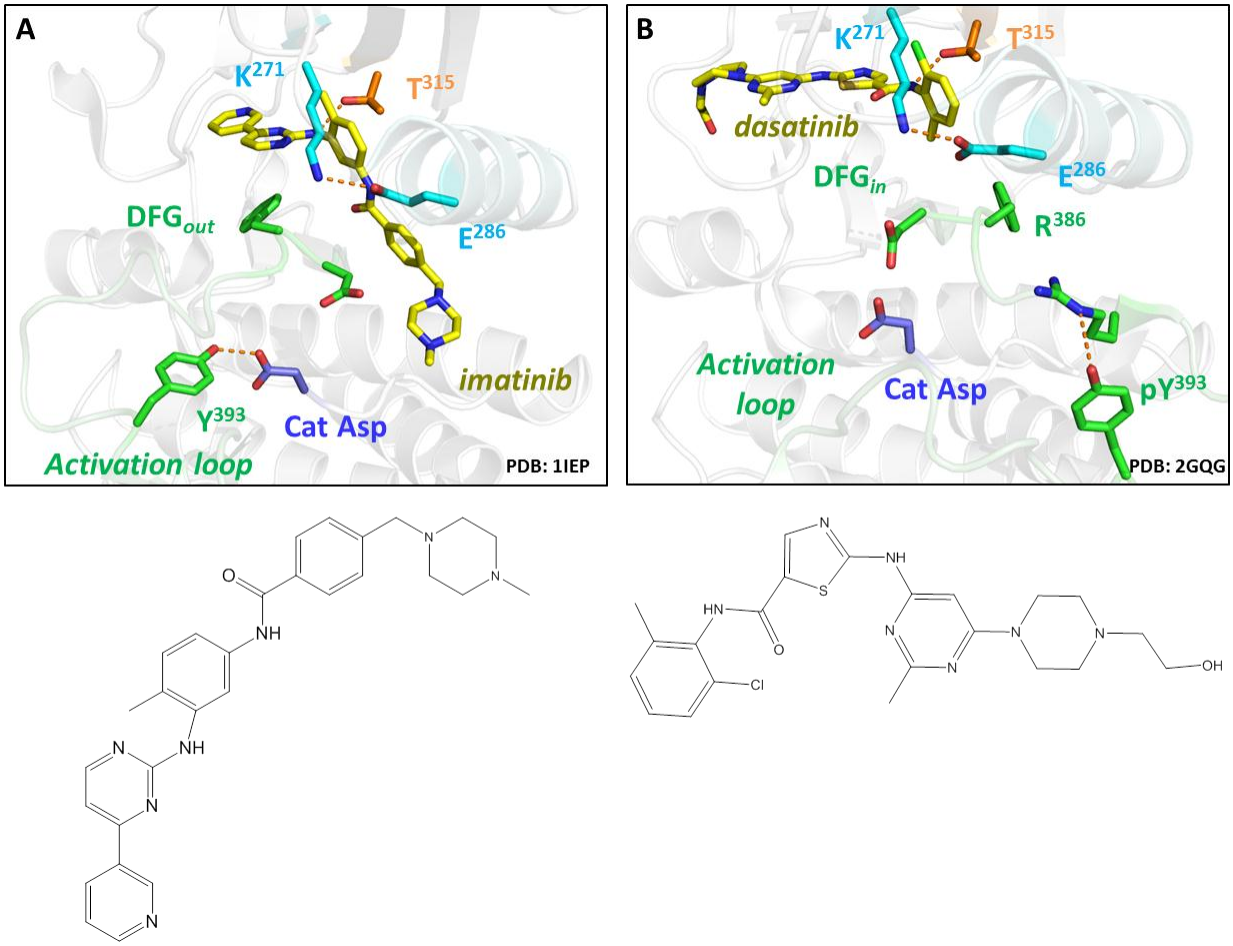

Figure 12. Binding modes of Bcr-Abl inhibitors imatinib and dasatinib to the c-Abl kinase domain

The x-ray crystal structure of the kinase domain of c-Abl has been solved in complex with the inhibitors imatinib (A, PDB ID: 1IEP) and dasatinib (B, PDB ID: 2GQG). Side chains of key residues are shown. In both structures, the K:E ion pair is present. A) Imatinib is a Type II kinase inhibitor that binds not only to the ATP-binding site of the kinase, but also to an allosteric site in the kinase domain that is only present in the inactive, DFG-out conformation. B) Dasatinib is a Type I kinase inhibitor that binds to the ATP-binding site of the kinase domain and shows no preference for the DFG-in or DFG-out conformation. The kinase is in the active, DFG-in conformation in the structure. Figure adapted from Panjarian, et al (*134*).

Conversely, the Type I inhibitor dasatinib shows no preference for the active or inactive kinase conformation. The structure of c-Abl with dasatinib bound (Figure 12B) is consistent with the

active conformation based on the presence of the K:E ion pair and the position of the activation loop. Though the activation loop tyrosine is not phosphorylated (since the kinase activity is inhibited by the presence of the drug), the tyrosine still pairs with R386 as it would in an active conformation. As mentioned before, dasatinib also binds and inhibits SFKs, which will be further discussed in the next section.

1.4.2 Src-Family Kinase Inhibitors

Dasatinib (structure in Figure 12B) is a dual SFK/Abl inhibitor that is currently approved for the treatment of CML in patients who are resistant to imatinib (*88*). As the SFKs are promising targets for cancer therapy due to their involvement in so many cellular processes, dasatinib has been tested in the laboratory setting for its ability to inhibit cancer cell growth, migration, and invasion. Dasatinib has shown much promise in these assays, leading to numerous clinical trials. Trials are currently in progress to test dasatinib for the treatment of metastatic breast cancer, head and neck cancer, glioblastoma multiforme, and metastatic colorectal cancer (*139-142*). Many of the clinical trials are testing dasatinib in combination with other first-line chemotherapeutic agents. As discussed above, dasatinib is a Type I, ATP-competitive kinase inhibitor. The activity of dasatinib is not restricted to c-Abl and the SFKs, as it also inhibits the PDGF receptor, c-Kit, and the ephrin type-A receptor 2 (EphA2). There have been some promising results from the clinical trials but at this point, none have led to approval for first-line therapy.

Saracatinib (AZD0530)

Saracatinib is a dual SFK/Abl inhibitor as well, with less off-target effects than dasatinib (*143*). No crystallography data is available for this drug in complex with a kinase, but it is known to be an ATP-competitive inhibitor. The success of this inhibitor in preclinical trials was similar to that of dasatinib and led to multiple clinical trials for the treatment of solid tumors (*144*). As personalized medicine is becoming more attainable, biomarkers are being investigated to preselect patients who may respond best to SFK inhibitor treatment. Once these are established, this and other SFK inhibitors may be reevaluated in patients who fit these criteria.

1.4.3 Focal Adhesion Kinase Inhibitors

As with the SFKs, a role for FAK in cancer metastasis has been established and inhibitors of FAK are being investigated as potential anti-cancer agents. There are currently no established FAK inhibitors used in the clinic, but there are clinical trials in progress with two compounds, PF-562,271 and VS-6068 (defactinib) (*145-147*). Both compounds were reported to decrease pY397 phosphorylation levels, which would be ideal so as to prevent formation of the c-Src:FAK complex. PF-562,271 was found to be very selective for FAK and the homolog Pyk2 in preclinical studies (*148-150*). Clinical trials with this compound were completed in patients with solid tumors of various sites and many patients showed no disease progression. Unfortunately, there was no positive partial or complete response reported in any patients. Defactinib is currently being investigated for the treatment of mesothelioma, lung cancer, and ovarian cancer (*145, 146*). This compound was very successful in preclinical studies as well, but clinical results are still pending. Based on the mechanism of FAK activity in cells, however, it would seem likely that using a FAK inhibitor in combination with traditional chemotherapy would be more

successful than monotherapy with the inhibitor alone. Many of the effects of FAK are elicited through the c-Src:FAK complex, so potential combination of SFK and FAK inhibitors could be useful in treatment of metastatic disease. An alternative approach may involve targeting of c-Src in the FAK-bound state; this possibility is explored experimentally in Chapter 3.

1.5 HYPOTHESIS AND SPECIFIC AIMS

The SFKs are thought to have redundant roles, yet evidence is accumulating for distinct primary functions by specific family members. Many studies have laid the foundation for what we know about kinase regulation, yet specifics about the differences between family members have yet to be determined. A role for the SFKs in cancer is well established, yet the current state of targeted therapies is limited to global SFK inhibition. In light of the differences in the functions of even the most closely related family members, I have attempted in this study to gain more insight into the diversity in the regulation of the individual members of the Src kinase family, and to exploit these differences for targeted inhibitor discovery.

Hypothesis

The SrcB subfamily of SFKs is more susceptible to activation by SH3:linker displacement alone, while SrcA subfamily members rely on additional displacement of the SH2:tail interaction for maximal activation.

Specific Aim 1

Determine whether linker displacement from the SH3 domain is sufficient to induce Src-family kinase activation.

Specific Aim 2

Develop a screening assay for conformation-specific inhibitors of c-Src using high affinity natural ligands to induce distinct kinase conformations.

2.0 DIVERSITY IN REGULATION OF SRC-FAMILY KINASES BY THEIR SH3 DOMAINS

2.1 INTRODUCTION

The Src family of non-receptor protein-tyrosine kinases is the largest tyrosine kinase family in the human kinome, with multiple members expressed in virtually every cell type. Three Src-family kinases (SFKs), c-Src, Fyn, and c-Yes, are found in most cell types while the remaining members have more restricted expression patterns, primarily in hematopoietic cell lineages (*151*). SFKs regulate multiple cellular processes, including proliferation, survival, differentiation, adhesion and migration (*4*). Strict control of SFK activity is essential to normal cellular and tissue homeostasis, while deregulation of SFK activity contributes to malignant transformation. Increased c-Src expression and activity are both observed in many forms of cancer and contribute to tumor cell proliferation, migration, and invasiveness (*71*).

All SFKs share a high degree of amino acid sequence homology and identical domain organization. The N-terminus of each family member encodes a signal sequence for myristoylation, a lipid modification critical to membrane localization. The myristoylation site is followed by a relatively short unique domain, which is the only non-homologous region across the kinase family. Most SFKs are also palmitoylated within this region, which contributes to membrane targeting (*152*). Following the unique region is an SH3 domain, which binds proline-

rich sequences that adopt a polyproline type-II (PPII) helical structure, an SH2 domain, which binds phosphotyrosine-containing sequences, an SH2-kinase linker, a bilobed kinase domain, and a C-terminal negative regulatory tail. All SFKs contain two conserved tyrosine phosphorylation sites important for regulation of kinase activity, which serve opposing roles (*153*). Phosphorylation of Y416 (all residue numbering as per the structure of c-Src; PDB code 2SRC) in the activation loop locks the kinase domain in the active conformation. Conversely, phosphorylation of Y527 in the C-terminal tail is required for downregulation of kinase activity. This site is phosphorylated by the separate regulatory kinases Csk and Chk (*154*).

Biochemical and structural studies have provided detailed insight regarding the mechanisms that keep SFKs in the inactive state. Both c-Src and the hematopoietic family member Hck have been crystallized in their inactive conformations (*6, 31, 32, 155*), revealing two intramolecular interactions essential for downregulation of kinase activity (Figure 1). One interaction involves pY527 in the C-terminal tail and the SH2 domain, while the other includes the SH3 domain and the PPII helix formed by the SH2-kinase linker. When both interactions are present, the SH3 and SH2 domains pack against the back of the kinase domain to stabilize the inactive conformation. In the inactive state, helix αC in the N-lobe is rotated away from the active site, preventing a conserved glutamate residue (E310 in c-Src) from forming a salt bridge with K295, a conserved interaction critical to the activity of c-Src and virtually all other kinases (*6, 155*). As a consequence, the activation loop adopts a helical structure with the autophosphorylation site (Y416) pointed inward.

Sequence homology and shared domain organization suggest that the structural basis of kinase downregulation is conserved across all Src-family members. However, distinct mechanisms of kinase activation have been reported for individual SFKs, including displacement

of the SH3 domain from the SH2-kinase linker (*41*), displacement of the C-terminal tail from the SH2 domain (*156*), displacement of both of these intramolecular interactions (*66*), and trans-phosphorylation of the activation loop tyrosine by another kinase (*153*). Further evidence suggests that these activation mechanisms may be unique to individual family members. For example, Hck is activated by the HIV-1 virulence factor Nef, which binds to the Hck SH3 domain. SH3 domain engagement by Nef displaces the Hck linker, leading to kinase activation without displacement of the tail from the SH2 domain (*157, 158*). In contrast, both the SH3:linker and SH2:tail interactions are disrupted when c-Src is activated by focal adhesion kinase (FAK), which contains tandem high-affinity binding sequences for the c-Src SH3 and SH2 domains (*66*).

Other evidence suggests that individual SFKs serve unique and non-redundant roles within the same cell type, despite their close structural homology. Recent work in murine embryonic stem (ES) cells provides a dramatic example of this phenomenon. Although c-Src and its closest phylogenetic relative, c-Yes, are both expressed in this cell type, c-Src activity drives ES cell differentiation while c-Yes suppresses differentiation and drives self-renewal (*159-161*). Along similar lines, RNAi-mediated knock-down of c-Yes expression in colon cancer cell lines increased apoptosis and reduced cell migration and tumor growth, while c-Src knock-down yielded a much less dramatic effect on the same phenotypes, suggestive of a dominant role for c-Yes vs. c-Src in colon cancer (*162*). These differences in individual functions raise fundamental questions about what mechanisms selectively regulate specific family members, especially in cellular contexts where multiple SFKs are co-expressed.

Biological evidence for diversity in SFK signaling prompted us to investigate whether individual family members are controlled by regulatory domain displacement and

autophosphorylation in an equivalent manner. For this study, we focused on four Src family members, c-Src, Lyn, Fyn and Hck, because they are broadly representative of the overall Src family from a phylogenetic point of view. First, we used a synthetic SH3-binding peptide with equal affinity for each of the recombinant purified kinases as an activating ligand. We found that all four representative SFKs are susceptible to activation by SH3 domain displacement, but the sensitivity to activation by this mechanism varied widely. In addition, we observed a major difference in sensitivity to activation of c-Src vs. Hck by SH3 domain displacement following autophosphorylation of the activation loop. Overall, these observations suggest that the mode of activation (activation loop phosphorylation vs. regulatory domain displacement) may reflect the evolution of individual SFKs to accommodate specific signaling environments.

2.2 MATERIALS AND METHODS

2.2.1 Cloning, expression, and purification of recombinant SH3 domains.

The coding sequences for the isolated SH3 domains of human c-Src, Fyn, Hck, and Lyn (corresponding to residues 81-142 of c-Src, numbering according to PDB ID: 2SRC) were amplified by PCR and subcloned into the bacterial expression vector pET21a (EMD Millipore) using NdeI and XhoI restriction sites. The C-terminus of each construct was modified by the addition of the sequence LPHHHHHH as encoded by the XhoI site and the His6 tag in the vector. E. coli strain Rosetta 2(DE3)pLysS (EMD Millipore) was transformed with each plasmid and cultures were grown at 37 °C until the OD600 reached 0.8-1.0. Protein expression was induced with 0.4 mM isopropyl β-D-thiogalactopyranoside (IPTG) for 4 h at 25 °C. For

purification, cell pellets were resuspended in ion-exchange start buffer (20 mM Tris-HCl, pH 8.5, 5 mM β-mercaptoethanol, 10% glycerol), sonicated, and clarified by centrifugation. Soluble SH3 domain proteins were purified from the clarified lysates by anion-exchange (HiPrep Q FF; GE Healthcare), immobilized metal ion affinity (HiTrap Chelating HP; GE Healthcare), and size-exclusion chromatography (HiLoad 26/60 Superdex 75; GE Healthcare). Purified SH3 domain proteins were buffer-exchanged with HBS-EP (10 mM HEPES, pH 7.4, 150 mM NaCl, 3 mM EDTA, 0.05% v/v P20 surfactant) using Amicon Ultra-15 Centrifugal Filter Units with Ultracel-10 Membranes (EMD Millipore) for storage and surface plasmon resonance experiments.

2.2.2 Expression and purification of recombinant SFK-YEEI proteins.

Human Hck, Lyn, Fyn and c-Src clones were modified on their C-terminal tails to encode the sequence Tyr-Glu-Glu-Ile-Pro (YEEI variants), to enable autophosphorylation of the tail and high-yield purification in the down-regulated state without co-expression of Csk (*163*). In addition, the N-terminal unique domain of each kinase was replaced with a hexahistidine tag, and each construct was used to produce a recombinant baculovirus in Sf9 insect cells using BaculoGold DNA and the manufacturer's protocol (BD Pharmingen) as previously described (*96*). Src-YEEI was co-expressed with the Yersinia pestis YopH phosphatase to promote dephosphorylation of the activation loop tyrosine to help downregulate kinase activity (*164, 165*). In this case, Sf9 cells were grown in a monolayer and infected with high-titer Src-YEEI and YopH baculoviruses. Cells were harvested 72 h after infection for Src-YEEI purification. All four kinases were purified as previously described (*96*). Purified proteins were stored in 20 mM Tris-HCl, pH 8.3, containing 100 mM NaCl.

2.2.3 Surface Plasmon Resonance (SPR).

SFK-YEEI proteins were buffer-exchanged with HBS-EP using Amicon Ultra-15 Centrifugal Filter Units with Ultracel-10 Membranes (EMD Millipore). SPR experiments were performed using a Biacore 3000 Instrument (GE Healthcare) on a streptavidin (SA) biosensor chip. The high-affinity Src SH3-binding peptide VSLARRPLPPLP (*166*) was synthesized and biotinylated by the University of Pittsburgh Peptide Synthesis Core. The peptide was solubilized in HBS-EP buffer to a concentration of 5 nM, injected onto the SA surface at 10 μl/min and immobilized to a level of 80 Response Units (RU). A biotinylated IκB kinase substrate peptide, RHDSGLDSMKD (Enzo Life Sciences), was immobilized to 80 RU on the reference flow cells as a control for nonspecific binding of analytes to the peptide SA surface. Each SFK SH3 domain and corresponding SFK-YEEI protein was injected in duplicate over a range of concentrations at 25 °C at a flow rate of 30 μl/min. Association was measured for 180 s, followed by 300 s of dissociation in HBS-EP running buffer. The chip surface was regenerated with HBS-EP buffer after each SH3 domain run or with 0.05% SDS in water after each SFK-YEEI protein run. In addition to reference flow cell subtraction, HBS-EP buffer-only cycles were used to allow double referencing for all analyses. Binding curves were fit using a 1:1 Langmuir binding model and the BIAevaluation software v. 4.1.1 (GE Healthcare) which was used to generate all kinetic data.

2.2.4 ADP Quest kinetic kinase assay.

Kinetic kinase assays were performed using the ADP Quest Assay (DiscoveRx), which fluorimetrically monitors the production of ADP (*167*). Briefly, the conversion of ATP to ADP is

coupled to the production of pyruvate from phosphoenolpyruvate (PEP) by pyruvate kinase (PK). Pyruvate is converted to hydrogen peroxide by pyruvate oxidase, which in turn oxidizes Amplex Red to the fluorescent product, resorufin. Accumulation of ADP is measured as the increase in resorufin fluorescence at excitation and emission wavelengths of 530 nm and 590 nm, respectively. All assays were performed in quadruplicate in black 384-well microplates (Corning Catalog # 3571). ATP stocks (10 mM; Sigma) were prepared in 10 mM Tris-HCl, pH 7.0. The SFK substrate peptide (5 mM; sequence YIYGSFK; Anaspec) (*168*) was prepared in ADP Quest assay buffer (15 mM HEPES, pH 7.4, 20 mM NaCl, 1 mM EGTA, 0.02% Tween-20, 10 mM MgCl2, 0.1 mg/ml bovine γ-globulins). Kinase reactions were initiated by the addition of 5 μl ATP to each well at 10 times the final concentration. The reactions were performed in a final assay volume of 50 μl/well at 25°C. Assay plates were read at 5 min intervals for 3 h on a Molecular Devices SpectraMax M5 microplate reader.

2.2.5 Substrate and ATP Km determination in the ADP Quest assay.

To measure the Km for the YIYGSFK substrate peptide, the ATP concentration was held constant at 200 μM, the maximum tolerated concentration in the assay. ATP is regenerated in the assay and is therefore not depleted as a function of substrate phosphorylation. Kinase concentrations were held constant at 150 ng/well for Src-YEEI, Fyn-YEEI, and Hck-YEEI, and 250 ng/well for Lyn-YEEI. The substrate peptide was titrated into the assay at various concentrations ranging from 1.95 to 500 μM. To measure the Km for ATP, the peptide substrate concentration was set to the K_m for each SFK, and kinase concentrations were held constant as

stated above. ATP was titrated into the assay over a concentration range of 6.25 to 200 μM. The resulting rate data were fit as described below.

2.2.6 ADP Quest Data Analysis.

Each ADP Quest assay included controls for non-enzymatic production of ADP and kinase autophosphorylation. Raw fluorescence data obtained from quadruplicate wells for each condition were averaged and corrected for the non-enzymatic rate of ADP production and SFK autophosphorylation. Corrected raw fluorescence units (RFU) were then plotted against time, in minutes, to determine the rate of each reaction. Linear regression analysis (GraphPad Prism) was performed on the linear portion of each corrected progress curve, and the slope yielded the reaction rate. Reaction rates were converted to pmol ADP produced/min using the correction factor 4.2 RU/pmol ADP, which was generated from a standard curve under identical reaction conditions. For ATP and substrate Km experiments, plots of the reaction rates at each substrate or ATP concentration obeyed Michaelis-Menten kinetics and were best-fit by nonlinear regression analysis (GraphPad Prism). K_m values were determined using the equation,

$$v = V_{max}[S]/(K_m+[S]) \qquad \text{(Eq. 1)}$$

where v = the measured velocity, V_{max} = the maximal reaction velocity, [S] = the substrate (peptide or ATP) concentration, and K_m = the concentration of substrate or ATP at which the reaction velocity is half of the maximal velocity.

2.2.7 SFK activation by the SH3 binding peptide in the ADP Quest Assay.

To test each SFK for sensitivity to activation by VSL12, ATP and substrate concentrations were set to their respective Km values for each SFK. Kinase concentrations were held constant for Src-YEEI (25 ng/well), Fyn-YEEI (30 ng/well), Hck-YEEI (80 ng/well), and Lyn-YEEI (120 ng/well), so as to yield a basal reaction rate of about 1 pmol ADP produced/min in each case. The VSL12 peptide was solubilized in ADP Quest assay buffer to 10 mM. The VSL12 peptide was titrated into the assay from 0.1 to 300 μM. VSL12 peptide and kinase were pre-incubated for 15 min at 25 °C before the addition of substrate, assay reagents, and ATP.

To test Src-YEEI and Hck-YEEI for sensitivity to activation by VSL12 after autophosphorylation, each kinase was pre-incubated in 550 μl of ADP Quest assay buffer with or without ATP at the K_m for each kinase for 3 h at 25 °C. Following pre-incubation, responsiveness to VSL12 activation was assayed as described above.

Kinase reaction rates at each VSL12 peptide concentration obeyed Michaelis-Menten kinetics and were best-fit by nonlinear regression. The V_{max} of each kinase reaction in the presence of VSL12 was determined using Equation 1. To calculate the activation constant (K_{act}), the basal rate (rate in the absence of VSL12) was subtracted from the rate in the presence of VSL12 at each concentration. The transformed rates were plotted against VSL12 concentration. The resulting curves also obeyed Michaelis-Menten kinetics and were best-fit by nonlinear regression as per the method of Boerner, et al., 1996 (*169*). K_{act} was calculated from

$$v_a = V_{act}[L]/(K_{act}+[L]) \qquad \text{(Eq. 2)}$$

where v_a = the measured velocity in the presence of VSL12 minus the velocity in the absence of VSL12, V_{act} = the maximal reaction velocity in the presence of VSL12 minus the velocity in the

absence of VSL12, [L] = the VSL12 concentration, and K_{act} = the concentration of VSL12 at which the reaction velocity is half of the V_{act}.

2.2.8 Pepsin digestion and peptide analysis.

For the elucidation of kinase autophosphorylation sites, 50 pmol of Src-YEEI and Hck-YEEI were digested online with pepsin in potassium phosphate buffer (150 mM KH2PO4/150 mM K2HPO4, pH 2.5). The resulting peptides were separated using a Waters nanoAcquity UPLC system (Waters Corp, Milford, MA), trapped and desalted for 3 min at 100 μL/min and then separated in 8 min by an 8%–40% acetonitrile:water gradient at 40 μL/min. The separation column was a 1.0 × 100.0 mm Acquity UPLC C18 BEH (Waters) containing 1.7 μm particles. Mass spectra were obtained with a Waters Xevo-QTOF equipped with standard ESI source (Waters Corp., Milford, MA, USA). Mass spectra were acquired over an m/z range of 100 to 1900. Mass accuracy was ensured by calibration with 100 fmol/μL Glu-fibrinopeptide, and was less than 10 ppm throughout all experiments. Identification of the peptic fragments was accomplished through a combination of exact mass analysis and MSE using custom IdentityE PLGS 2.5 Software from the Waters Corporation (*170*). MSE was performed by a series of low-high collision energies ramping from 5-30 V, therefore ensuring proper fragmentation of all the peptic peptides eluting from the LC system.

2.3 RESULTS

2.3.1 Structural basis of high affinity VSL12 peptide binding to SFK SH3 domains.

To test c-Src, Fyn, Hck, and Lyn for their susceptibility to activation by SH3 domain displacement, we first identified a peptide ligand with similar affinity for each of their SH3 domains. VSL12, a 12-mer peptide with the sequence VSLARRPLPPLP, was originally discovered in a phage-display screen for sequences that bind to the c-Src SH3 domain in the low micromolar range (*166*). Subsequent structural studies showed that VSL12 binds to the Src SH3 domain through a polyproline type II helix found in the C-terminal end of the peptide, with the adjacent arginine making contact with an aspartate in the RT-loop of the c-Src SH3 domain (*22*). These observations suggest that VSL12 may bind SFK SH3 domains with similar potency, thereby representing a useful ligand to probe the role of the SH3 domain in kinase regulation across the Src family.

The amino acid sequence of VSL12 is aligned with the SH2-kinase linker of c-Src in Figure 13A, and structural models of the c-Src SH3 domain bound to VSL12 vs. its own SH2-kinase linker are presented in Figure 13B. Comparison of these structures reveals that VSL12 forms a much more extensive interface with the SH3 domain compared to the natural linker. Proline residues at VSL12 positions 12 and 9, together with adjacent leucine residues (L11 and L8), occupy grooves formed by conserved SH3 domain residues Y90, Y92, W118, and Y136 (see Figure 5 for SH3 domain alignment).

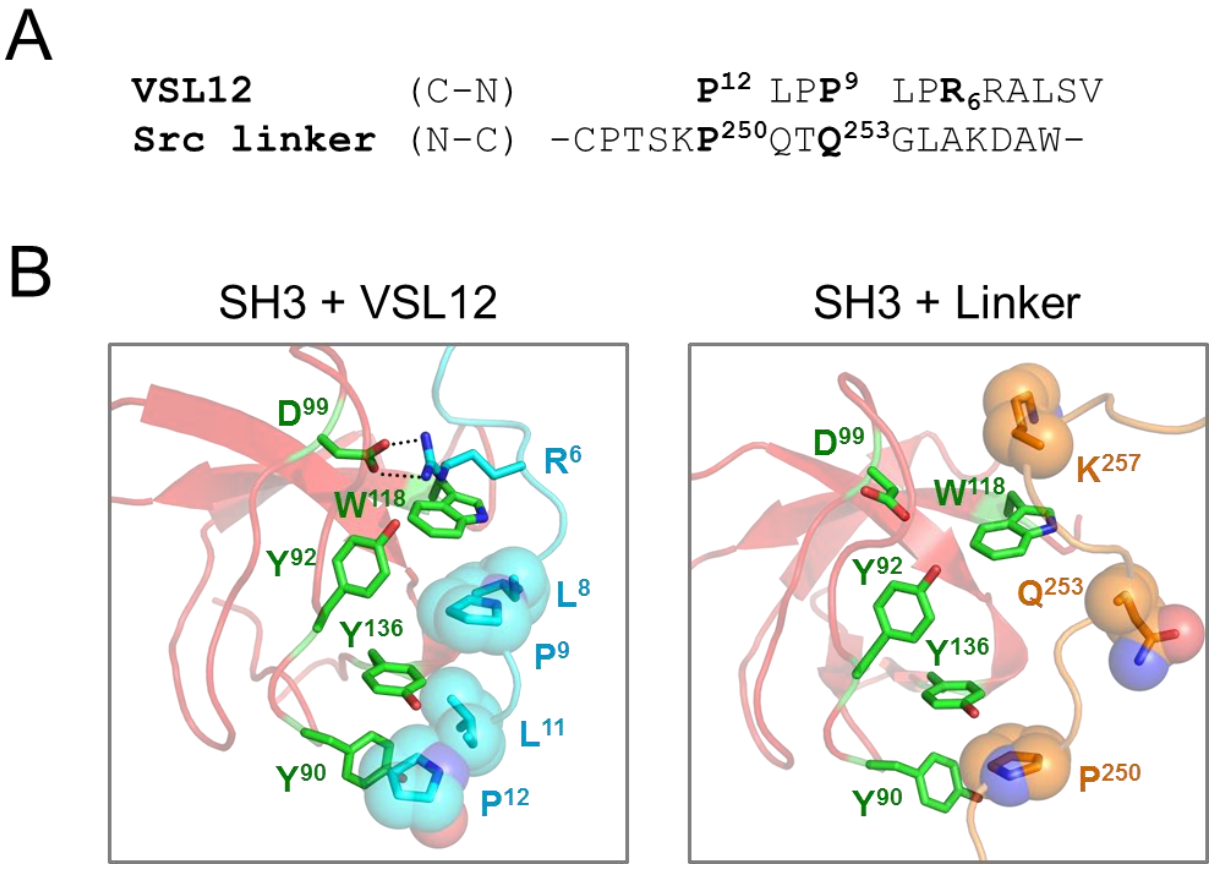

Figure 13. Interaction of the VSL12 peptide with the SH3 domain of c-Src

A) Comparison of the sequence of the SH3-binding peptide VSL12 (top) with that of the c-Src SH2-kinase linker (bottom). Note that prolines occupy the critical P0 and P+3 positions of the PPII helix in VSL12, which intercalate into the aromatic binding grooves of the SH3 surface. The Src linker, by contrast, has a single proline at P0 and glutamine at P+3. Note that the VSL12 sequence is presented in the C- to N-terminal orientation relative to the linker. B) Comparison of the c-Src interaction with the VSL12 peptide and the SH3-kinase linker. The NMR solution structure of the Src SH3 domain (red) with the VSL12 peptide (cyan) is modeled on the left (PDB: 1QWF) (*22*). The side chains of the SH3 domain residues that interact with VSL12 are shown in green (Y90, Y92, Y136 and W118), and interacting VSL12 side chains are shown in cyan (P12, L11, P9, and L8). The salt bridge between VSL12 R6 and SH3 D99 is also shown. The analogous interaction of the Src SH3 domain with the SH2-kinase linker from the inactive structure of c-Src is shown on the right (PDB: 2SRC) (*6*). Linker residue P250 contributes to this interaction in the P0 position, while Q253 occupies the P+3 position and is rotated away from the SH3 surface. The position of K257 is also shown; it does not contact D99 in this structure.

In addition, VSL12 has an arginine residue in position 6, which forms a salt bridge with D99 in the Src SH3 domain; aspartate is found at this position all SFK SH3 domains as well (Figure 5). By comparison, the c-Src SH2-kinase linker forms fewer contacts with the SH3 domain in the context of the overall downregulated structure of c-Src. While the linker does form a PPII helix, only one proline is present in the sequence (P250) and packs between SH3 Y90 and Y136 in a similar position as P12 in the SH3:VSL12 peptide structure (P0 position; Figure 13B). However, Q253 occupies the P+3 position, normally occupied by proline in high-affinity SH3 ligands (P9 in VSL12). The long polar side chain of Q253 is too bulky to fit in the pocket formed by SH3 Y92, W118, and Y136, and points away from the SH3 domain. While a basic residue (K257) is present near the C-terminal end of the linker SH3-binding sequence, it does not form a salt bridge with the conserved aspartate (D99) in the SH3 domain. These observations suggest that the linker sequence represents a suboptimal SH3 ligand, and that VSL12 may be able to compete with the linker for SH3 binding.

2.3.2 The VSL12 peptide binds SFK SH3 domains with similar affinity and competes with the linker for near-full-length kinase binding.

We first measured the affinity of the isolated SFK SH3 domains for the VSL12 peptide using surface plasmon resonance (SPR). For these experiments, VSL12 was immobilized on a biosensor chip, and the recombinant SH3 domains were flowed past the peptide as described under Materials and Methods. Surface densities were kept low to ensure that binding conformed to a 1:1 Langmuir interaction. Sensorgrams for the interaction of the SFK SH3 domain to the VSL12 peptide-coated surface are shown in Figure 14.

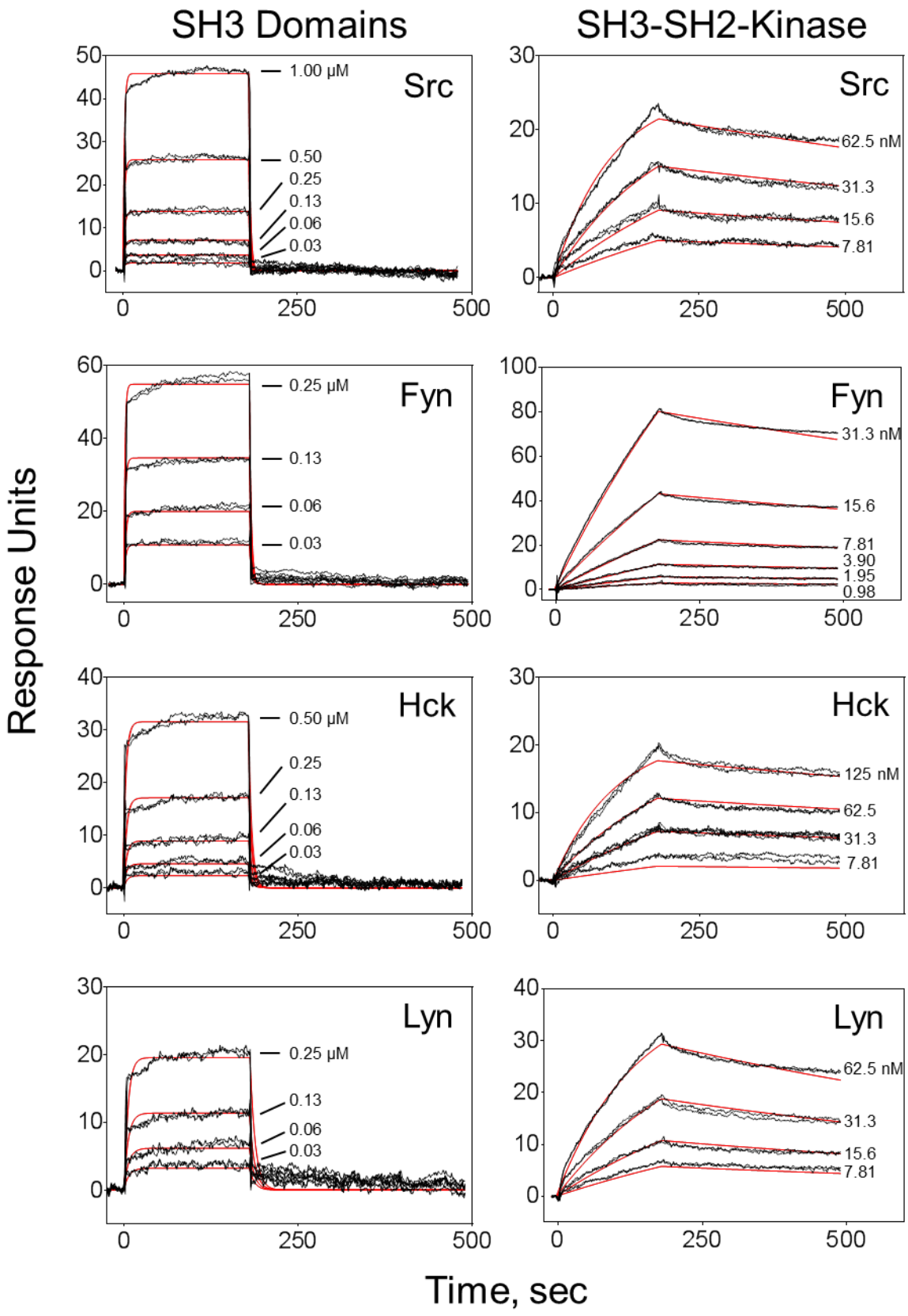
SH3 Domains
SH3-SH2-Kinase
Src
1.00 μM
0.50
0.25
0.13
0.06
0.03
62.5 nM
31.3
15.6
7.81
Fyn
0.25 μM
0.13
0.06
0.03
31.3 nM
15.6
7.81
3.90
1.95
0.98
Hck
0.50 μM
0.25
0.13
0.06
0.03
125 nM
62.5
31.3
7.81
Lyn
0.25 μM
0.13
0.06
0.03
62.5 nM
31.3
15.6
7.81
Response Units
Time, sec

Figure 14. VSL12 binds to SH3 domains and near-full length SFK-YEEI proteins by SPR

Surface plasmon resonance (SPR) was used to evaluate VSL12 peptide binding kinetics and affinity for the isolated SFK SH3 domains (left) as well as near-full-length SFK-YEEI proteins (right). The biotinylated peptide was immobilized to 80 Response Units (RU) on the surface of a streptavidin (SA) biosensor chip. The recombinant purified SH3 and SFK-YEEI proteins were flowed over the peptide over the concentration ranges shown. Association was measured for 180 s, followed by a 300 s dissociation phase. Each panel shows a representative sensorgram, with the double-referenced binding data (black trace) fit to a 1:1 Langmuir binding model (red trace). Kinetic constants derived from this experiment are presented in Table 3. The VSL12 peptide binds with similar affinities to near-full-length Src-family kinases and their isolated SH3 domains.

All four SH3 domains bound to VSL12 in a concentration-dependent manner with rapid on-rates, and showed complete dissociation from the peptide following washout. Table 3 summarizes the resulting association (k_a) and dissociation (k_d) constants as well as the equilibrium dissociation constants derived from them (K_D). All four SH3 domains bound to VSL12 with low micromolar affinities, consistent with previously published values for the c-Src and Hck SH3 domains (*166, 171*).

We next explored the binding of recombinant, purified near-full-length Src-family kinase proteins to VSL12 using the same approach (Figure 14). For these studies, we used purified recombinant SFK proteins in which the natural C-terminal tails were replaced with the sequence pTyr-Glu-Glu-Ile-Pro (referred to hereafter as SFK-YEEI proteins). This tail modification creates an optimal SH2-binding sequence and has been used in previous structural and enzymatic studies to ensure downregulation of kinase activity through enhanced binding of the tail to the SH2 domain in the absence of Csk co-expression (*32*, *96*). Surprisingly, each of the near-full-length SFKs bound to VSL12 with low nanomolar affinity. Comparison of the k_a values for the

SFKs with those for the isolated SH3 domains shows nearly identical association constants for the two sets of proteins (Table 3).

Table 3. Kinetic Constants for SH3 Domains and Near-Full-Length SFKs for the VSL12 Peptide Measured by Surface Plasmon Resonance

Protein	k_a ($M^{-1}s^{-1}$)	k_d (s^{-1})	K_D (M)	χ^2
Src SH3[a]	1.21×10^5	4.14×10^{-1}	3.42×10^{-6}	0.570
Fyn SH3[b]	1.06×10^6	3.72×10^{-1}	3.51×10^{-7}	1.890
Hck SH3[c]	7.88×10^4	2.17×10^{-1}	2.76×10^{-6}	1.360
Lyn SH3[b]	2.12×10^5	1.37×10^{-1}	6.47×10^{-7}	1.850
Src-YEEI[d]	1.57×10^5	6.33×10^{-4}	4.03×10^{-9}	0.374
Fyn-YEEI[e]	5.39×10^4	$5.53 \times 10\text{-}^4$	1.03×10^{-8}	0.765
Hck-YEEI[f]	7.13×10^4	4.54×10^{-4}	6.36×10^{-9}	0.667
Lyn-YEEI[d]	1.05×10^5	8.71×10^{-4}	8.28×10^{-9}	0.567
Hck-YEEI[c,g]	1.12×10^4	5.49×10^{-4}	4.90×10^{-8}	0.126

[a] 31.25, 62.5, 125, 250, 500, 1000 nM
[b] 31.25, 62.5, 125, 250 nM
[c] 31.25, 62.5, 125, 250, 500 nM
[d] 7.81, 15.62, 31.25, 62.5 nM
[e] 0.98, 1.95, 3.9, 7.81, 15.62, 31.25 nM
[f] 7.81, 31.25, 62.5, 125 nM
[g] This analysis was performed with a lower amount of VSL12 peptide immobilized on the SA chip surface to rule out re-binding artifacts (25 RU rather than 80 RU).

SPR analysis was performed with biotinylated VSL12 peptide bound to a streptavidin biosensor chip as described under Materials and Methods. Each protein was flowed past the chip surface over the concentration ranges indicated in the footnotes. Duplicate runs were performed for each concentration. A control cycle of buffer only was subtracted from all concentrations of reference-subtracted curves. Interaction data were curve-fit using a 1:1 binding model, and the kinetic constants and chi-square values were calculated using BIAevaluation software (v. 4.1.1).

However, the k_d values for the SFK proteins are roughly 1000-fold lower than for the SH3 domains, suggesting that VSL12 binding induces a stabile kinase-peptide complex. To exclude the possibility that this lower dissociation rate constant results from rebinding events during the dissociation phase, an additional SPR experiment was conducted using the minimum surface level of VSL12 peptide required for kinetic analysis (25 response units) to determine the K_D for Hck-YEEI. The resulting k_a, k_d, and K_D values were similar to those generated on the higher surface level of VSL12 (Table 3). These SPR results show that the VSL12 peptide binds with similar kinetics to each Src-family member, and is a suitable ligand to test for SH3-based activation of each kinase by SH3 domain displacement.

2.3.3 Characterization of recombinant SFK-YEEI protein kinase activity in vitro.

In order to characterize the sensitivity of individual SFKs to SH3-based activation, we initiated kinetic kinase assays with each of the recombinant SFK-YEEI proteins in the presence of the SH3-binding peptide, VSL12. As described in the preceding section, the YEEI tail modification allows for purification of each Src-family member in the downregulated state. In addition, the increased affinity of the tyrosine-phosphorylated YEEI tail for the SH2 domain ensured that kinase activation observed in response to VSL12 binding can be attributed to the displacement of the SH3 domain rather than complete disruption of the regulatory apparatus.

Prior to testing for SH3-based kinase activation using the VSL12 peptide, uniform assay conditions were established for each SFK. We first determined the K_m values for both ATP and the peptide substrate, YIYGSFK, for all four of the SFK-YEEI proteins using a kinetic assay. As shown in Figure 15, all of the SFKs obey Michaelis-Menten kinetics for both ATP and the peptide substrate. Table 4 summarizes the K_m values determined for each kinase.

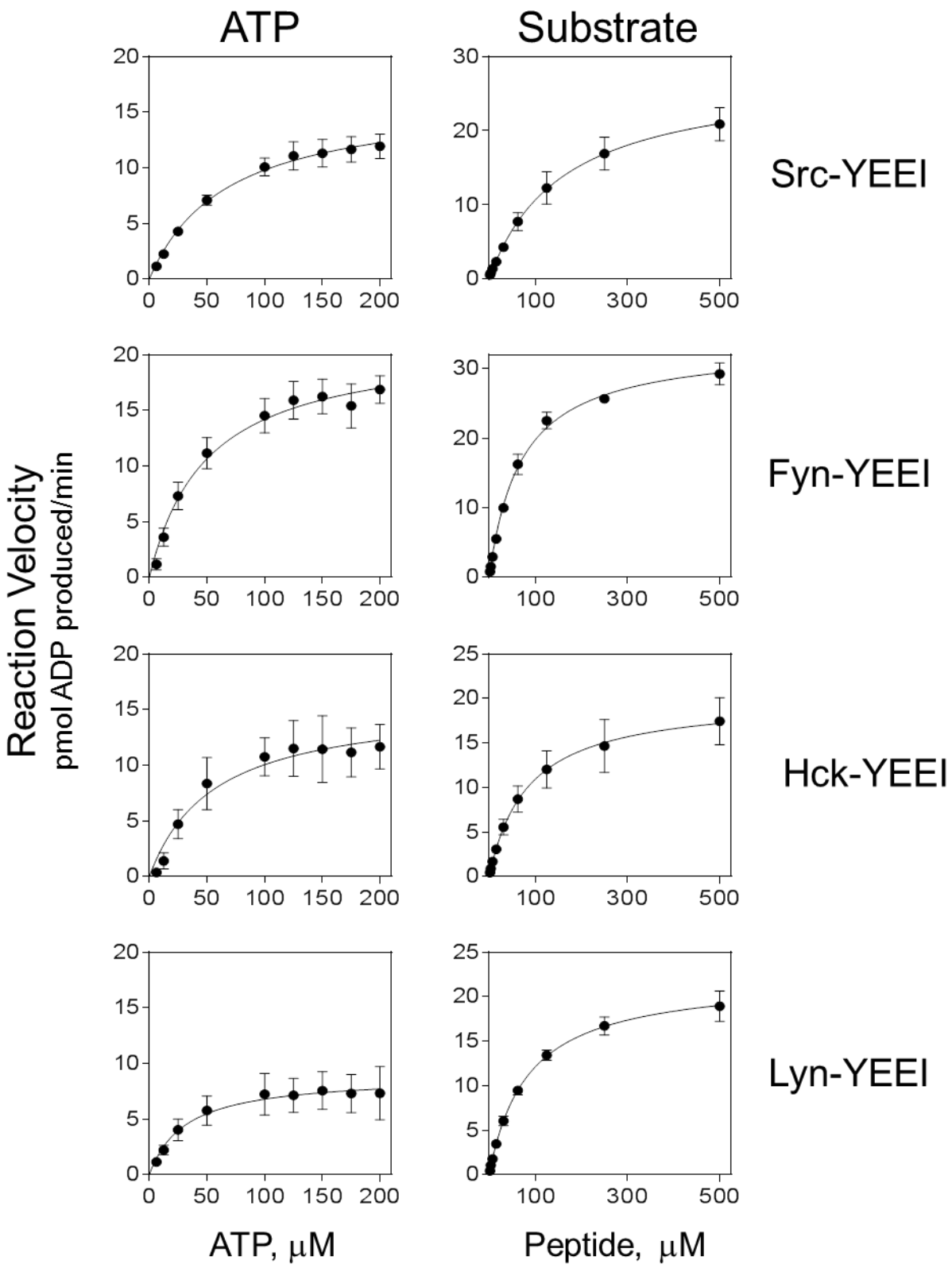
ATP
Substrate
Src-YEEI
Fyn-YEEI
Hck-YEEI
Lyn-YEEI
Reaction Velocity
pmol ADP produced/min
ATP, μM
Peptide, μM

Figure 15. Recombinant near-full-length Src-family kinases obey Michaelis-Menten kinetics.

Initial reaction velocities for each of the SFK-YEEI proteins shown were determined over a range of ATP and peptide substrate (sequence YIYGSFK) concentrations as described under Materials and Methods. Plots of reaction velocity vs. the concentration of ATP (*left panels*) and substrate (*right panels*) exhibited saturation kinetics and were fit to the Michaelis-Menten equation by non-linear regression analysis (GraphPad Prism Software). The resulting K_m and V_{max} values are presented in Table 4.

Table 4. K_m Values for ATP and Peptide Substrate for Near-Full-Length SFKs

Kinase	ATP (μM)	YIYGSFK (μM)
Src-YEEI	67.0 ± 10.3	159.1 ± 20.9
Fyn-YEEI	49.7 ± 8.2	69.6 ± 3.7
Hck-YEEI	55.8 ± 18.5	83.8 ± 12.5
Lyn-YEEI	31.1 ± 9.70	83.2 ± 4.9

The K_m values for ATP and the substrate peptide, YIYGSFK, were determined for each SFK-YEEI protein using the ADP Quest assay as described under Materials and Methods. ATP experiments were performed three times for each kinase and substrate experiments were performed four times for each kinase, except for Src-YEEI, where ATP experiments were performed twice and substrate experiments were performed three times. Mean values are shown for each kinetic constant ± S.E.

All four Src-family members showed very similar K_m values for ATP, ranging from 31 to 67 μM. These values are in the same range as those reported previously for these kinases, despite the use of different assay methods (29-31). K_m values for the substrate peptide also varied by about two-fold, with Src-YEEI exhibiting the highest value (159 μM) and Fyn-YEEI the lowest (70 μM). To control for inherent variations in substrate utilization by each Src-family member, all subsequent experiments were done with the ATP and peptide substrate concentrations set to

the respective K_m values for each kinase. Finally, kinase titrations were performed to determine enzyme concentrations that yielded a basal rate of about 1 pmol ADP produced/min. Figure 16 shows the production of ADP over time for a range of six Src-YEEI concentrations.

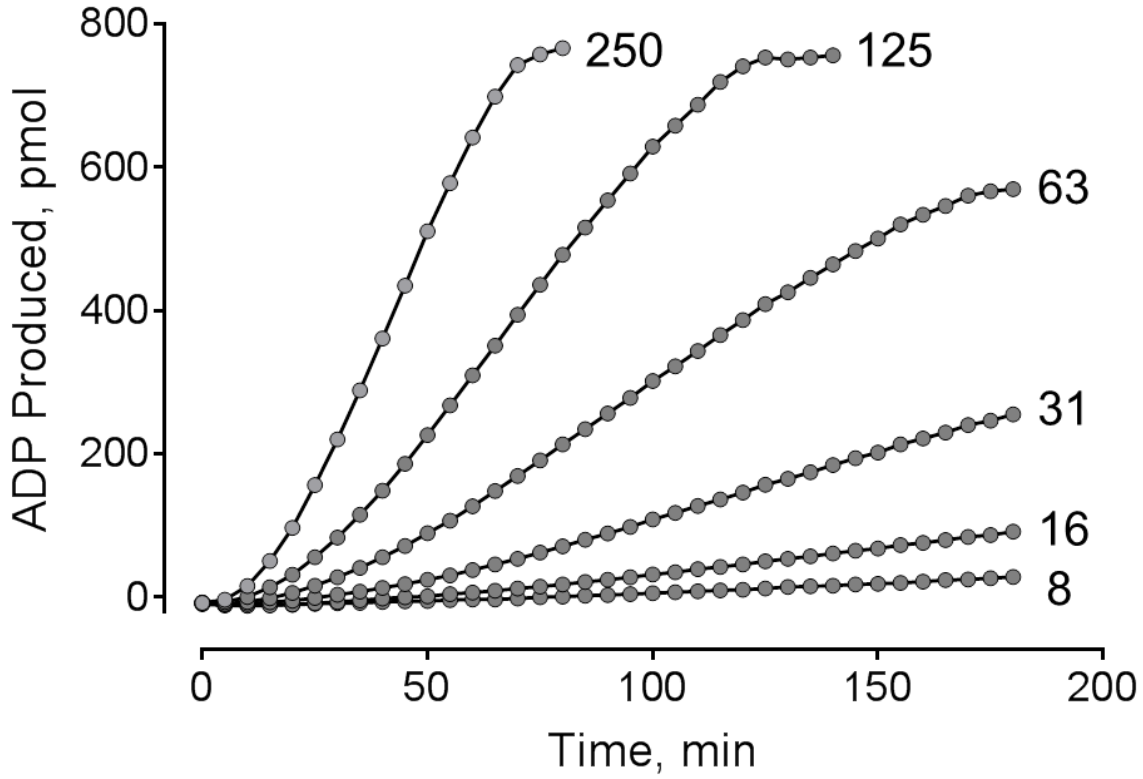

Figure 16. Time course of ADP production for a concentration range of Src-YEEI

Representative time course of ADP production for six concentrations of Src-YEEI. At higher kinase concentrations, the reaction rates plateau as the fluorescence reading reaches saturation. The linear portion of each curve was fit by linear regression analysis to provide the slope, which corresponds to the rate of the reaction in pmol ADP produced/min.

The reaction rate increases as a function of kinase concentration, as reflected in the increase in the slope of the linear portion of the curve for each kinase concentration. Reaction

rates were determined in the same way for the remaining SFK-YEEI proteins, and the results are shown in Figure 17.

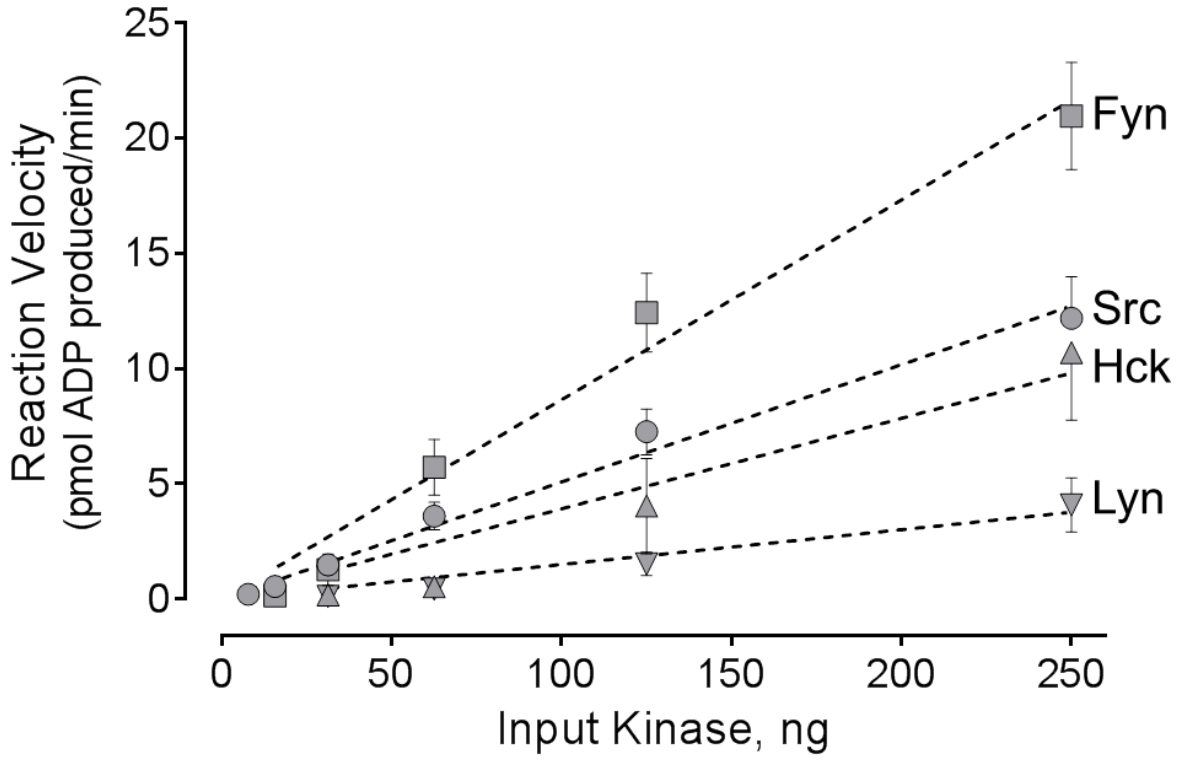

Figure 17. Linear relationship between SFK-YEEI activity and input kinase

Reaction rates for each SFK-YEEI protein are plotted against input kinase concentration. Curves were best-fit by linear regression analysis (dotted lines) and used to estimate the basal reaction rate for each kinase.

All four kinases showed a linear relationship between input kinase amount and reaction velocity over the range of kinase concentrations tested. Because the specific kinase activity differs for each family member, these experiments allowed us to identify input kinase amounts that yielded equivalent basal rates for subsequent SH3 domain-displacement experiments with VSL12.

2.3.4 Differential sensitivity of Src-family members to activation by VSL12 peptide binding.

We next tested the susceptibility of each Src-family member to SH3-based activation using the VSL12 peptide as an SH3 domain 'agonist'. Using the established conditions for substrate, ATP, and kinase concentration as described above, the VSL12 peptide was titrated into the assay over a concentration range of 0.1 to 300 μM. Figure 18A shows the reaction velocity for each kinase as a function of VSL12 peptide concentration. These data show that all four Src-family members are susceptible to activation by the VSL12 peptide, providing strong evidence that SH3:linker interaction has an important role in kinase regulation across the entire Src family.

Data presented in Figure 18A demonstrate that the extent of kinase activation is saturable at higher concentrations of the VSL12 peptide. These data were therefore fit to Equation 1 to determine the V_{max} for each kinase reaction as a measure of the highest level of SH3-dependent activation attainable for each kinase. Figure 18B compares the basal reaction rate to the V_{max} for each kinase in the presence of VSL12. This analysis revealed that Src-family kinases have remarkably different responses to SH3-based kinase activation. Lyn-YEEI showed the smallest response, with a V_{max} of about 5 pmol ADP produced/min, while Hck-YEEI showed a much higher response, approaching 30 pmol ADP produced/min. Fyn-YEEI and Src-YEEI exhibited intermediate responses with values of 11 and 16 pmol ADP produced/min, respectively. These results support the idea that individual Src-family members have very different inherent enzymatic capacities, at least in response to SH3 domain-based activation.

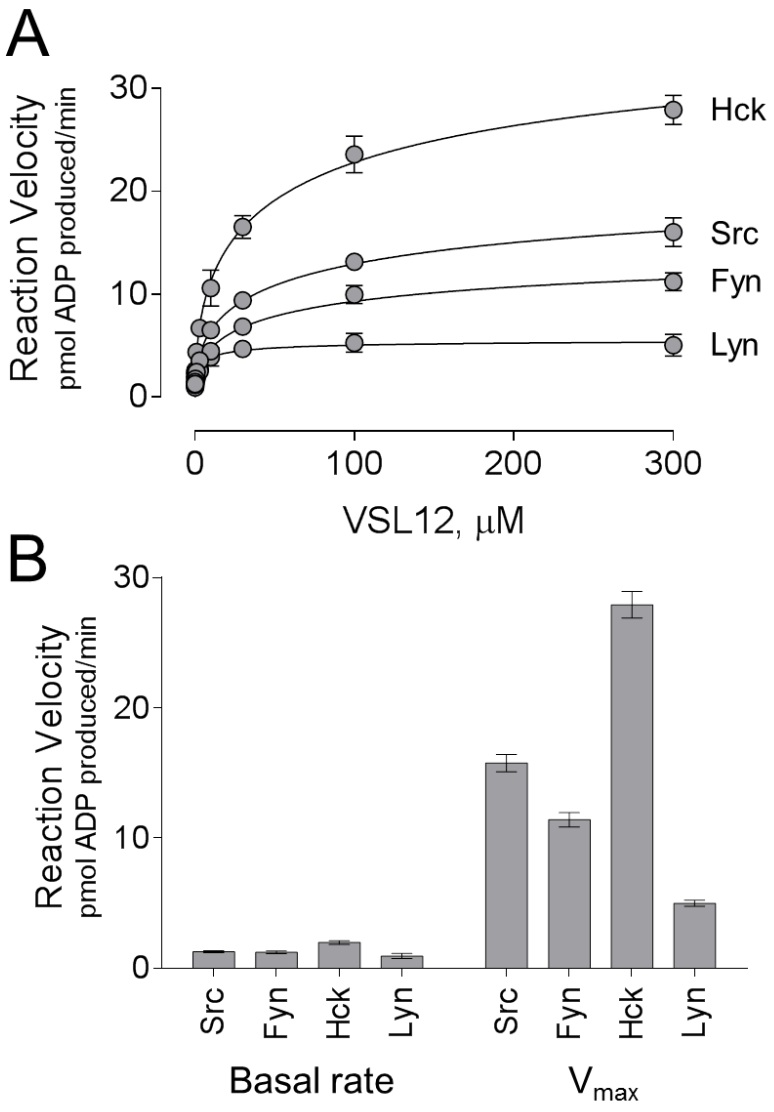

Figure 18. Differential sensitivity of individual SFK-YEEI proteins to activation by SH3 domain displacement

Each of the SFK-YEEI proteins shown was assayed in the presence of VSL12 over a range of concentrations (0.1 to 300 μM). ATP and substrate concentrations were set to the K_m for each kinase, and input kinase concentrations were set to achieve a basal reaction velocity of 1 pmol ADP produced/min. A) Each of the kinases is activated by VSL12 in a concentration-dependent manner. Plots of reaction velocity vs. VSL12 concentration were best-fit by the Michaelis-Menten equation, allowing for the determination of the V_{max}. Each data point was assayed in triplicate and is shown as the mean ± S.E. B) Comparison of basal rate (left) and V_{max} (right) for each kinase in the presence of VSL12. Bars heights correspond to the mean values from triplicate experiments ± S.E.

In addition to defining the extent to which each kinase can be activated by VSL12 (V_{max}), we also calculated an activation constant (K_{act}) for each kinase in response to this SH3-binding peptide. K_{act} defines the concentration of VSL12 required to increase the reaction rate to one-half of the V_{max}, and is calculated by subtracting the basal kinase activity (without VSL12) from the reaction rate observed at each VSL12 concentration and performing nonlinear regression analysis using Equation 2 (see Materials and Methods). As shown in Table 5, the K_{act} values for VSL12-based activation of Src-YEEI, Fyn-YEEI, and Hck-YEEI were all remarkably similar (22-25 μM). In contrast, Lyn-YEEI displayed a lower K_{act} compared to the other kinases (4 μM), which may suggest higher sensitivity to activation by SH3 domain displacement, although the maximum response observed was the lowest among the four kinases tested. Interestingly, Lyn and Hck are the most closely related among the SFKs tested in terms of phylogeny, yet their sensitivity to VSL12-induced activation is the most diverse.

Table 5. Basal Rate, Maximal Velocity, and Activation Constants for VSL12 with each SFK

Kinase	Basal reaction velocity (pmol ADP produced/min)	V_{max} (pmol ADP produced/min)	K_{act} (μM)
Src-YEEI	1.27 ± 0.08	15.77 ± 0.67	22.42 ± 2.23
Fyn-YEEI	1.22 ± 0.10	11.41 ± 0.55	24.95 ± 1.91
Hck-YEEI	1.97 ± 0.14	27.94 ± 1.02	22.38 ± 2.18
Lyn-YEEI	0.93 ± 0.20	5.00 ± 0.24	4.03 ± 0.61

The basal reaction velocity, maximum velocity (V_{max}), and activation constant (K_{act}) were determined for each kinase in the ADP Quest assay as described under Materials and Methods. Basal velocity is the rate of kinase activation in the absence of the VSL12 peptide. Kinetic constants were determined in triplicate and are presented as the mean ± S.E.

2.3.5 Hck and c-Src remain susceptible to activation by SH3 domain displacement after autophosphorylation.

In addition to regulatory domain engagement, SFK activity is also regulated by the phosphorylation state of the kinase domain activation loop (Figure 1). However, whether or not activation loop phosphorylation results in maximal kinase activation or whether the autophosphorylated kinase is still susceptible to further activation by SH3 domain displacement is not known. To explore this question, we focused on c-Src and Hck, because these are the only two family members for which the crystal structures of their downregulated states are known. Before examining the impact of VSL12 binding on SFK activity as a function of autophosphorylation, we first confirmed that the activation loops of recombinant Hck-YEEI and Src-YEEI were not phosphorylated prior to addition to the assay. To do this, the recombinant purified kinases were digested with pepsin and the phosphorylation states of the activation loop and tail tyrosines were determined by mass spectrometry. As shown in Figure 19, the C-terminal tail tyrosines are phosphorylated in both Src-YEEI and Hck-YEEI as expected for the inactive conformations, while no activation loop tyrosine phosphorylation was detected in either case.

A

Src-YEEI Tail YFTSTESQpY^{527}EEIP

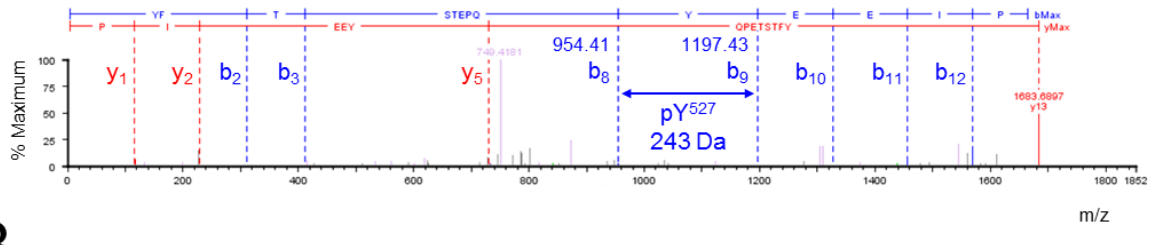

B

Src-YEEI Loop Y^{416}TARQGAKF

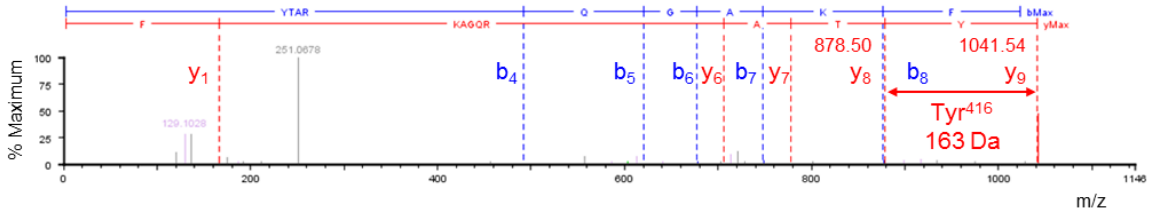

C

Hck-YEEI Tail ESQpY^{527}EEIP

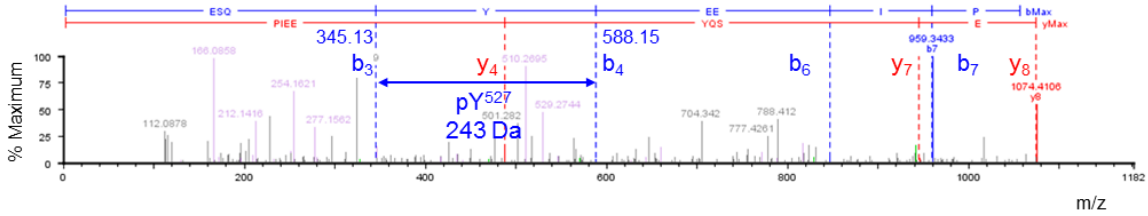

D

Hck-YEEI Loop Y^{416}TAREGAKF

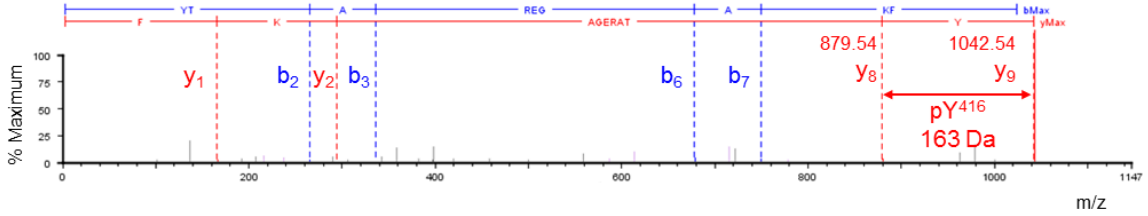

Figure 19. Mass spectrometric analysis of Src-YEEI and Hck-YEEI tail and activation loop tyrosine phosphorylation.

A) ESI-MS/MS spectra of Src-YEEI peptic peptide YFTSTESQpY^{527}EEIP ($[M+H]^+$ = 1683.68 Da), which is derived from the C-terminal tail, indicates that Tyr527 is phosphorylated (numbering as per crystal structure of c-Src; PDB ID: 2SRC). The mass difference between fragment ions b_8 and b_9 (blue) indicates the presence of a phosphate group attached to the tyrosine residue (243 Da). The y ions are colored in red. B) ESI-MS/MS spectra of Src-YEEI peptic peptide Y^{416}TARQGAKF ($[M+H]^+$ = 1041.54 Da), which maps to the activation loop in the kinase domain, indicates that Tyr416 is not phosphorylated (163 Da). The mass difference between fragment ions y_8 and y_9 (red) corresponds to the unphosphorylated tyrosine. C) ESI-MS/MS spectra of Hck-YEEI peptic peptide ESQpY^{527}EEIP ($[M+H]^+$ = 1074.40 Da), derived from the C-terminal tail, indicates that Tyr527 is phosphorylated. The mass difference between fragment ions b_3 and b_4 (blue) indicates the presence of a phosphate group attached to the tyrosine residue. D) ESI-MS/MS spectra of the Hck-YEEI peptic peptide Y^{416}TAREGAKF ($[M+H]^+$ = 1042.54 Da), derived from the activation loop, indicates that Tyr416 is not phosphorylated. The mass difference between fragment ions y_8 and y_9 (red) corresponds to the unphosphorylated tyrosine.

To test whether Src-YEEI and Hck-YEEI can be activated further by SH3 domain displacement after activation loop autophosphorylation, both kinases were preincubated in the presence or absence of ATP prior to testing for sensitivity to activation by VSL12. Time-course experiments in a kinetic kinase assay revealed that kinase autophosphorylation reached a plateau after three hours of incubation with ATP (data not shown), so preincubation was conducted for this time period prior to assessment of the VSL12-induced response. In both cases, the basal rate of kinase activity (no VSL12) was dramatically increased after pre-incubation with ATP. For Src-YEEI, the basal rate increased from 1.74 pmol ADP produced/min in the absence of ATP to 6.38 in the presence of ATP following the preincubation step. Similarly, the basal rate of Hck-YEEI activation increased from 1.27 to 9.04 pmol ADP produced/min following preincubation with ATP. This increase is presumably due to autophosphorylation of the activation loop tyrosine

and stabilization of the active site conformation. Note that the basal rate of each kinase following preincubation in the absence of ATP is consistent with the basal rates shown in Figure 18B and Table 5, indicating that the preincubation step did not compromise basal kinase activity.

Figure 20 shows the effect of SH3 domain displacement by VSL12 on Src-YEEI and Hck-YEEI activity as a function of autophosphorylation. In each case, the basal rate observed in the absence of VSL12 was subtracted from the rate at each peptide concentration to reveal additional activation resulting from VSL12 binding to the SH3 domain.

Autophosphorylated Src-YEEI and Hck-YEEI were both activated by VSL12 in a concentration-dependent manner, demonstrating that phosphorylation of the activation loop does not uncouple the kinase domain from the regulatory influence of the SH3 domain. However, we observed remarkable differences in the responses of Src-YEEI vs. Hck-YEEI to VSL12 following pre-incubation with ATP. The curves for Hck-YEEI activation by VSL12 were identical, whether the kinase was preincubated with ATP or not. This observation suggests that activation of Hck-YEEI by SH3 domain displacement is independent of activation loop phosphorylation. Conversely, preincubation of Src-YEEI with ATP enhanced the response to VSL12, indicating that autophosphorylation of Src-YEEI sensitizes the kinase domain to further activation by SH3 domain displacement. These differences suggest that c-Src and Hck may have evolved to respond to different types of cellular inputs for activation and have important implications for signaling.

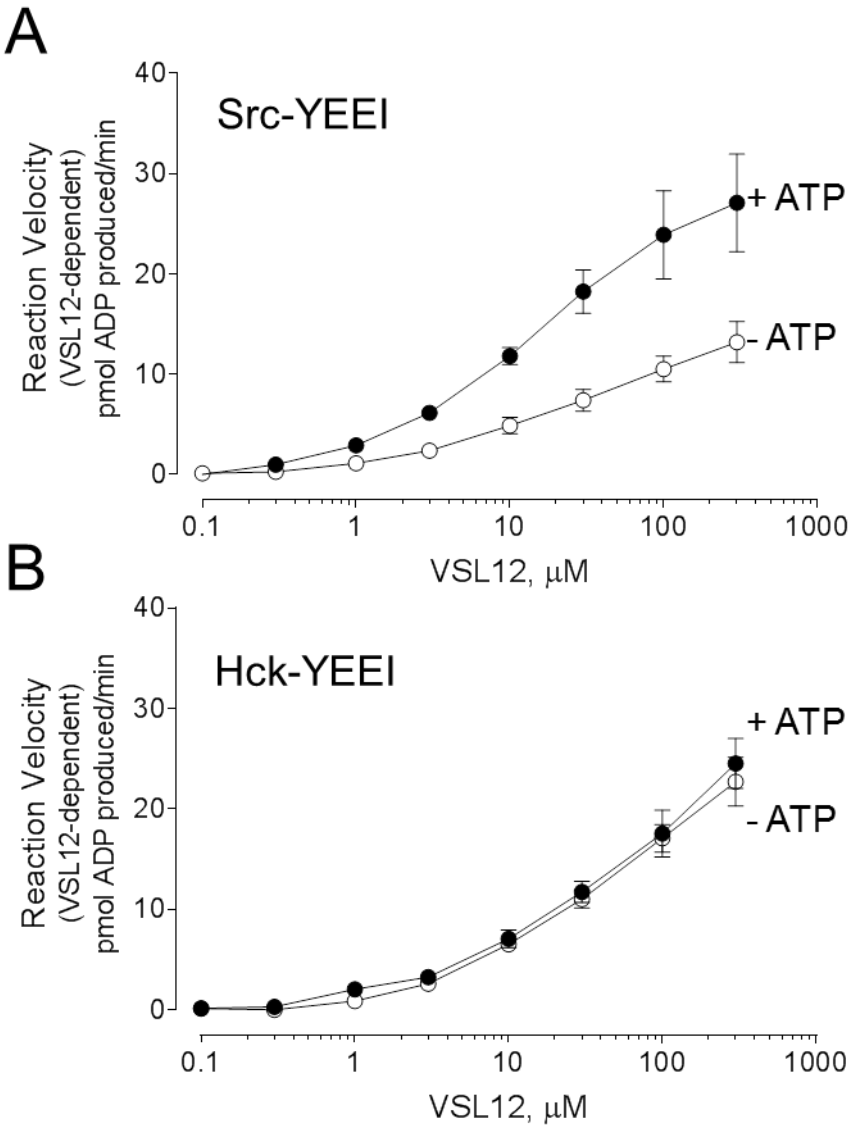

Figure 20. Src-YEEI and Hck-YEEI retain sensitivity to activation by SH3 domain displacement after autophosphorylation.

Src-YEEI (A) and Hck-YEEI (B) were incubated in the absence or presence of ATP (at the K_m) for 3 hours at 25 °C to induce autophosphorylation of Tyr416 in the activation loop. The autophosphorylated kinases were then assayed for responsiveness to the SH3-binding peptide, VSL12. The basal reaction velocity (no VSL12) was subtracted from the rate at each VSL12 concentration, and the resulting linear reaction velocities were plotted as a function of VSL12 concentration as shown. Each data point was assayed in triplicate and the average value is plotted ± S.E.

2.4 DISCUSSION

The mechanisms responsible for SFK downregulation have been established by extensive biochemical and structural studies and appear to be conserved among all family members. The precise mechanisms of kinase activation, and whether or not they are also conserved across this kinase family, are less clear. Displacement of intramolecular regulatory interactions involving the SH2 and/or SH3 domains can cause kinase activation, suggesting that individual family members may be finely tuned to respond to inputs through their regulatory domains in specific ways. In this study, we provide direct evidence in support of this idea. Using a peptide ligand (VSL12) to induce kinase activation by SH3 domain displacement, we showed a wide range of sensitivities to this allosteric activation mechanism across the Src kinase family. Furthermore, we observed that c-Src becomes more susceptible to activation by SH3 domain displacement after autophosphorylation of the activation loop tyrosine. In contrast, activation of Hck through its SH3 domain was independent of kinase domain autophosphorylation, revealing a very different response to this activating input despite the remarkable similarity to c-Src in terms of the structure of the inactive state (*6, 31, 32, 155*).

We chose the VSL12 peptide as the SH3 ligand for these studies because previous work showed that it binds to the c-Src, Fyn, and Lyn SH3 domains with similar micromolar affinities (*19, 166*). SPR results presented here show that VSL12 bound to the SH3 domains of these three SFKs as well as that of Hck with low micromolar dissociation constants, providing a useful peptide ligand to compare the effect of SH3 domain displacement on kinase activity across the kinase family. The solution structure of the Src SH3 domain in complex with VSL12 reveals the key SH3 residues that interact with the peptide that suggest a mechanism for linker displacement (*22*). The hydrophobic pocket formed by SH3 Y90 and Y136 is occupied by the lone proline

residue in the Src SH2-kinase linker (P250; Figure 13B). This interaction is likely displaced by VSL12 L11 and P12 which occupy the same pocket in the NMR structure. In addition, VSL12 L8 and P9 both make contacts with the SH3 domain, while the analogous positions are occupied by T252 and Q253 in the linker; Q253 does not contact the SH3 domain in the inactive c-Src structure (Figure 13B). Furthermore, VSL12 R6 forms a stabilizing ionic contact with conserved SH3 D99, and also makes a hydrogen bond with the side chain of W118. This interaction is missing in the SH3:linker interface in downregulated c-Src. The SH3 domain residues involved in VSL12 binding are conserved across the four SFKs studied here, consistent with the similarities in binding kinetics and affinities observed by SPR (Table 3).

In addition to the isolated SH3 domains, we also determined the interaction of VSL12 with the corresponding downregulated, near-full-length SFK proteins by SPR for the first time. In this case, we anticipated a lower apparent affinity of VSL12 for the SH3 domain in the context of the near-full-length kinase, because of competition with the linker. Such a phenomenon has been reported previously for the interaction of HIV-1 Nef with Hck, which exhibits a higher affinity for the isolated SH3 domain vs. the near-full length kinase (*98, 157*). Instead, we observed much higher affinity of VSL12 for all four near-full-length kinases, with equilibrium dissociation constants in the low nanomolar range. While the kinetic association constants for the individual SH3 domains and SFK-YEEI proteins were similar, the dissociation constants for the SFK-YEEI protein were roughly 1000-fold lower. These observations suggest that the SH3:VSL12 complex may be stabilized in the near-full-length kinase through additional interactions, possibly with the N-lobe of the kinase domain or with the displaced linker itself. Identification of residues that stabilize the VSL12 interaction with the near-full-length kinase may guide the future development of Src-family kinase agonists.

Work presented here supports the idea that Src-family kinases are generally susceptible to activation by SH3 domain displacement. In addition, VSL12-based activation of recombinant SFK proteins with YEEI tails shows that disruption of SH2:tail interaction is not required for SH3-based activation, as the pYEEI sequence has a much higher affinity for the SH2 domain than the natural tail sequence (*32, 172*). While the VSL12 peptide bound to and activated all of the kinases, differences in the extent of activation were striking. Particularly surprising was the difference in sensitivity to SH3-based activation between Hck and Lyn, as they are the most similar in amino acid sequence among the entire Src kinase family. Our observation that Hck and Lyn demonstrate very different responses to SH3-based activation by VSL12 is consistent with previous reports with the Nef protein of HIV-1. Like VSL12, Nef binds to the SH3 domains of Hck and Lyn with similar affinity, yet Nef activates Hck more strongly both in vitro and in cell-based assays (*90, 173*). One possibility is that maximal activation of Lyn may also require displacement of the C-terminal tail from the SH2 domain, which does not appear to be the case for Hck.

To understand how interaction with VSL12 induces kinase activation, the structures of Src-family kinases in the active vs. inactive conformations must be considered. In the downregulated structure of c-Src, the SH3 domain contacts both the SH2-kinase linker (as described above) and R318 in the N-lobe of the kinase domain through D117. Additionally, a key residue that has been shown to couple the SH3-SH2 region of the protein to the kinase domain is W260 at the C-terminal end of the linker (*163*). In the inactive conformation, conserved W260 packs against helix αC, helping to position it away from the active site and preventing formation of a salt bridge between E310 and K295 that is required for kinase activity. Because VSL12 has a relatively high affinity for the SH3 domains of the SFKs, it is likely to

bind to the SH3 domain, displace the linker and shift W260 away from the αC helix. The stabilizing interaction between SH3 domain D117 and N-lobe R318 may also be disrupted as a consequence. Removal of these inhibitory constraints would allow the αC helix to rotate inward, with E310 forming the critical salt bridge with K295. This rearrangement also exposes activation loop Y416 for autophosphorylation. By analogy to the active structure of the Lck kinase domain (*34*), phosphorylation of Y416 is anticipated to result in an intrastrand ionic contact with R409. This interaction stabilizes the active conformation of the conserved DFG motif at the N-terminal end of the activation loop and is essential for phosphate binding and catalysis.

Another remarkable difference between the SFKs relates to the coupling of activation loop autophosphorylation and sensitivity to SH3 domain displacement. Autophosphorylation of Y416 strongly stimulated both Hck and c-Src kinase activity in the absence of the VSL12 peptide. In addition, both kinases were further activated by VSL12 in a concentration-dependent manner, demonstrating that activation loop phosphorylation enhances kinase activity independently of regulatory domain displacement. This observation suggests that Y416 phosphorylation alone is sufficient to reorganize the active site for phosphotransfer. However, our data show that autophosphorylation alone does not maximally increase kinase activity, because addition of VSL12 enhanced both c-Src and Hck kinase activity to an even greater extent. The additional impact of this SH3 domain ligand on autophosphorylated SFKs implies that displacement of the SH3 domain relieves additional allosteric constraints on the kinase domain, possibly through W260 or direct SH3 interaction with the N-lobe as described above. Furthermore, this observation implies that autophosphorylation of the activation loop does not cause release of the SH3 domain from the linker, at least for c-Src and Hck.

Our finding that autophosphorylated c-Src and Hck are still under the allosteric control of the SH3 domain is consistent with recent studies of c-Abl kinases. Like SFKs, the c-Abl kinase 'core' consists of a similar arrangement of SH3 and SH2 domains, an SH2-kinase linker, followed by the kinase domain. In this system, intramolecular interaction of the SH3 domain with the linker is also essential for downregulation of Abl kinase activity (*174*). Interestingly, active mutants of c-Abl, as well as the constitutively active Bcr-Abl fusion protein associated with chronic myelogenous leukemia, are both sensitive to linker proline substitutions that enhance interaction with the SH3 domain (*175*). Together with our data, these observations support the idea that activation loop phosphorylation and regulatory domain displacement represent independent modes of SFK and Abl regulation.

While activation of Hck-YEEI by VSL12 binding was not enhanced by autophosphorylation, Src-YEEI was primed for further activation by VSL12 upon preincubation with ATP. This observation suggests distinct regulatory controls for each of these kinases, despite the fact that they are composed of the same component parts. These differences may have evolved to meet specific needs for kinase regulation under distinct physiological conditions. For example, c-Src is locally active in focal adhesions, where it regulates their turnover during cell adhesion and migration. One important mechanism of c-Src activation in focal contacts involves direct interaction with FAK. In this case, the SH3 and SH2 domains of c-Src interact with FAK, integrating the localization of c-Src to focal adhesions with kinase activation via regulatory domain displacement (*66*). This interaction juxtaposes the c-Src and FAK kinase domains, raising the possibility of direct phosphorylation of the c-Src activation loop by FAK (*176*). Maximal c-Src activation in focal adhesions may therefore require displacement of both regulatory domains plus trans-phosphorylation by another kinase, consistent with our findings. In

contrast, Hck is expressed primarily in cells of innate immunity and is activated by diverse upstream signals including hematopoietic cytokines and Fc receptors (*177-180*). In this case, receptor engagement with Hck through its SH3 and/or SH2 domains may be sufficient to induce a rapid and transient response, without the need for secondary phosphorylation on the activation loop. These intrinsic differences in the sensitivity of c-Src, Hck and other SFKs to activating signals may provide opportunities for discovery of selective small molecule probes of their functions.

3.0 IDENTIFICATION OF INHIBITORS SELECTIVE FOR C-SRC IN COMPLEX WITH THE FAK SH3-SH2-BINDING REGION

3.1 INTRODUCTION

The c-Src protein-tyrosine kinase is the prototype of the Src kinase family and is broadly expressed in virtually every mammalian cell type (*156*). The domain organization of c-Src is shared by all eight mammalian Src-family kinases (SFKs; Figure 21A). At the N-terminus is a signal sequence for myristoylation, which targets c-Src to the cell membrane. Membrane association facilitates interactions of c-Src with binding partners such as receptor tyrosine kinases (RTKs) and is essential for function (*7*). The myristoylation signal is followed by a unique domain, which contains the most divergent sequences among the kinase family. C-terminal to the unique region are the modular SH3 and SH2 domains, which bind to polyproline-rich and phosphotyrosine-containing sequences, respectively. The SH3 and SH2 domains are important for interactions with other cellular proteins as well as kinase regulation. These domains are followed by an SH2-kinase linker, the kinase domain, and a C-terminal tail with a conserved tyrosine residue essential for negative regulation of kinase activity.

SFKs maintain their inactive state through two intramolecular interactions involving the SH2 and SH3 domains. The SH3 domain interacts with a polyproline type II helix formed by the SH2-kinase linker while the SH2 domain binds to the tyrosine-phosphorylated tail (*153*). Tail

phosphorylation is mediated by the independent regulatory kinase Csk as well as the related kinase, Chk (*154, 181*). Both interactions are present in the x-ray crystal structure of c-Src in the downregulated conformation, shown in Figure 1 (*6*).

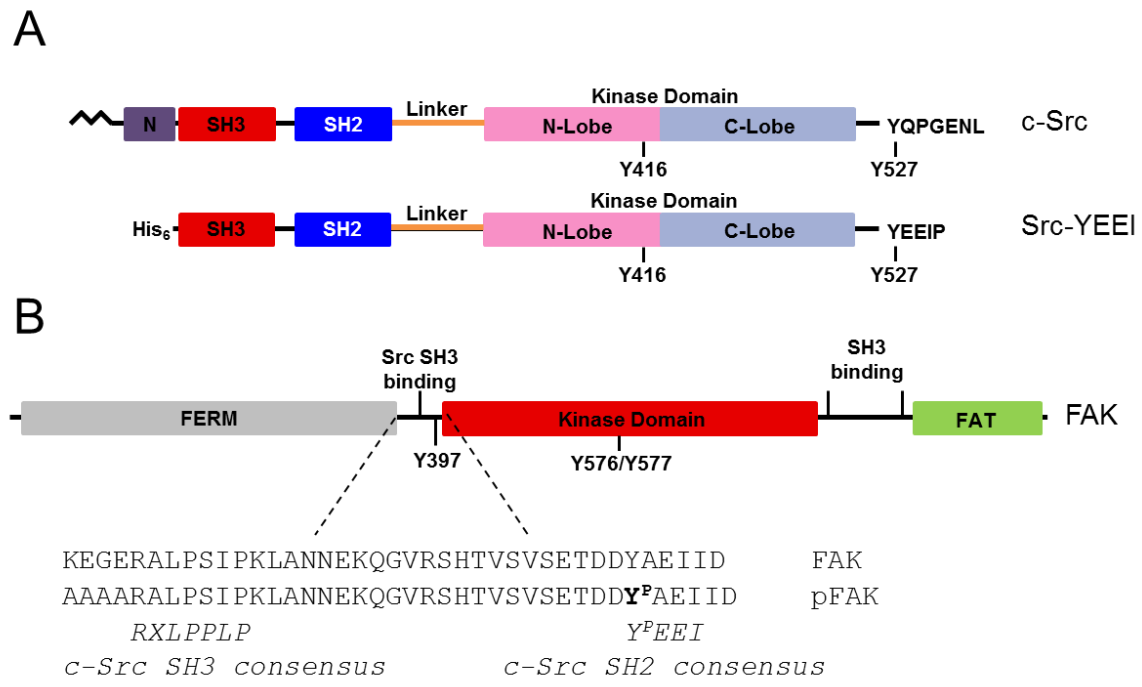

Figure 21. Domain organization of c-Src and FAK

A) The modular domain organization of c-Src is shown, which corresponds to the x-ray crystal structure of the downregulated conformation in Figure 1 (PDB ID: 2SRC). The conserved tyrosine residues in the activation loop (Y416) and the tail (pY527) are shown. Intramolecular interactions between the SH3 domain and the SH2-kinase linker as well as the SH2 domain and the tyrosine-phosphorylated tail are required to maintain the inactive state. The unique N-terminal domain and myristoylation site are not present in the crystallized protein. The domain organization of recombinant Src-YEEI used for this study is also shown, which lacks the N-terminal unique domain, and has the modified C-terminal tail sequence, YEEI. B) Modular domain organization of focal adhesion kinase (FAK) which consists of the N-terminal FERM domain (blue) the kinase domain (green), a proline-rich region containing SH3 binding sites for other focal adhesion proteins, and the C-terminal FAT domain (red). The linker connecting the FERM and kinase domains encompasses the binding site for c-Src, consisting of a PxxP motif (SH3

binding) and an autophosphorylation site in the sequence context pYAEI (SH2 binding). The sequence of the pFAK peptide used in the screening assay is also shown.

Multiple mechanisms of SFK activation have been reported, including dephosphorylation of the C-terminal tail tyrosine, leading to the loss of the SH2:tail interaction (*182*), and displacement of one or both of the intramolecular interactions as a result of binding to peptides or other proteins (*40, 171*). Based on their sequences, the SH2-kinase linker and C-terminal tail represent low affinity ligands for their respective target domains. Displacement of these interactions by proteins with higher affinity for the SH3 and/or SH2 domains provides a mechanism for SFK activation by both physiological substrates as well as foreign proteins expressed as a result of microbial infection. For example, the Nef protein encoded by HIV-1 binds to the SH3 domain of the Src-family member Hck, resulting in linker displacement and constitutive kinase activation. Alternatively, juxtamembrane autophosphorylation sites on active RTKs recruit c-Src through its SH2 domain, resulting in displacement of the tail and kinase activation. Other cellular protein partners for c-Src contain both SH3- and SH2-binding sequences to displace both intramolecular interactions, such as p130Cas (*183*) and the focal adhesion kinase (FAK) (*66*).

FAK is a non-receptor protein tyrosine kinase that localizes to focal adhesions, the intracellular structures formed at sites of cell adhesion to the extracellular matrix (ECM). The domain organization of FAK consists of a protein 4.1/ezrin/radixin/moesin (FERM) domain, followed by high affinity binding sites for the c-Src SH3 and SH2 domains (Figure 21B) and the kinase domain. C-terminal to the kinase domain is a proline-rich region with binding sites for the SH3 domains of p130Cas and other proteins involved in the focal adhesion complex, followed by the focal adhesion targeting (FAT) domain that targets FAK to focal adhesions upon integrin

stimulation (*103, 104, 184*). Once recruited to focal adhesions, FAK autophosphorylates on Y397 creating a high-affinity binding site for the c-Src SH2 domain. Additionally, the c-Src SH3 domain binds to a proline-rich sequence adjacent to the SH2 binding site. These tandem binding events displace both intramolecular regulatory interactions, leading to c-Src kinase activation. Once active, c-Src then phosphorylates FAK at multiple tyrosine residues. Two of these, pY576 and pY577, localize to the activation loop of the kinase domain and are important for full FAK kinase activity. The others recruit SH2-containing proteins like p130Cas, which binds to pY861, and Grb2, which binds pY925 (*113-115, 185*). Coordinated activation of c-Src and FAK stimulates multiple signaling pathways linked to focal adhesion turnover and cell migration, an essential process in embryonic development, wound healing, and the immune response. Tight control of both c-Src and FAK activity is therefore very important for both cellular and tissue integrity. Indeed, cells lacking c-Src and FAK show a dramatically reduced rate of migration (*51, 121*), while the hyperactivation of these kinases leads to an increased rate of migration that has been implicated in tumorigenesis.

Overexpression and increased activity of both c-Src and FAK has been reported in multiple tumor sites, including colon, head and neck, breast, and ovary (*67-69, 186-191*). Hyperactivation of the c-Src:FAK complex not only increases cell migration and invasion as a result of increased focal adhesion turnover, but also drives cell proliferation and survival (*192, 193*). The recruitment of Grb2 to pY925 leads to the activation of the Ras pathway and stimulates cell proliferation. Additionally, the p85 subunit of phosphatidylinositol-3-kinase (PI3K) can bind to the pY397 site and lead to activation of Akt, which prevents apoptosis.

The relationship of the c-Src:FAK complex to cancer progression highlights the potential for c-Src and FAK as targets for cancer therapy (*194-197*). Multiple inhibitors of both c-Src and FAK

have been discovered and some have progressed into clinical trials. However, the success of these inhibitors, especially as monotherapy, has been limited (*192, 198*). One disadvantage of SFK inhibitors is their lack of selectivity for c-Src over other members of this kinase family. Kinase domain sequence and structural homology makes isoform-selective inhibitor targeting quite challenging. In this study, we approached this problem by developing a screening assay for inhibitors of c-Src in complex with the SH3-SH2-binding region of FAK. We hypothesized that binding of FAK to c-Src induces a unique active conformation that may be amenable to selective inhibitor targeting. In an effort to find a selective c-Src:FAK complex inhibitor, we identified in vitro kinase assay conditions such that the activation of c-Src was entirely dependent on the presence of a phosphopeptide based on the FAK SH3/SH2-binding sequences for c-Src. We then screened a kinase-biased inhibitor library and identified four compounds selective for the Src:FAK peptide complex versus Src alone. The most promising compound showed a five-fold preference for the active complex in both endpoint and kinetic kinase assays. Computational docking studies suggest that this compound prefers the 'DFG-out' conformation of the kinase active site, suggesting that binding of the pFAK peptide induces this kinase domain conformation. Our results provide an important proof-of-concept that state-selective ATP site inhibitors for c-Src can be identified under appropriate screening assay conditions. This approach may provide an additional avenue for inhibitor specificity in the context of large kinase families with highly homologous active sites.

3.2 MATERIALS AND METHODS

3.2.1 Expression and purification of recombinant SFK-YEEI proteins.

A human c-Src cDNA clone was modified on its C-terminal tail to encode the sequence Tyr-Glu-Glu-Ile-Pro (YEEI) as described previously for Hck (*163*). In addition, the N-terminal unique domain of c-Src was replaced with a hexa-histidine tag. The resulting sequence was used to produce a recombinant baculovirus in Sf9 insect cells using BaculoGold DNA and the manufacturer's protocol (BD Pharmingen) as previously described (*96*). Src-YEEI was co-expressed with the Yersinia pestis YopH phosphatase to promote dephosphorylation of the activation loop tyrosine to help downregulate kinase activity (*164, 165*). Sf9 cells were grown in monolayer and co-infected with Src-YEEI and YopH baculoviruses. Cells were harvested 72 h after infection for Src-YEEI purification as previously described (*96*). Purified Src-YEEI protein was stored in 20 mM Tris-HCl, pH 8.3, containing 100 mM NaCl. Kinase protein used in the Z'Lyte in vitro kinase assays also contained 3 mM DTT. The molecular weight of purified Src-YEEI was confirmed by mass spectrometry and determined to be phosphorylated on the YEEI tail but not the activation loop, consistent with the structure of the downregulated conformation (*6*).

3.2.2 Chemical library screen.

A library of 586 kinase-biased inhibitors (*199*) was screened using the FRET-based Z'Lyte in vitro kinase assay and Tyr2 peptide substrate (Life Technologies) (*200*). Assays were performed in quadruplicate in 384-well low-volume nonbinding surface black polystyrene

microplates (Corning) according to the manufacturer's instructions and as described previously (*96, 199, 201*). Briefly, the assay measures phosphorylation of the Tyr2 FRET-peptide substrate which is labeled with coumarin and fluorescein on its N- and C-terminii, respectively, which form a FRET pair. After the kinase reaction, a development step involves site-specific proteolytic cleavage of the unphosphorylated but not the phosphorylated peptide. Peptide cleavage results in loss of a FRET signal.

Src-YEEI was first titrated into the assay over a concentration range of 0.5 – 500 ng/well (0.908 – 908 nM). Kinase activity was measured in the absence and presence of a 10-fold molar excess of the pFAK peptide with the sequence AAAARALPSIPKLANNEKQ-GVRSHTVSVETDDYPAEIID (*66*) as well as the control peptides pYEEI (EPQYPEEIPIYL) (*202*), and VSL12 (VSLARRPLPPLP) (*166*). All peptides were synthesized by the University of Pittsburgh Genomics and Proteomics Core Laboratories and the mass and purity of each compound was confirmed by LC-MS. The kinase was pre-incubated with or without the peptides for 15 min, and the reaction was initiated by the addition of ATP (100 μM) and Tyr2 peptide substrate (1 μM). The kinase reaction was incubated 1 h, followed by addition of the development protease to cleave the unphosphorylated substrate. Coumarin and fluorescein fluorescence were measured 1 h later on a Molecular Devices SpectraMax M5 plate reader. Results are expressed as percent of maximum kinase activity relative to a stoichiometrically phosphorylated positive control peptide and negative control wells where no ATP is present.

Screening assays were performed with Src-YEEI (30 ng) in the presence of a 10-fold molar excess of the pFAK peptide (545 nM pFAK to 54.5 nM Src-YEEI) or with Src-YEEI alone (125 ng; 227 nM). These conditions yielded about 75% of maximum kinase activity in the absence of compounds. Each compound was assayed at a final concentration of 10 μM with carrier solvent

(DMSO) at 2.5%. After peptide preincubation, the compound was added and incubated for 30 minutes before initiating the kinase reaction. The IC50 values for the hit compounds were determined over a concentration range of 3 nM to 30 μM, and the resulting concentration-response curves were best-fit by nonlinear regression analysis to obtain the compound IC50 (GraphPad Prism). Results are expressed as percent inhibition, calculated relative to negative control wells without ATP (maximum inhibition) and DMSO only control wells (minimum inhibition).

3.2.3 Kinetic Kinase Assays.

The ADP Quest Assay (DiscoveRx) is a fluorescence-based assay used to monitor the production of ADP in kinase reactions (*167*). All assays were performed in quadruplicate in black 384-well microplates (Corning # 3571), in a final assay volume of 50 μl/well at 25°C as previously described (Chapter 2). ATP stocks were prepared in 10 mM Tris-HCl, pH 7.0, and the ATP concentration in each assay was held constant at 100 μM. The SFK substrate peptide, YIYGSFK (Anaspec) (*168*) was prepared in ADP Quest assay buffer (15 mM HEPES, pH 7.4, 20 mM NaCl, 1 mM EGTA, 0.02% Tween-20, 10 mM MgCl2, 0.1 mg/ml bovine γ-globulins). The substrate concentration in the assay was set to the Km value (162 μM) determined previously (Chapter 2). In kinase inhibition assays, Src-YEEI concentration in the absence of peptide was 40 ng/well (14.5 nM) and in the presence of the peptide was 15.6 ng/well (5.7 nM). Kinase reactions were initiated by the addition of ATP. Assay plates were read every 5 min for 3 h on a Molecular Devices SpectraMax M5 microplate reader. Results are expressed as percent of maximum kinase activity relative to the activity of the kinase in the absence of inhibitor.

3.3 RESULTS

3.3.1 Development of a screening assay for Src:FAK selective inhibitors

In order to screen for inhibitors selective for the c-Src:FAK kinase complex, we used a synthetic peptide based on the c-Src SH3 and SH2 binding sites from the FAK sequence, pFAK, to activate recombinant Src-YEEI. Our goal was to model the specific conformation of active c-Src that results from interaction with FAK in focal adhesions. The pFAK peptide has been shown to bind to the tandem SH3-SH2 protein with low nanomolar affinity and to activate c-Src in vitro (*66*).

Before initiating the chemical library screen, we first established kinase assay conditions where recombinant Src-YEEI activity was dependent upon binding to the pFAK peptide. The Src-YEEI protein has a modified tail in which the wild-type sequence, Y527QPGENL, is replaced with YEEI to create a high affinity SH2-binding sequence. This modification allows the kinase to be purified in the downregulated state (*32, 96*). We first measured purified Src-YEEI activity over a range of kinase concentrations in the absence or presence of the pFAK peptide. As shown in Figure 22, the extent of substrate phosphorylation increased in sigmoidal fashion as a function of input kinase concentration, with an EC50 value of 151 ng in the absence of peptide. When this experiment was repeated in the presence of the pFAK peptide, the activation curve was shifted markedly to the left, yielding an EC50 value of 34 ng. This result is consistent with the interaction of the pFAK peptide with the Src-YEEI SH3 and SH2 domains, resulting in displacement of the regulatory apparatus from the back of the kinase domain and subsequent activation.

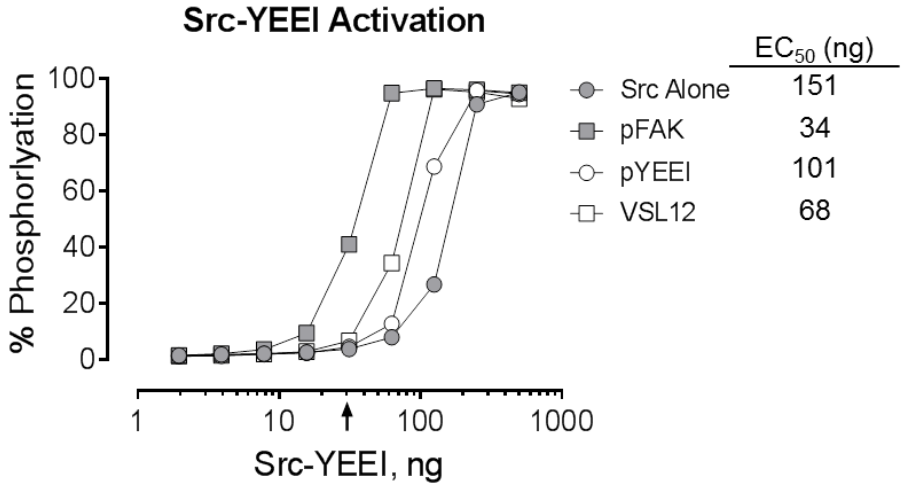

Peptide	Sequence	Target
pFAK	AAAARALPSIPKLANNEKQGVRSHTVSVSETDDY^{P}AEIID	SH3-SH2
VSL12	VSLARRPLPPLP	SH3
pYEEI	EPQY^{P}EEIPIYL	SH2

Figure 22. Activation of Src-YEEI by SH3- and SH2-binding peptides

The activity of Src-YEEI was measured in the Z'Lyte in vitro kinase assay in the absence and presence of peptides that bind to the SH3 domain alone (VSL12), the SH2 domain alone (pYEEI), or to both (pFAK). Recombiant Src-YEEI kinase protein was titrated into the assay over the range of 2-500 ng as shown, and peptides were added at a 10-fold molar excess at each kinase concentration. The concentration of kinase that yielded 50% activation for each condition is shown (EC_{50}). The arrow indicates the Src-YEEI concentration used in the screening assay, where Src-YEEI activity is dependent on the pFAK peptide (30 ng kinase input). The sequences of the peptides are shown below the graph, and the docking sites for the Src SH3 and SH2 domains are indicated.

To provide additional evidence that dual engagement of the SH3 and SH2 domains is necessary for maximal activation of Src-YEEI in our assay, we examined the effect of peptides that bind individually to the SH3 domain (VSL12) or the SH2 domain (pYEEI) on kinase activity. Both peptides activated Src-YEEI to a lesser extent than the pFAK peptide (Figure 22). The pYEEI peptide, which binds to the SH2 domain, decreased the EC50 value for Src-YEEI activation from

151 ng to 101 ng, while the VSL12 peptide, which exclusively engages the SH3 domain, decreased it to 68 ng. The finding that the VSL12 and pYEEI peptides do not activate Src-YEEI to the same extent as the pFAK peptide suggests that displacement of a single regulatory interaction is not sufficient for full kinase activation. The pFAK peptide, on the other hand, simultaneously displaces both of these interactions, presumably releasing all conformational constraints on the kinase domain.

3.3.2 Identification of inhibitors selective for Src-YEEI in complex with the pFAK peptide

For inhibitor screening, we chose a concentration of Src-YEEI that was dependent on the pFAK peptide for activity so as to model the kinase conformation induced by FAK binding. As indicated by the arrow in Figure 22, roughly 30 ng of Src-YEEI alone was inactive in the assay, while addition of the pFAK peptide resulted in 40% of maximal activation. We also identified the concentration of Src-YEEI alone that resulted in the same level of activity (125 ng/well), which provided a basis of comparison in the screen. The ATP concentration was set to 100 μM, which is in excess of published Km values for c-Src (*203-205*), and the substrate concentration was set to 1 μM. Using these assay conditions, we screened a kinase-biased small-molecule library (586 compounds) for preferential inhibitors of Src-YEEI in the presence of the pFAK peptide compared to Src-YEEI alone. Compounds were screened at a final concentration of 10 μM. The rank order of inhibitory potency for each compound is presented in Figure 23A, with the percent inhibition values shown in Table 7 (Appendix A).

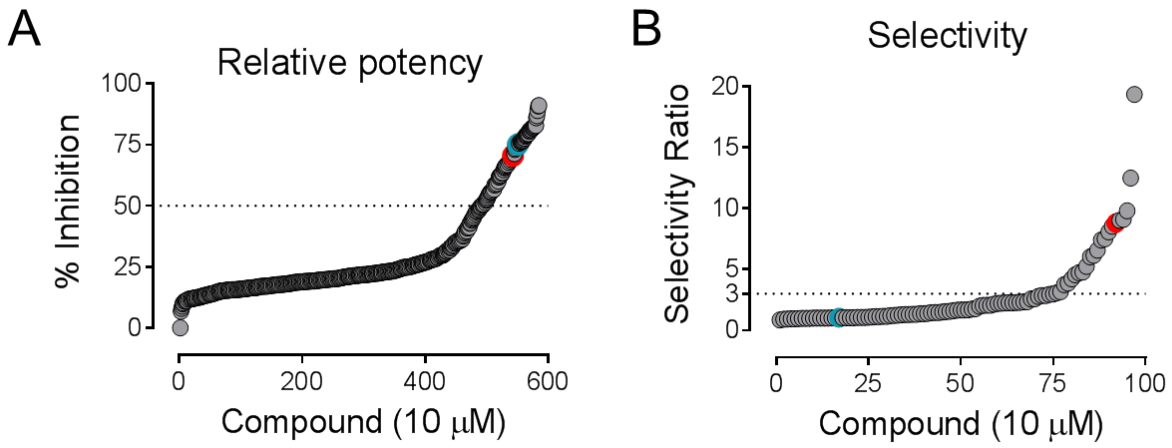

Figure 23. Pilot screen for selective inhibitors of pFAK-dependent Src-YEEI activity

A kinase-biased library of 586 compounds was screened for inhibitors of Src-YEEI activity in the presence of the pFAK peptide using the FRET-based Z'Lyte assay as described in the text. WH-4-124-2 is indicated in each graph by a red dot. WH-4-023 is indicated in each graph with a blue dot. A) Inhibitory activity for all compounds ranked by percent inhibition relative to the unphosphorylated substrate peptide control. Ninety-seven compounds inhibited kinase activity by at least 50% (dotted line). B) The Selectivity Ratio (SR) was calculated for the compounds showing greater than 50% inhibition of the Src-YEEI:pFAK complex in part A. This ratio was calculated as the percent inhibition of the Src-YEEI:pFAK complex divided by the percent inhibition observed with Src-YEEI alone. Twenty-four compounds exhibited a selectivity ratio greater than 3 (dotted line).

The ninety-seven compounds that showed at least 50% inhibition of the complex were then assessed for inhibition of Src-YEEI alone. Results from these compounds were then ranked according to their selectivity ratio (SR), defined as:

$$SR = \frac{\text{\% Inhibition of Src-YEEI:pFAK peptide complex}}{\text{\% Inhibition of Src-YEEI alone}}$$

Twenty-four compounds with an SR greater than 3 (Figure 23B) were selected for further evaluation in concentration-response experiments. Of these, four compounds reproducibly inhibited Src-YEEI in the presence of the pFAK peptide to a greater extent than Src-YEEI alone (Figure 24 and 25A). The aminopyrimidinyl carbamate designated WH4-124-2 was chosen for further evaluation because it was the most potent and selective inhibitor of Src-YEEI in the presence of the pFAK peptide (Table 7, compound 543). As shown in Figure 25A and Table 6, this compound inhibited the Src-YEEI:pFAK peptide complex with an IC50 value of 0.88 μM in the Z'Lyte assay, as compared to 4.95 μM for Src-YEEI alone.

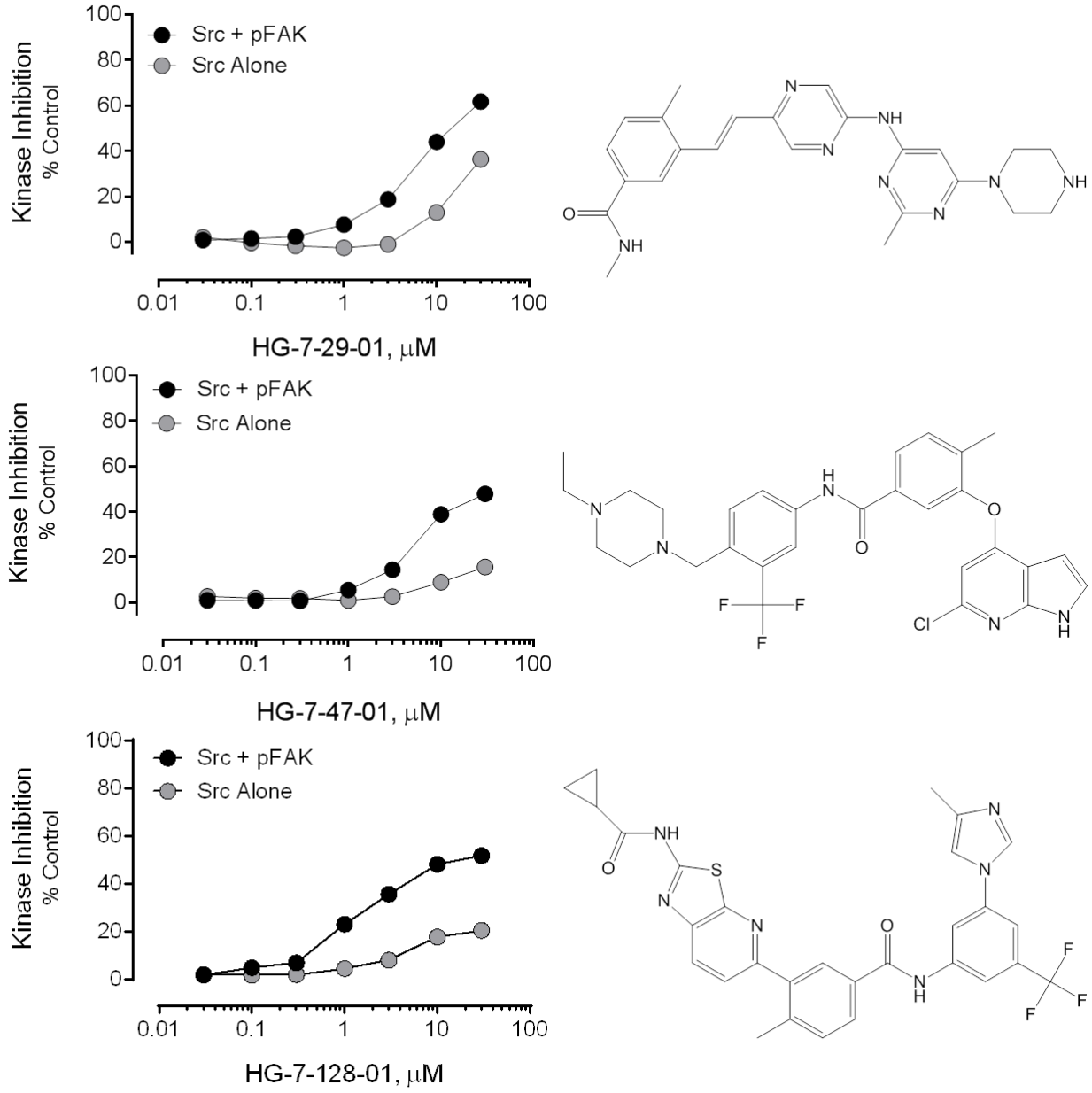

Figure 24. Inhibition of Selective inhibition of Src-YEEI by three compounds in the presence of the pFAK peptide

HG-7-29-01, HG-7-47-01, and HG-7-128-01 were assayed against Src-YEEI alone (gray circles) and the Src-YEEI:pFAK complex (black circles) over the range of inhibitor concentrations shown using the Z'Lyte assay. These inhibitors were selective for the complex in the primary screen and maintained selectivity in dose response experiments.

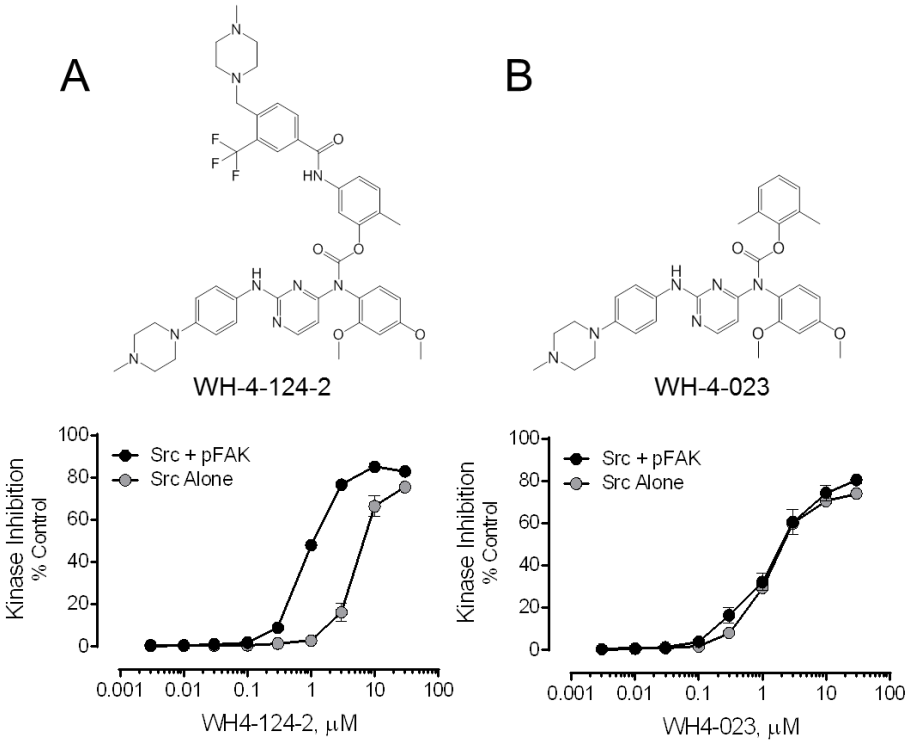

Figure 25. Selective inhibition of Src-YEEI by WH-4-124-2 in the presence of the pFAK peptide but not by the analog, WH-4-023

WH-4-124-2 (A) and WH-4-023 (B) were assayed against Src-YEEI alone (gray circles) and the Src-YEEI:pFAK complex (black circles) over the range of inhibitor concentrations shown using the Z'Lyte assay. IC_{50} values were determined by curve-fitting and are shown in Table 6.

3.3.3 WH-4-124-2 is a selective inhibitor of the Src-YEEI:pFAK complex

To further characterize the selective inhibitor WH-4-124-2, we first identified an analog of this compound with similar inhibitor potency for both Src-YEEI alone and in complex with the pFAK peptide. The compound WH-4-023 is very similar in structure to WH-4-124-2 (Figure 25B) and inhibited both the complex and Src-YEEI alone by more than 70% in the screening assay (Table 7, compound 551). We then performed a concentration-response experiment with

this compound in the Z'-Lyte assay, and found that it inhibited Src-YEEI both alone and in complex with the pFAK peptide with an IC50 value of about 1.3 μM. This result strongly suggests that the additional substituent present in WH-4-124-2 is responsible for inhibitor selectivity.

Selective inhibitor discovery and characterization described so far was performed using an end-point kinase assay, which does not provide direct information about the effect of either the activator peptide or the inhibitors on the kinase reaction rate. To further evaluate these compounds in a kinetic assay, we turned to the ADP Quest assay, which measures the progress of the kinase reaction as the accumulation of ADP. We began by performing a titration of Src-YEEI activity in the absence and presence of the pFAK peptide to establish conditions for testing the compounds (Figure 26A). As in the Z'Lyte assay, we chose a concentration of Src-YEEI such that activation was dependent on the presence of the pFAK peptide (15.6 ng per reaction). The rate of activity at this concentration alone was barely detectable, with 0.2 pmol ADP produced per minute and increased to 1.0 pmol ADP/produced per minute in the presence of the pFAK peptide at a concentration of 30 μM. To test for inhibition of Src-YEEI alone, we used 40 ng kinase per reaction to achieve the same basal rate of 1.0 pmol ADP produced per minute.

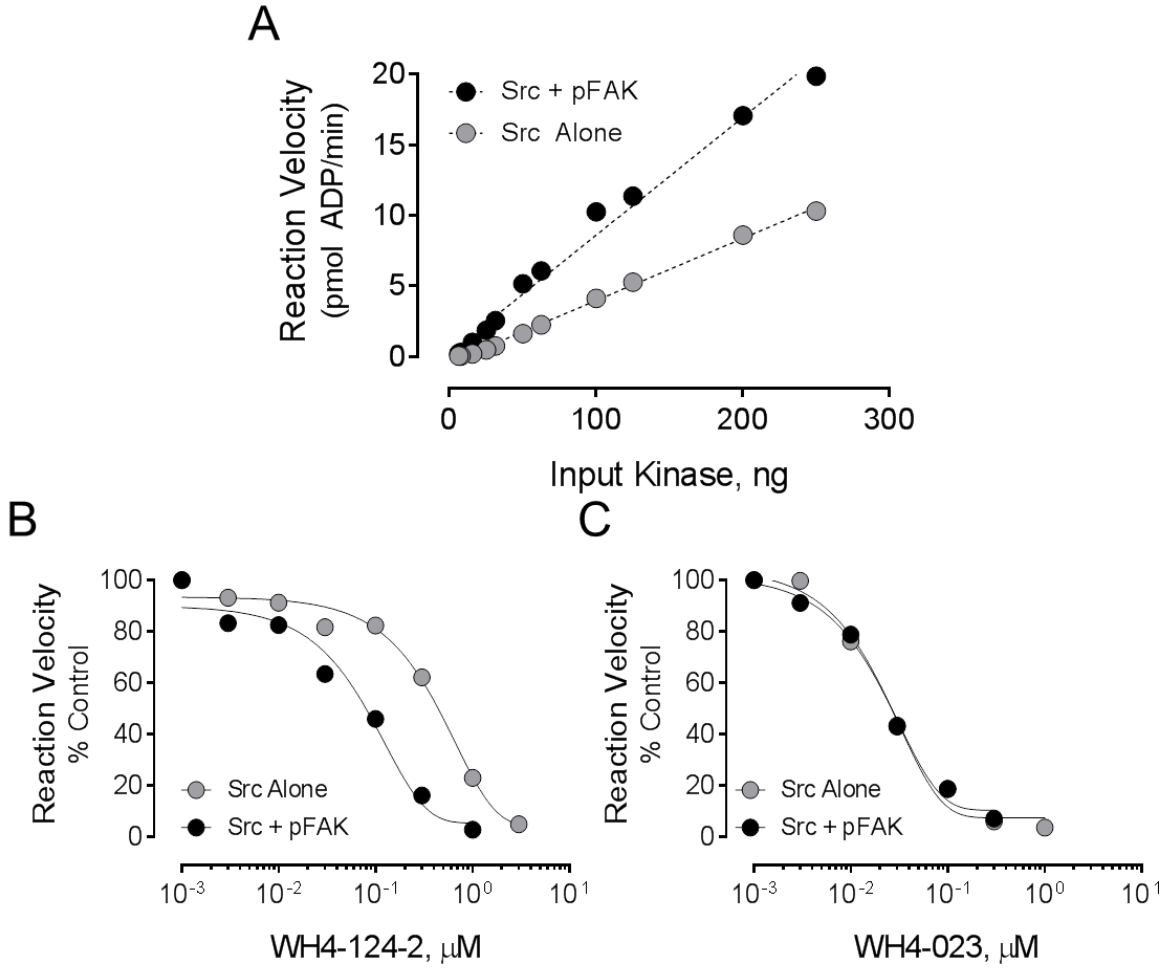

Figure 26. WH-4-124-2 exhibits increased potency while maintaining selectivity in a kinetic kinase assay

A) The activity of Src-YEEI was measured in the ADP Quest kinetic kinase assay in the absence (gray circles) and presence (black circles) of 30 μM pFAK peptide. WH-4-124-2 (B) and WH-4-023 (C) were assayed against Src-YEEI alone and the Src-YEEI:pFAK complex in the ADP Quest assay over the range of inhibitor concentrations shown. IC_{50} values were determined by curve-fitting and are shown in Table 6.

Both WH-4-124-2 and WH-4-023 inhibited Src-YEEI activity in this assay in a concentration-dependent manner (Figure 26B and C). As observed previously with the Z'Lyte assay, WH-4-124-2 demonstrated selective inhibition of Src-YEEI in the presence of the pFAK peptide, while WH-4-023 did not. Table 6 compares the IC50 values generated in the ADP Quest assay for each

of these compounds to those from the Z'Lyte assay. WH-4-124-2 is more potent against Src-YEEI in complex with the pFAK peptide than Src-YEEI alone with IC50 values of 114 vs. 531 nM, respectively. By contrast, WH-4-023 inhibited Src-YEEI alone and the complex with very similar potencies, yielding IC50 values of 19 and 25 nM, respectively. While the IC50 values generated for both inhibitors in the ADP Quest assay are lower than those generated in the Z'Lyte assay, the relative selectivity for the Src-YEEI:pFAK complex is the same in both. This difference in apparent potency may be due to the different peptide substrates used in each assay, the ATP concentrations, or both.

Table 6. IC50 values for kinase inhibitors WH-4-124-2 and WH-4-023 against Src-YEEI in the presence and absence of the pFAK peptide

Compound	**WH-4-124-2**		**WH-4-023**	
Assay	Z'Lyte	ADP Quest	Z'Lyte	ADP Quest
Src-YEEI + pFAK	0.885	0.114	1.36	0.025
Src-YEEI alone	4.95	0.531	1.28	0.019

IC_{50} values (μM) were generated in the Z'Lyte endpoint assay used for the library screen and in the ADP Quest kinetic kinase assay for Src-YEEI in complex with the pFAK peptide vs. Src-YEEI alone.

3.3.4 Docking studies of WH-4-124-2 with the c-Src and Lck kinase domains

Data presented in the previous sections suggest that binding of pFAK to c-Src may induce a conformation of the kinase active site that is stabilized by WH-4-124-2 binding. One well-known determinant of inhibitor specificity relates to the conformation of the highly conserved Aspartate-Phenylalanine-Glycine ('DFG') motif at the N-terminal end of the activation loop in the kinase active site (*138, 206*). In the active state, the aspartate in the DFG motif moves into the active site where it contributes to the coordination of ATP-Mg++. In the

inactive state, however, this aspartate residue moves away from the active site while the phenylalanine moves inward, resulting in the so-called 'DFG-out' conformation. Previous structural studies have shown that inhibitors such as imatinib prefer the DFG-out conformation of the Abl kinase domain, a therapeutically relevant target for this drug (*135, 138*). Interestingly, imatinib has also been co-crystallized with both c-Src and Lck, where it binds to a very similar DFG-out conformation (*207, 208*). These observations led us to consider whether WH-4-124-2 may exhibit some of its selectivity by inhibiting a similar DFG-out state of the kinase domain.

Comparison of the chemical structures of WH-4-124-2 and imatinib reveals significant overlap, allowing us to align the structure of WH-4-124-2 with imatinib in the X-ray crystal structure of the Lck kinase domain bound to this compound (Figure 27). This structure was chosen because all of its kinase domain features are resolved, including the activation loop and autophosphorylation site which are missing from the c-Src structure with imatinib. Figure 27 shows imatinib bound to the Abl (A) and Lck (B) kinase domains, highlighting the positions of key active site features in the presence of imatinib. In these structures, the DFG motif is flipped outward. The Lck activation loop and tyrosine autophosphorylation site are extended outward, whereas in Abl the equivalent tyrosine is hydrogen-bonded to the catalytic aspartate. This comparison suggests that in Lck, imatinib traps a 'primed' or intermediate state between the downregulated and fully active forms of the kinase domain. WH-4-124-2 was then aligned with imatinib using the docking routine smina (*209*), a modified version of AutoDock Vina optimized for user-specified custom scoring functions (Figure 27C).

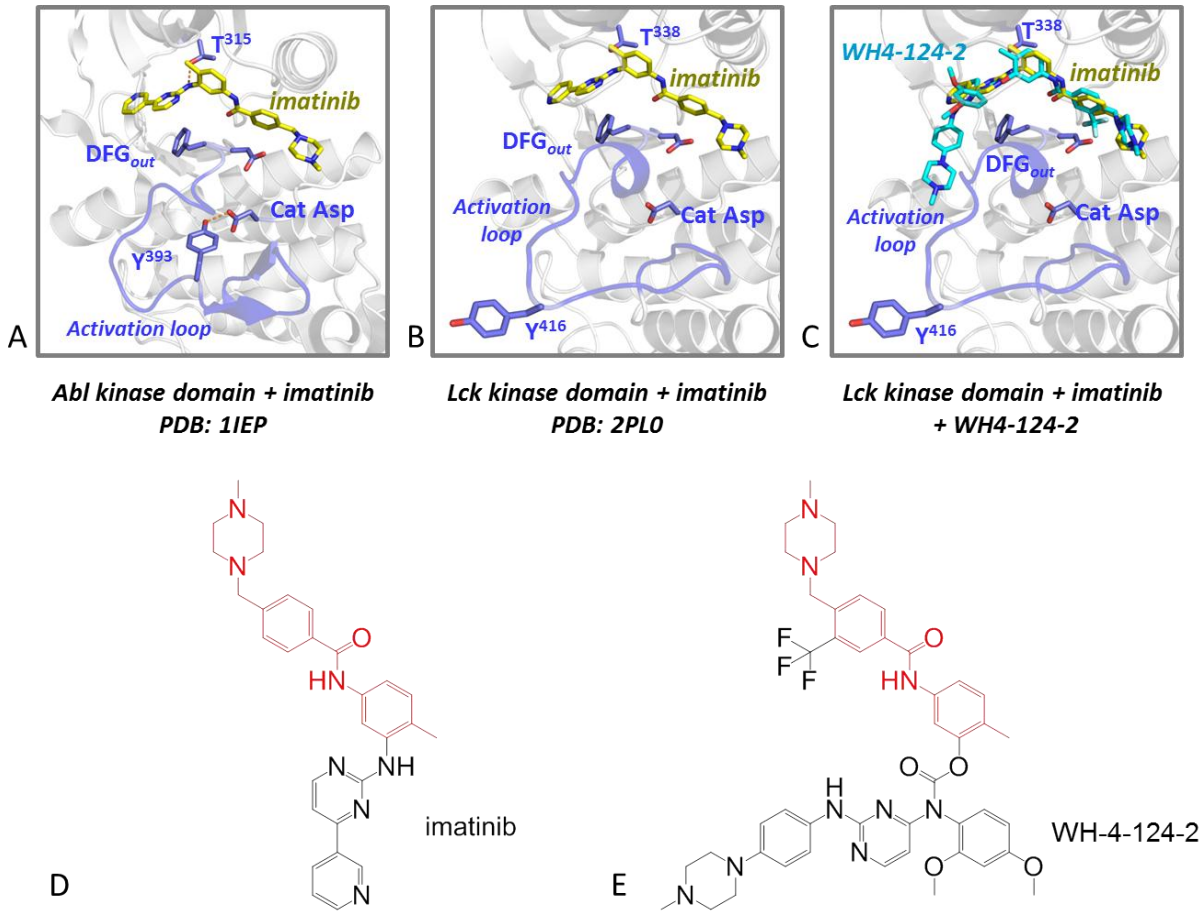

Figure 27. Computational docking of WH-4-124-2 to the x-ray crystal structure of the Lck kinase domain bound to imatinib.

A) The active site of c-Abl with imatinib bound. Key side chains are displayed and labeled. Imatinib (carbon atoms in yellow) binds to the DFG-out conformation. The activation loop tyrosine (Y393) points inward and H-bonds to the catalytic aspartate in the kinase domain. B) The active site of Lck with imatinib bound. The same side chains are labeled as in A. Imatinib binds to the Lck activation loop in a manner analogous to the Abl kinase domain. Unlike Abl, however, the activation loop adopts an extended conformation, with the tyrosine autophosphorylation site (Y394) exposed. C) WH-4-124-2 (carbon atoms in cyan) was aligned with the analogous portion of imatinib using smina, a modified form of AutoDock Vina developed by the Camacho group (Computational and Systems Biology, University of Pittsburgh School of Medicine). WH-4-124-2 was readily accommodated by the imatinib-binding conformation of the Lck kinase domain, with only minimal changes to the crystallographic positions of side chains that come in close contact with the compound. D and E show the structures of imatinib and WH-4-124-2 with the overlapping portion highlighted in red.

WH-4-124-2 was accommodated by the conformation of the imatinib-bound Lck active site, supporting the idea that this inhibitor also prefers the DFG-out state of the kinase active site. A similar docking routine was also performed using the X-ray crystal structure of the c-Src kinase domain bound to imatinib (PDB: 2OIQ) and yielded an almost identical result, although the activation loop is not resolved in this structure (data not shown). In summary, this docking model suggests that binding of the pFAK peptide and displacement of the SH3-SH2 regulatory subunits allows the kinase to adopt the DFG-out conformation, which in turn is trapped by the inhibitor.

3.4 DISCUSSION

In this study, we describe a screening assay that has enabled discovery of a conformationally selective inhibitor of the c-Src protein tyrosine kinase. SFKs are involved in a wide variety of cellular signaling pathways and most cells express multiple members of Src-kinase family, making the search for isoform- and pathway-selective inhibitors difficult. Rather than focusing on the kinase itself, we developed an assay method that models a disease-specific conformation of c-Src that is induced by interaction with FAK. Using a synthetic tyrosine phosphopeptide containing the natural FAK sequence known to bind to the SH3 and SH2 domains of c-Src, we first identified screening assay conditions where Src-YEEI activity was dependent on the presence of the pFAK peptide. Comparative studies with shorter peptides that bind only to the SH3 (VSL12) or the SH2 (pYEEI) domains individually demonstrated that displacement of both intramolecular interactions was required for maximal activation of Src-YEEI. Using pFAK-activated Src-YEEI, we then screened a small library of kinase-biased

inhibitors and identified WH-4-124-2, an aminopyrimidinyl carbamate with enhanced potency for Src-YEEI in the presence of the pFAK peptide. This compound exhibited five-fold greater potency for the Src-pFAK peptide complex relative to Src-YEEI alone in both endpoint and kinetic kinase assays. Interestingly, a smaller structural analog of WH-4-124-2 showed no preference, supporting the idea that WH-4-124-2 stabilizes a specific conformation of the kinase active site that is induced by interaction with the pFAK peptide.

Docking studies with WH-4-124-2 and the imatinib-bound crystal structures of both the Lck and c-Src kinase domains suggest that binding to the pFAK peptide may induce a unique DFG-out conformation that is preferentially inhibited by this compound. In this conformation, the αC-helices of both kinase domains are rotated inward, allowing the formation of the conserved lysine to glutamate salt bridges. The DFG motif at the distal end of the activation loop in each kinase is also rotated outward, in the same manner originally observed for imatinib binding to the Abl kinase domain. However, in the Lck structure, the autophosphorylation site is also extended outward, although the tyrosine is not phosphorylated (this region is not resolved in the c-Src kinase domain structure with imatinib). Using the structural overlap with imatinib as a starting point, WH-4-124-2 was readily docked into this unique Lck kinase domain conformation, requiring only minimal changes to the positions of side chains already present in the crystal structure. The implication, therefore, is that pFAK peptide binding may induce this kinase domain conformation in c-Src, thereby accounting for preferential inhibition of the kinase by this compound in the presence of the pFAK peptide. Whether or not binding to full-length FAK results in similar changes to the c-Src active site in a cellular context will require further investigation. Nevertheless, these studies support the more general concept that unique disease-

state specific conformations of Src-family kinases exist in cells that may be amenable to selective inhibition with active-site inhibitors.

4.0 GENERAL DISCUSSION

The Src-family of kinases has been extensively studied as a whole, yet there is still much to be learned about the regulation of individual family members. In this study, I have shown differences in regulation of four of the Src-family members through extensive biochemical and kinetic studies. Further, I have shown that it is possible to target a specific kinase conformation induced by high-affinity ligand binding with a small molecule kinase inhibitor. The data presented here provides insight into a new way of targeting a specific member of a homologous protein family through targeting specific active kinase conformations.

I hypothesized that regulation of the Src-family members would vary based on the phylogenetic breakdown of the eight members into two subfamilies. The experiments presented in Chapter 2 examined the regulation of two kinases from each subfamily: c-Src and Fyn from subfamily A and Hck and Lyn from subfamily B. Each of these members was chosen based on previous work from our laboratory, literature available on the known mechanisms of regulation, and evidence that supported a difference in regulation between subfamily members. Interestingly, results presented here have shown that differences in regulation cannot be explained solely by sequence differences, but are in fact unique for each family member.

The SFKs are kept in a downregulated state by two intramolecular interactions. Disruption of either one or both of these interactions has been shown to result in kinase activation for multiple members of the kinase family. Mutation of the C-terminal tail tyrosine in

various members of each subfamily results in kinase activation, demonstrating an absolute requirement for tail phosphorylation by Csk in kinase regulation. The diversity of control among the family members by the SH3:linker interaction is less clear. For most of the SFKs, it is not known whether disruption of one interaction requires the disruption of the other before the kinase can become activated. The exception to this is Hck, as studies have confirmed that the tail remains bound to the SH2 domain while Hck is bound and activated by Nef. For c-Src, however, it was possible that when activated by ligand binding to the SH3 domain, a conformational change resulted in the release of the tail from the SH2 domain before kinase activation. The studies performed here were a means to elucidate this mechanism.

In Chapter 2 of this thesis, I focused on SH3:linker displacement-induced activation of the Src-family kinases. By using SFK proteins with YEEI-tail mutations that increased the affinity for the SH2 domain, I was able to ensure that kinase activation would not be influenced by this intramolecular interaction and was due only to SH3:linker displacement. In addition, it was imperative to ensure that there would be no bias in the system regarding the ligand used to displace the SH3:linker interaction. In past studies of SH3 ligand binding, the VSL12 peptide was discovered as a high-affinity ligand for the c-Src SH3 domain. In this study, VSL12 was confirmed to have similar affinities for the isolated SH3 domains of all of the SFKs tested in SPR binding assays. To ensure that the peptide could bind to the downregulated kinases for use in kinase assays, I also measured the affinity for the near-full-length proteins. The result was surprising, as the affinity increased roughly 1000-fold compared to the isolated SH3 domains. The expectation for this experiment was that there would be a lower affinity, or at least a lower rate of association, for the near-full length proteins for VSL12, as there would be competition for the SH3 domain from SH2-kinase linker which is bound in the downregulated state. However,

the association rates of the peptide to the isolated SH3 domain and the near full length kinase were nearly identical for each SFK. Surprisingly, the dissociation rates were 1000-fold lower for the near-full-length proteins than for the isolated SH3 domains. This suggests that VSL12 binding to the SH3 domain in the context of the entire protein induces a favorable, stabilized conformation, which will require further study to establish. Another explanation for the higher affinity is that the VSL12 peptide actually binds to a second site on the near-full length kinase domain. The binding affinity of VSL12 has been measured for the isolated SH3, SH2, tandem SH3-SH2, and SH3-SH2-linker proteins from c-Src, Fyn, Hck, and Lyn. None of these results suggest a second binding site in any of these areas of the protein, and there is no evidence in the literature to suggest that the peptide would bind on its own to the isolated kinase domain. Furthermore, if there were a second binding site, there would likely be a different rate of association since there would be more binding events occurring at those additional sites. There are currently plans underway to test this by SPR using the isolated kinase domain proteins and eliminate the possibility of a second binding site for the peptide.

To test whether the binding of VSL12 actually stabilizes the complex, structural dynamics studies could be utilized. Using hydrogen exchange mass spectrometry (HXMS, (*210*)), the changes in protein structure could be investigated by comparing Src-YEEI in the absence and presence of the peptide. This technique measures the incorporation of deuterium into solvent-exposed areas of a protein. Binding of the peptide would potentially prevent deuterium exchange in certain areas that are covered by peptide binding. However, other areas may become more solvent-exposed through conformational rearrangements and consequently incorporate more deuterium, since the peptide is known to activate the kinase. These changes can be mapped to specific areas of the protein structure by analysis of changes in mass of peptide

sequences. If the hypothesis that VSL12 induces a stabilized conformation of the kinase is true, this technique would enable us to determine if and where the peptide makes contact with the kinase domain to do so. These data in addition to an x-ray crystal structure of Src-YEEI in complex with VSL12 would be the most useful to visualize how the conformation of the entire kinase changes in response to SH3:linker displacement.

Despite the surprising result of the high-affinity binding of VSL12 to the near-full-length kinases, I was able to validate the use of VSL12 as an agonist for the SFKs with equal affinity for each family member. Subsequently, I showed that this peptide was able to activate all SFKs tested to varying degrees. This disproves the original hypothesis, which stated that SrcA subfamily members would not be susceptible to activation by SH3:linker displacement alone. However, the activation mechanisms of all family members are not the same, which supports the idea that regulation across the kinase family is diverse, despite the homology of the family members. It was not surprising that the activity of Src-YEEI and Fyn-YEEI was similar in response to VSL12 binding since they are members of the same subfamily. The difference between Hck and Lyn was unexpected because they are the closest phylogenetic relatives in the SrcB subfamily. Similarly, recent evidence supports opposing roles for c-Src and c-Yes in both development and cancer. These two family members are the closest phylogenetic relatives in the SrcA subfamily, yet their functions are proving to be unique. This is not simply a consequence of expression patterns as these are two of the three SFKs (Fyn being the third) that are expressed ubiquitously. At the time this study was designed, the evidence for differences between c-Src and c-Yes was not as prevalent. Continuation of this study with Yes-YEEI would be a logical next step to further the evidence for diversity in the regulation of the Src kinase family.

Another significant finding in this study was that autophosphorylation of Src-YEEI seemed to prime the kinase for activity, while it had no such effect on Hck-YEEI. The overall activity of both autophosphorylated kinases was increased in both the absence and presence of the peptide, showing that autophosphorylation of the activation loop alone does not stimulate the kinase to its maximum activity. However, the result with Hck-YEEI showed that activity induced by SH3 domain displacement is not influenced by the phosphorylation state of the kinase while the result with Src-YEEI supports a different mechanism of regulation. Further studies are in progress with linker mutants of both Src-YEEI and Hck-YEEI that will abolish the SH3:linker interaction. These experiments will hopefully determine whether the differences observed between Src-YEEI and Hck-YEEI are merely result of peptide disassociation and linker reassociation rather than a real difference in regulation between the two kinases.

Overall, the study in Chapter 2 has utilized knowledge gained from previous research on the regulation of the SFKs and provides a new view of the diversity in kinase regulation. Some differences may be accounted for by variation in the cellular expression patterns of the kinases. For example, the results presented here suggest that Hck is generally more susceptible to activation by perturbation of any interaction that supports downregulation of activity, and this may correspond to a requirement for fast Hck activation in a cellular context. Conversely, c-Src may be more tightly regulated and require more than just displacement of one interaction to result in maximal kinase activity. Alternatively, different levels of c-Src activity may be elicited by activation through different mechanisms. For example, in the context of c-Src activation by FAK, both intramolecular interactions are displaced by FAK binding, resulting in complete release of autoinhibitory control. In a situation where c-Src is activated by displacement of only one interaction, it may be in a context where less c-Src activity is required.

This could be an evolutionary mechanism for controlling the amount of activity elicited from one kinase. Results from Chapter 3 support that different levels of kinase activity result from displacement of one, the other, or both intramolecular interactions.

In Chapter 3, I focused on exploiting the differences in mechanisms of kinase activation to screen for conformationally selective inhibitors of c-Src kinase activity. As mentioned above, FAK activates c-Src by binding both the SH3 and SH2 domains, resulting in a loss of regulatory control of activity by these domains. Rather than trying to model the system using the full-length FAK protein, I was able to use a peptide comprised of the FAK sequence that binds the c-Src SH3 and SH2 domains, pFAK. This peptide activated the Src-YEEI protein in kinase assays better than peptides that targeted either the SH3 or SH2 domain alone. Even when using both of the individual domain-binding peptides together, the activation by the pFAK peptide, which has the binding sequences for both domains in tandem, was much higher. This supports the idea presented in Chapter 2 that disruption of the regulatory control by the different intramolecular interactions can have a different result.

By determining conditions in the Z'Lyte in vitro kinase assay such that activation of Src-YEEI was dependent on the presence of the pFAK peptide, I was able to ensure that any active protein in the assay would be in a pFAK-induced conformation. Using these assay conditions, I screened a kinase-biased inhibitor library to see if inhibitors could be identified that preferentially inhibited the pFAK-bound state of Src. Out of 586 screened compounds, 97 were able to inhibit the Src-YEEI:pFAK complex in the primary screen. As a counterscreen, I used a concentration of Src-YEEI protein alone that resulted in the same basal level of activity that was elicited by the Src-YEEI:pFAK complex. The mechanism of activation in the Src-only kinase reactions is likely trans-autophosphorylation of the activation loop, as there are no ligands

present to displace the intramolecular regulatory interactions. Only 21 of the 97 compounds tested here were selective for the Src-YEEI:pFAK complex. Further testing of these compounds identified WH-4-124-2 as the most potent and selective inhibitor of the Src-YEEI:pFAK complex. This compound showed a five-fold selectivity for the complex in endpoint and kinetic kinase assays.

Although the compound is selective for the pFAK-induced conformation of Src-YEEI compared to Src-YEEI alone, there is still a matter of selectivity of Src-YEEI over other members of the kinase family. Currently, plans are underway to test the ability of the pFAK peptide to activate Hck-YEEI, Fyn-YEEI, and Lyn-YEEI. This will not only extend the study performed in Chapter 2, but will also enable me to determine whether the conformation of c-Src induced by FAK binding is unique to Src. I would predict that Fyn-YEEI will show similar inhibition by WH-4-124-2 due to the similarities observed in Chapter 2, as well as evidence that Fyn is bound and activated by FAK in cells as well. There is also uncertainty as to whether this active conformation is induced solely by FAK or if another ligand can bind and induce a similar conformation. Studies are also underway to test this question using VSL12 and pYEEI, the peptides used in Chapter 2 that bind to the individual SH3 or SH2 domains, respectively.

In addition to the discovery of the selective compound WH-4-124-2, a structural analog, WH-4-023, was also discovered and shows a similar level of potency but no selectivity for either the pFAK bound or unbound kinase. Based on the modeling studies performed with WH-4-124-2 and the Lck kinase domain bound to imatinib, we can speculate that the selectivity observed with WH-4-124-2 is due to the imatinib-like part of the structure, which is not present in WH-4-023. The facile docking of WH-4-124-2 to the imatinib-bound conformation of Lck suggests that the pFAK-bound conformation of Src-YEEI may also be sensitive to inhibition by

imatinib itself. Therefore, plans are underway to test the ability of imatinib to inhibit the Src-YEEI:pFAK complex. Experiments have already demonstrated that imatinib has no effect on Src-YEEI alone. In addition, further studies will be required to elucidate the mechanism of selectivity of WH-4-124-2. Crystallographic studies would be ideal in the determination of the actual binding mode of the compound to Src-YEEI in the pFAK-bound state.

This dissertation provides strong evidence for the diversity in regulation among the Src-kinase family. Despite their homology and apparent redundancy in certain cellular processes, eight SFKs are conserved and functional in mammalian species. This suggests that in cells, each family member has a unique role and function. Otherwise, evolutionary mechanisms would likely result in the loss of expression of the individual kinase gene. Therefore, it is important to understand the differences in the mechanisms of kinase regulation. While the search for selective inhibitors of SFKs has remained elusive, a new approach could be to target a disease-induced conformation of that kinase, as I have demonstrated here. This would not only target the specific member involved in deregulation of cellular processes, but would target the specific effects that result from the deregulation, rather than all effects of that kinase in a cell. The results presented here will hopefully lay the foundation for further exploitation of these differences as a means to generate selective inhibitors.

APPENDIX A

INHIBITION RESULTS FROM SCREENED COMPOUNDS

Table 7. Inhibition of Src-YEEI +/- pFAK by entire kinase-biased library

Compound	% Inhibition of Src + pFAK	% Inhibition of Src Alone	Selectivity Ratio
1	-1.05676	1.655786	-0.63822
2	0.163812	0.3165	0.517573
3	6.932333	0.723222	9.58534
4	8.072438	5.989337	1.347802
5	9.060375	-0.00341	-2655.99
6	9.992882	1.834704	5.446591
7	10.35875	2.077826	4.98538
8	10.3591	2.962374	3.496891
9	10.95063	0.190116	57.59982
10	10.96882	1.396072	7.856915
11	11.07077	0.416142	26.60337
12	11.23091	6.413868	1.751035
13	11.23474	0.178414	62.9699
14	11.34642	0.072944	155.5488
15	11.78764	4.872591	2.419173
16	11.93701	0.472202	25.27947
17	11.96135	2.030002	5.892281
18	11.97477	0.080071	149.552
19	12.04613	0.526966	22.85939
20	12.06802	2.265138	5.327719
21	12.09864	2.009403	6.021013
22	12.1222	0.45286	26.76807
23	12.15354	0.668505	18.18018
24	12.16973	1.37497	8.850902
25	12.25697	0.492325	24.89607

26	12.36962	0.334352	36.99582
27	12.39133	1.243784	9.96261
28	12.47908	1.179349	10.58133
29	12.49611	1.205771	10.36358
30	12.5152	0.233681	53.55671
31	12.54649	0.610832	20.54
32	12.59205	0.312733	40.26446
33	12.59697	2.413911	5.21849
34	12.63199	3.235642	3.904013
35	12.71639	0.169952	74.82322
36	12.92122	2.385509	5.416547
37	13.03294	0.433512	30.06363
38	13.03578	0.811205	16.06965
39	13.06999	0.189005	69.15156
40	13.13507	0.976308	13.45382
41	13.29562	0.306635	43.35971
42	13.36031	1.875123	7.125031
43	13.39715	0.880146	15.22151
44	13.43963	0.50675	26.5212
45	13.50299	0.575847	23.44891
46	13.69583	1.125914	12.16419
47	13.79031	0.562839	24.50136
48	13.79358	3.596688	3.835078
49	13.79764	2.301167	5.99593
50	13.809	1.165683	11.84628
51	13.91971	0.330409	42.12871
52	13.97795	1.161069	12.03887
53	13.9996	1.70548	8.208599
54	14.04175	3.491324	4.021897
55	14.0982	3.776451	3.733188
56	14.20927	0.766384	18.54066
57	14.29919	1.963669	7.281872
58	14.33865	0.339257	42.26485
59	14.44022	1.991091	7.252417
60	14.64863	5.43356	2.695954
61	14.74163	1.850993	7.964175
62	14.78307	0.476555	31.0207
63	14.81299	0.852896	17.36787
64	14.90194	4.322087	3.447858
65	14.91428	5.139667	2.901798
66	15.04176	0.171605	87.65331
67	15.14022	1.316583	11.49963
68	15.15493	0.5189	29.20587

69	15.207	1.602411	9.490073
70	15.21608	5.626585	2.704319
71	15.26731	1.384225	11.0295
72	15.28375	2.238258	6.828411
73	15.36021	1.668255	9.207347
74	15.39262	3.541223	4.346697
75	15.43114	4.433202	3.480811
76	15.4541	0.711395	21.72366
77	15.45672	2.489578	6.20857
78	15.46411	3.688976	4.19198
79	15.47341	5.432503	2.848303
80	15.52328	1.777295	8.734217
81	15.57905	1.727185	9.019908
82	15.595	5.460282	2.85608
83	15.59569	5.031421	3.099659
84	15.59698	0.990891	15.74036
85	15.61003	4.829234	3.232404
86	15.66209	2.21828	7.060464
87	15.71785	2.368916	6.635042
88	15.72532	1.814356	8.667164
89	15.731	1.032196	15.24032
90	15.73691	0.649149	24.24239
91	15.77856	1.276891	12.35701
92	15.79068	1.04673	15.08572
93	15.80384	0.968309	16.32108
94	15.81084	2.128113	7.429512
95	15.81354	2.255275	7.011803
96	15.81975	1.853161	8.536629
97	15.86506	3.168779	5.006678
98	15.89999	0.306859	51.81527
99	15.9053	4.044773	3.93231
100	16.00257	-0.0182	-879.146
101	16.0104	4.177361	3.832658
102	16.01528	1.705898	9.388187
103	16.03526	2.109545	7.601289
104	16.03562	0.704495	22.76187
105	16.08144	5.147984	3.123833
106	16.11301	0.491412	32.78921
107	16.11854	1.899874	8.484007
108	16.14144	0.415573	38.8414
109	16.16575	5.708494	2.831877
110	16.18453	0.422172	38.33637
111	16.30427	1.682273	9.691811

112	16.33012	2.636524	6.193808
113	16.35565	1.524521	10.72838
114	16.40199	4.953346	3.311295
115	16.40327	9.409703	1.74323
116	16.43318	2.531134	6.49242
117	16.44527	0.991622	16.58421
118	16.48619	2.344932	7.030565
119	16.50209	1.011425	16.31569
120	16.51153	1.771861	9.318749
121	16.54542	1.841976	8.982428
122	16.56777	0.889823	18.61917
123	16.57569	2.783934	5.954053
124	16.58759	-0.76161	-21.7796
125	16.65627	3.040621	5.477919
126	16.71397	2.315421	7.218546
127	16.75849	1.0254	16.34337
128	16.75948	2.132881	7.857674
129	16.81444	2.1346	7.877091
130	16.92674	1.333665	12.69189
131	16.9689	1.684544	10.07329
132	16.9858	7.49533	2.266185
133	17.04722	0.985629	17.29577
134	17.11595	1.677682	10.20214
135	17.12142	3.604939	4.749435
136	17.12829	2.862867	5.982914
137	17.1423	2.063506	8.307364
138	17.14735	4.900618	3.499017
139	17.15576	1.016171	16.88274
140	17.16765	4.231094	4.057495
141	17.17136	4.254814	4.035748
142	17.17161	1.257587	13.65441
143	17.18536	1.696379	10.13061
144	17.2227	5.219989	3.299374
145	17.29945	4.691753	3.687205
146	17.31235	6.810871	2.541871
147	17.3157	3.056804	5.664641
148	17.32184	1.058492	16.36464
149	17.3592	1.802853	9.628739
150	17.46806	1.222445	14.28945
151	17.46919	4.584605	3.810403
152	17.55299	3.803062	4.615489
153	17.58265	2.280118	7.71129
154	17.6048	0.6494	27.10934

155	17.60619	1.735818	10.14288
156	17.63935	2.263221	7.793915
157	17.68061	3.076253	5.747449
158	17.68725	2.77381	6.376515
159	17.73131	2.894009	6.126901
160	17.77415	0.531531	33.43953
161	17.80178	3.004909	5.924233
162	17.82029	1.357896	13.12345
163	17.83988	3.918228	4.553047
164	17.84686	5.58684	3.194445
165	17.85086	1.860486	9.59473
166	17.86324	2.84523	6.278312
167	17.8862	2.481988	7.206399
168	17.94522	0.759405	23.63063
169	17.94541	5.513314	3.254922
170	17.96896	1.620392	11.08926
171	18.012	6.160427	2.923823
172	18.01849	6.850245	2.630342
173	18.04526	6.280004	2.873448
174	18.10991	1.848794	9.795526
175	18.13973	2.653361	6.836509
176	18.17835	4.81625	3.774379
177	18.18355	1.994071	9.118808
178	18.18915	2.883705	6.307562
179	18.26126	3.395294	5.378402
180	18.26662	5.847018	3.124091
181	18.29516	4.875219	3.752685
182	18.39449	0.719205	25.57614
183	18.42219	6.063894	3.038012
184	18.42479	4.512916	4.08268
185	18.54931	3.399552	5.456398
186	18.56268	1.050138	17.67642
187	18.61456	11.33862	1.641695
188	18.64668	11.3112	1.648515
189	18.67018	0.925332	20.17673
190	18.71215	8.306225	2.252787
191	18.71628	4.137643	4.523416
192	18.77632	2.098926	8.945681
193	18.79972	5.827661	3.225945
194	18.86006	0.218172	86.44573
195	18.86682	4.612238	4.0906
196	18.8917	1.145236	16.4959
197	18.91364	4.607624	4.104857

198	18.91686	6.585651	2.872436
199	18.94533	6.883961	2.752097
200	18.94985	7.225188	2.622748
201	19.00018	9.366412	2.028544
202	19.02491	1.535469	12.39029
203	19.03255	8.446746	2.253241
204	19.04837	2.697357	7.061863
205	19.06512	4.740793	4.021504
206	19.0805	1.000644	19.06821
207	19.08629	3.196386	5.97121
208	19.09558	2.883811	6.621648
209	19.09763	1.477835	12.9227
210	19.1226	2.209382	8.65518
211	19.17345	10.73205	1.786561
212	19.18682	2.194995	8.741165
213	19.20305	2.921629	6.57272
214	19.23632	2.354028	8.171661
215	19.26003	1.830156	10.52371
216	19.28432	0.256555	75.16644
217	19.30576	3.366114	5.735325
218	19.30644	1.904126	10.13926
219	19.32286	5.8618	3.296403
220	19.33435	10.33571	1.870636
221	19.34707	3.123534	6.193967
222	19.35713	0.68338	28.32557
223	19.41792	1.509819	12.86109
224	19.4511	2.434682	7.989175
225	19.4664	0.689136	28.24756
226	19.58305	1.108829	17.66101
227	19.59132	2.269926	8.630822
228	19.59706	0.804041	24.37319
229	19.60199	1.416402	13.83928
230	19.65425	2.787192	7.051632
231	19.68339	3.144848	6.258934
232	19.69547	1.423277	13.83811
233	19.70379	0.738251	26.68984
234	19.74426	0.134214	147.1102
235	19.76831	2.260167	8.746395
236	19.79042	6.03248	3.280644
237	19.84852	2.413714	8.22323
238	19.85368	3.411658	5.819363
239	19.87076	4.593318	4.326015
240	19.88866	0.434671	45.75565

241	19.92979	5.557315	3.586227
242	19.95027	1.342512	14.8604
243	19.95534	1.675157	11.91252
244	19.9575	0.853028	23.39607
245	20.08805	3.86926	5.191704
246	20.15019	2.798649	7.199969
247	20.15795	6.828059	2.952222
248	20.16847	1.933273	10.43229
249	20.18099	7.242125	2.786611
250	20.19599	4.046453	4.991037
251	20.24027	5.74521	3.522982
252	20.24227	1.61215	12.55607
253	20.25652	1.829986	11.06922
254	20.26385	2.500671	8.103367
255	20.27183	1.659013	12.21921
256	20.28649	10.62399	1.909499
257	20.31189	3.15401	6.440018
258	20.36185	0.564643	36.06145
259	20.42407	3.049191	6.698195
260	20.43454	4.835686	4.225779
261	20.49723	2.961052	6.922279
262	20.50293	1.948552	10.52214
263	20.54781	7.142816	2.87671
264	20.594	1.771467	11.62539
265	20.68611	0.911173	22.70271
266	20.70482	1.164637	17.77791
267	20.77176	6.560689	3.166094
268	20.86818	1.992543	10.47314
269	20.87983	0.858199	24.32981
270	20.93926	4.424301	4.732784
271	20.98057	2.596462	8.080445
272	21.01502	1.977238	10.62847
273	21.06786	3.256582	6.469315
274	21.06871	1.680771	12.53514
275	21.11059	4.090139	5.161338
276	21.18226	2.613532	8.104839
277	21.22806	6.644819	3.194679
278	21.23069	2.13653	9.936997
279	21.23992	1.467505	14.47348
280	21.27217	2.957533	7.192536
281	21.30167	5.366592	3.969311
282	21.35399	2.814206	7.587929
283	21.43445	4.040181	5.30532

284	21.45311	2.697569	7.952758
285	21.4544	0.76346	28.10153
286	21.45599	9.693888	2.213352
287	21.46337	1.407575	15.24847
288	21.50144	1.626783	13.21716
289	21.52096	5.698776	3.776418
290	21.61413	4.682928	4.615515
291	21.6365	9.862598	2.193793
292	21.65885	2.342564	9.24579
293	21.66703	5.086634	4.259601
294	21.67073	2.786231	7.777795
295	21.71572	0.904725	24.00256
296	21.77027	3.215607	6.77019
297	21.8215	6.767834	3.224297
298	21.82485	2.363574	9.233834
299	21.85556	6.471891	3.376997
300	21.88715	1.085466	20.16383
301	21.89106	0.802309	27.28506
302	21.89941	2.140717	10.22994
303	21.90803	1.829838	11.97266
304	21.91875	2.862399	7.657474
305	21.94416	12.06805	1.818368
306	21.98736	9.362538	2.34844
307	22.03226	0.808497	27.25088
308	22.07407	4.366075	5.055816
309	22.07567	2.480137	8.900986
310	22.12202	6.189841	3.573923
311	22.15849	6.713122	3.300773
312	22.17154	2.204149	10.059
313	22.21643	1.176531	18.883
314	22.24552	5.987367	3.715409
315	22.25149	5.849676	3.803885
316	22.34234	4.510814	4.953061
317	22.36725	2.448038	9.136807
318	22.40685	5.03983	4.445954
319	22.40814	0.741583	30.21664
320	22.45977	8.557571	2.624549
321	22.46989	2.725341	8.244799
322	22.49281	2.989513	7.523903
323	22.51359	0.564222	39.90204
324	22.52635	2.673513	8.425749
325	22.52802	4.497976	5.008479
326	22.52815	2.856011	7.887976

327	22.64176	72.71791	0.311364
328	22.65512	1.914439	11.83382
329	22.83849	3.528867	6.471905
330	22.85895	2.949407	7.750354
331	22.88449	2.362755	9.685509
332	22.93358	6.554792	3.49875
333	22.95248	0.765936	29.96657
334	23.00546	3.119458	7.374826
335	23.0519	4.010902	5.747311
336	23.06352	0.963265	23.94307
337	23.09069	1.518701	15.20423
338	23.1162	3.114203	7.42283
339	23.12427	4.719586	4.899639
340	23.15909	3.9591	5.849585
341	23.20349	3.034142	7.647463
342	23.23682	0.720193	32.2647
343	23.26771	2.633605	8.83493
344	23.31819	8.641714	2.69833
345	23.32219	5.504323	4.237068
346	23.3589	2.093275	11.15902
347	23.37214	2.771005	8.434535
348	23.41181	2.273653	10.297
349	23.44929	2.072386	11.31512
350	23.56061	11.45885	2.056107
351	23.67623	3.585305	6.603685
352	23.70001	0.891746	26.57708
353	23.85296	0.120265	198.3369
354	23.92814	5.604663	4.269328
355	23.94154	6.788116	3.526979
356	23.97567	3.599649	6.660557
357	24.01254	2.673408	8.981997
358	24.09887	2.181363	11.04762
359	24.27753	2.703082	8.981426
360	24.3443	2.114586	11.51256
361	24.50473	4.554958	5.379792
362	24.52534	5.486157	4.470404
363	24.60242	1.432879	17.16992
364	24.61553	1.615061	15.24124
365	24.81927	1.738463	14.27656
366	24.84319	3.038074	8.17728
367	24.84698	2.704623	9.186856
368	24.87162	2.433226	10.22166
369	24.90368	8.862551	2.80999

370	24.99238	4.563348	5.476764
371	24.99341	3.951553	6.324958
372	24.99756	4.706412	5.311384
373	25.02731	3.269253	7.655361
374	25.1131	5.228041	4.803538
375	25.131	0.661042	38.01726
376	25.21191	3.152715	7.996888
377	25.23346	3.318526	7.603815
378	25.27587	5.541839	4.560917
379	25.37291	2.635982	9.625601
380	25.54346	4.252182	6.007141
381	25.62895	2.365323	10.83528
382	25.63698	2.210234	11.59921
383	25.76067	4.951151	5.202966
384	25.84048	5.62677	4.592417
385	25.90044	0.541828	47.80199
386	25.95216	0.123742	209.7272
387	26.00165	27.96519	0.929786
388	26.10944	3.363417	7.762773
389	26.1432	5.969808	4.379235
390	26.17746	5.881064	4.451144
391	26.21946	1.563799	16.76652
392	26.30028	2.072044	12.69292
393	26.35175	7.022937	3.75224
394	26.37367	2.706137	9.745875
395	26.64323	3.900551	6.830633
396	26.70871	2.248114	11.8805
397	26.75591	1.471119	18.18746
398	26.92577	0.688596	39.10243
399	26.92975	2.56796	10.48682
400	26.97072	1.540368	17.50927
401	27.02576	2.028461	13.32328
402	27.06865	3.311966	8.172984
403	27.13756	4.425018	6.132756
404	27.22	1.033836	26.32914
405	27.39722	4.392506	6.237265
406	27.51366	5.983969	4.597894
407	27.71676	7.866016	3.523608
408	27.76915	2.25391	12.32043
409	27.86996	5.846687	4.766794
410	28.06458	5.413553	5.184133
411	28.10224	6.240326	4.503329
412	28.11628	2.617852	10.74021

413	28.17053	5.919262	4.759129
414	28.18318	7.381958	3.817845
415	28.25317	3.627821	7.787917
416	28.41126	7.365603	3.857289
417	28.44473	4.138555	6.873107
418	28.49778	4.152056	6.863535
419	28.77416	5.897155	4.879329
420	28.84867	1.73684	16.60986
421	28.99892	3.739222	7.755334
422	29.24637	5.068919	5.769745
423	29.48036	6.367003	4.630179
424	29.69964	12.15198	2.444015
425	29.72595	0.192798	154.182
426	29.75817	2.668217	11.15283
427	29.76183	3.511646	8.475179
428	29.81552	0.740569	40.2603
429	29.87519	2.091589	14.28349
430	30.07509	3.277198	9.177075
431	30.34321	6.535819	4.642603
432	30.64462	6.739447	4.547052
433	30.75738	8.233717	3.73554
434	31.29992	6.94687	4.505615
435	31.48084	3.963236	7.943216
436	31.52943	0.82734	38.10941
437	31.6026	2.634184	11.99711
438	31.70059	4.996491	6.344571
439	31.78471	3.673678	8.652012
440	31.98826	1.840115	17.38384
441	32.87826	8.054362	4.082044
442	32.89764	5.275902	6.235452
443	32.98506	12.49736	2.639362
444	32.99549	2.64094	12.49384
445	33.6758	1.619684	20.79159
446	34.11444	8.424692	4.04934
447	34.36854	4.843944	7.095156
448	34.81288	2.28041	15.26607
449	34.87136	6.293887	5.540513
450	34.96772	8.937881	3.912306
451	35.28426	1.32676	26.59431
452	35.28474	2.106262	16.7523
453	35.55667	3.408221	10.43262
454	35.57448	6.035911	5.893804
455	35.60313	1.23368	28.8593

456	35.7842	20.7126	1.727654
457	35.85878	5.545079	6.466775
458	36.01615	2.109476	17.07351
459	36.03274	9.348708	3.854301
460	36.09289	3.786467	9.532075
461	36.54945	2.662703	13.72645
462	37.65126	2.628152	14.32614
463	38.08169	2.219599	17.15702
464	38.96175	10.8227	3.600004
465	39.51385	2.251894	17.54694
466	39.54234	3.249312	12.16945
467	39.72978	2.159644	18.39645
468	39.76753	12.55135	3.168386
469	40.94203	2.241568	18.2649
470	41.03104	2.664609	15.39852
471	41.03848	2.179901	18.82584
472	41.32028	7.951909	5.196273
473	42.93393	3.516578	12.20901
474	43.12494	43.44659	0.992597
475	43.18875	10.29582	4.194784
476	44.11608	2.378152	18.55057
477	44.51732	3.699749	12.03253
478	44.97484	17.62204	2.552193
479	45.38656	4.564718	9.942906
480	46.12428	35.93889	1.283408
481	46.14673	5.013126	9.20518
482	46.93707	16.62757	2.822846
483	47.65766	2.733428	17.43513
484	47.7562	9.863722	4.8416
485	47.83338	3.334384	14.34549
486	47.97869	4.789824	10.01679
487	48.32626	16.07747	3.005837
488	48.54235	14.5496	3.336335
489	49.22858	9.960055	4.942601
490	49.64085	5.065599	9.799601
491	49.7736	5.513021	9.028371
492	49.91057	13.32076	3.746826
493	50.21187	12.97195	3.870805
494	50.56013	59.26862	0.853067
495	50.82563	22.81096	2.228123
496	50.97693	24.58849	2.073203
497	51.10337	39.32116	1.29964
498	51.46565	48.39147	1.063527

499	52.23165	52.6742	0.991598
500	52.63766	22.37459	2.352564
501	52.93405	49.51545	1.069041
502	53.43816	17.31123	3.086908
503	54.17965	8.980643	6.032937
504	54.85789	24.09676	2.276567
505	54.94217	6.032605	9.107536
506	55.39324	9.008973	6.148674
507	55.73821	4.461786	12.49235
508	55.85976	7.533579	7.414771
509	56.09981	24.3892	2.300191
510	56.32542	40.57499	1.388181
511	56.62043	21.80912	2.596182
512	56.7919	2.936605	19.33931
513	58.54569	41.7275	1.403048
514	58.74441	60.98616	0.963242
515	58.76811	25.94905	2.26475
516	58.78421	8.941683	6.574178
517	59.19019	61.95816	0.955325
518	59.20395	28.68338	2.064051
519	60.1261	33.78708	1.779559
520	61.76831	8.230116	7.505156
521	62.0322	35.39425	1.752607
522	62.34861	57.76247	1.079397
523	62.51814	65.08594	0.960548
524	62.6514	37.93071	1.651733
525	63.28499	7.825515	8.087007
526	63.6624	7.452366	8.542576
527	63.72227	15.0294	4.239842
528	64.80812	14.20631	4.561925
529	65.60772	21.87967	2.998569
530	65.79678	20.69193	3.179827
531	66.22396	71.1194	0.931166
532	66.63691	28.34065	2.351283
533	66.66137	23.25005	2.86715
534	66.89158	65.58633	1.019901
535	67.20214	54.48069	1.233504
536	67.84205	54.65182	1.24135
537	68.25685	12.99121	5.254077
538	68.46062	40.79924	1.677988
539	68.49612	52.18501	1.312563
540	69.00923	65.82745	1.048335
541	70.07565	27.04345	2.591224

542	70.61014	41.81457	1.688649
543	70.64229	8.029943	8.797359
544	71.02607	32.90741	2.158361
545	71.43963	47.04741	1.51846
546	73.10076	55.4468	1.318395
547	73.54171	15.35718	4.78875
548	74.28116	75.00011	0.990414
549	74.66246	45.87899	1.627378
550	75.0141	26.24327	2.858413
551	75.10517	72.27594	1.039145
552	75.25645	34.06319	2.209319
553	75.65577	48.84848	1.548784
554	75.70339	71.61728	1.057055
555	76.17291	33.72893	2.258385
556	76.2484	27.30264	2.792711
557	76.33412	48.57994	1.571309
558	76.53089	55.10378	1.38885
559	76.68709	59.6991	1.28456
560	77.05621	33.66234	2.289093
561	77.67972	68.26015	1.137995
562	77.72795	46.12522	1.685151
563	78.50181	85.32508	0.920032
564	78.88049	67.80825	1.163287
565	78.90148	53.30199	1.480273
566	79.18738	67.9731	1.164981
567	79.3689	76.11435	1.042759
568	79.60867	40.05725	1.987372
569	80.58981	79.72105	1.010898
570	80.71724	80.58911	1.00159
571	80.76031	66.34898	1.217205
572	81.20856	73.57013	1.103825
573	81.20908	82.31402	0.986577
574	81.85259	80.71004	1.014156
575	81.92597	78.80328	1.039626
576	82.02912	80.68384	1.016673
577	82.33925	79.63629	1.033941
578	82.43232	81.12737	1.016085
579	82.86357	56.63505	1.463115
580	82.91347	62.63022	1.323857
581	86.05231	29.1152	2.95558
582	86.92015	18.35838	4.734631
583	89.02011	84.46587	1.053918
584	90.836	62.53645	1.452529

585	91.09277	44.49977	2.047039
586	102.776	90.46986	1.136024

Percent inhibition of Src-YEEI activity in the presence and absence of the pFAK peptide is shown. Percent inhibition is calculated based on the maximum inhibition, where no ATP is present, and the minimum inhibition, where only DMSO is present. Compounds are sorted by their percent inhibition of the Src-YEEI:pFAK complex, which is reflected in the compound number column. This corresponds to Figure 23A in the main text. The compounds characterized in the study are highlighted in gray. Compound 543 is the selective WH-4-124-2 and compound 551 is the non-selective analog WH-4-023.

APPENDIX B

COMMONLY USED ABBREVIATIONS

AIDS	Acquired Immunodeficiency Syndrome
CML	Chronic myelogenous leukemia
Csk	C-terminal Src kinase
ECM	Extracellular matrix
EGFR	Epidermal growth factor receptor
FAK	Focal adhesion kinase
FAT	Focal adhesion targeting
FERM	Four-point-one/ezrin/radixin/moesin
FGFR	Fibroblast growth factor receptor
HIV	Human immunodeficiency virus
PDB	Protein data bank
PDGFR	Platelet derived growth factor receptor
PPII	Polyproline type II
PTP	Protein tyrosine phosphatase
RTK	Receptor tyrosine kinase
SFK	Src family kinase
SH2	Src homology 2
SH3	Src homology 3
SPR	Surface plasmon resonance
SYF	Src-Yes-Fyn
TCR	T-cell receptor

BIBLIOGRAPHY

Reference List

1. P. Rous, *J. Exp. Med.* **13**, 397 (1911).
2. S. R. Weiss, H. E. Varmus, J. M. Bishop, *Cell* **12**, 983 (1977).
3. J. S. Brugge, R. L. Erikson, *Nature* **269**, 346 (1977).
4. S. M. Thomas, J. S. Brugge, *Annu. Rev. Cell Dev. Biol.* **13**, 513 (1997).
5. M. S. Serfas, A. L. Tyner, *Oncol. Res.* **13**, 409 (2003).
6. W. Xu, A. Doshi, M. Lei, M. J. Eck, S. C. Harrison, *Mol. Cell* **3**, 629 (1999).
7. M. D. Resh, *Cell* **76**, 411 (1994).
8. M. L. Thomas, E. J. Brown, *Immunol. Today* **20**, 406 (1999).
9. M. Okada, H. Nakagawa, *J. Biol. Chem.* **264**, 20886 (1989).
10. M. Okada, S. Nada, Y. Yamanashi, T. Yamamoto, H. Nakagawa, *J. Biol. Chem.* **266**, 24249 (1991).
11. D. Davidson, L. M. Chow, A. Veillette, *J. Biol. Chem.* **272**, 1355 (1997).
12. I. Hamaguchi *et al.*, *Biochem. Biophys. Res. Commun.* **224**, 172 (1996).
13. P. Filippakopoulos, S. Muller, S. Knapp, *Curr. Opin. Struct. Biol.* **19**, 643 (2009).
14. M. L. Stahl, C. R. Ferenz, K. L. Kelleher, R. W. Kriz, J. L. Knopf, *Nature* **332**, 269 (1988).
15. H. Yu *et al.*, *Science* **258**, 1665 (1992).
16. D. A. Horita *et al.*, *J. Mol. Biol.* **278**, 253 (1998).
17. P. Cicchetti, B. J. Mayer, G. Thiel, D. Baltimore, *Science* **257**, 803 (1992).

18. B. Nagar *et al.*, *Cell* **112**, 859 (2003).

19. R. J. Rickles *et al.*, *EMBO J.* **13**, 5598 (1994).

20. D. C. Dalgarno, M. C. Botfield, R. J. Rickles, *Biopolymers* **43**, 383 (1997).

21. W. A. Lim, F. M. Richards, R. O. Fox, *Nature* **372**, 375 (1994).

22. S. Feng, C. Kasahara, R. J. Rickles, S. L. Schreiber, *Proc. Natl. Acad. Sci. U. S. A* **92**, 12408 (1995).

23. I. Sadowski, J. C. Stone, T. Pawson, *Mol. Cell. Biol.* **6**, 4396 (1986).

24. W. Zhang, T. E. Smithgall, W. H. Gmeiner, *J. Biomol. NMR* **10**, 263 (1997).

25. T. D. Mulhern, G. L. Shaw, C. J. Morton, A. J. Day, I. D. Campbell, *Structure.* **5**, 1313 (1997).

26. G. Waksman, S. E. Shoelson, N. Pant, D. Cowburn, J. Kuriyan, *Cell* **72**, 779 (1993).

27. M. F. Moran *et al.*, *Proc. Natl. Acad. Sci. USA* **87**, 8622 (1990).

28. Z. Songyang *et al.*, *Cell* **72**, 767 (1993).

29. S. A. Courtneidge *et al.*, *J. Virol.* **65**, 3301 (1991).

30. J. R. Engen *et al.*, *Cell Mol. Life Sci.* **65**, 3058 (2008).

31. F. Sicheri, I. Moarefi, J. Kuriyan, *Nature* **385**, 602 (1997).

32. T. Schindler *et al.*, *Mol. Cell* **3**, 639 (1999).

33. S. S. Taylor, A. P. Kornev, *Trends Biochem. Sci.* **36**, 65 (2011).

34. H. Yamaguchi, W. A. Hendrickson, *Nature* **384**, 484 (1996).

35. A. P. Czernilofsky *et al.*, *Nature* **287**, 198 (1980).

36. J. E. Smart *et al.*, *Proc. Natl. Acad. Sci. U. S. A* **78**, 6013 (1981).

37. T. E. Kmiecik, D. Shalloway, *Cell* **49**, 65 (1987).

38. A. B. Reynolds *et al.*, *EMBO J.* **6**, 2359 (1987).

39. C. A. Cartwright, W. Eckhart, S. Simon, P. L. Kaplan, *Cell* **49**, 83 (1987).

40. E. C. Lerner, T. E. Smithgall, *Nat. Struct. Biol.* **9**, 365 (2002).

41. S. D. Briggs, T. E. Smithgall, *J. Biol. Chem.* **274**, 26579 (1999).

42. M. Okada, *Int. J. Biol. Sci.* **8**, 1385 (2012).

43. J. F. Cloutier, A. Veillette, *EMBO J.* **15**, 4909 (1996).

44. D. Davidson, J. F. Cloutier, A. Gregorieff, A. Veillette, *J. Biol. Chem.* **272**, 23455 (1997).

45. E. Ingley, *Biochim. Biophys. Acta* **1784**, 56 (2008).

46. J. D. Bjorge, A. Pang, D. J. Fujita, *J. Biol. Chem.* **275**, 41439 (2000).

47. J. Su, M. Muranjan, J. Sap, *Curr. Biol.* **9**, 505 (1999).

48. A. K. Somani, J. S. Bignon, G. B. Mills, K. A. Siminovitch, D. R. Branch, *J. Biol. Chem.* **272**, 21113 (1997).

49. S. Irtegun, R. J. Wood, A. R. Ormsby, T. D. Mulhern, D. M. Hatters, *PLoS. One.* **8**, e71035 (2013).

50. G. Sun *et al.*, *Arch. Biochem. Biophys.* **397**, 11 (2002).

51. R. A. Klinghoffer, C. Sachsenmaier, J. A. Cooper, P. Soriano, *EMBO J.* **18**, 2459 (1999).

52. F. Meng, C. A. Lowell, *J. Exp. Med.* **185**, 1661 (1997).

53. C. A. Lowell, P. Soriano, *Genes Dev.* **10**, 1845 (1996).

54. D. S. Aaronson, C. M. Horvath, *Science* **296**, 1653 (2002).

55. L. C. Cantley, *Science* **296**, 1655 (2002).

56. W. Zhang, H. T. Liu, *Cell Res.* **12**, 9 (2002).

57. D. K. Luttrell, L. M. Luttrell, S. J. Parsons, *Mol. Cell Biol.* **8**, 497 (1988).

58. L. K. Wilson, D. K. Luttrell, J. T. Parsons, S. J. Parsons, *Mol. Cell Biol.* **9**, 1536 (1989).

59. S. A. Courtneidge *et al.*, *EMBO J.* **12**, 943 (1993).

60. D. M. Kilkenny, J. V. Rocheleau, J. Price, M. B. Reich, G. G. Miller, *J. Biol. Chem.* **278**, 17448 (2003).

61. J. Liu, C. Huang, X. Zhan, *Oncogene* **18**, 6700 (1999).

62. M. A. Broome, S. A. Courtneidge, *Oncogene* **19**, 2867 (2000).

63. R. A. Blake *et al.*, *Mol. Cell Biol.* **20**, 9018 (2000).

64. G. M. Twamley-Stein, R. Pepperkok, W. Ansorge, S. A. Courtneidge, *Proc. Natl. Acad. Sci. U. S. A* **90**, 7696 (1993).

65. M. L. Hermiston, Z. Xu, R. Majeti, A. Weiss, *J. Clin. Invest* **109**, 9 (2002).

66. J. W. Thomas *et al.*, *J. Biol. Chem.* **273**, 577 (1998).

67. D. K. Luttrell *et al.*, *Proc. Natl. Acad. Sci. USA* **91**, 83 (1994).

68. R. B. Irby, T. J. Yeatman, *Oncogene* **19**, 5636 (2000).

69. W. Mao *et al.*, *Oncogene* **15**, 3083 (1997).

70. J. R. Wiener *et al.*, *Gynecol. Oncol.* **88**, 73 (2003).

71. T. J. Yeatman, *Nat. Rev. Cancer* **4**, 470 (2004).

72. M. C. Maa, T. H. Leu, D. J. McCarley, R. C. Schatzman, S. J. Parsons, *Proc. Natl. Acad. Sci. U. S. A* **92**, 6981 (1995).

73. D. A. Tice, J. S. Biscardi, A. L. Nickles, S. J. Parsons, *Proc. Natl. Acad. Sci. U. S. A* **96**, 1415 (1999).

74. R. J. Jones *et al.*, *Br. J. Cancer* **87**, 1128 (2002).

75. P. M. Termuhlen, S. A. Curley, M. S. Talamonti, M. H. Saboorian, G. E. Gallick, *J. Surg. Res.* **54**, 293 (1993).

76. M. S. Talamonti, M. S. Roh, S. A. Curley, G. E. Gallick, *J. Clin. Invest* **91**, 53 (1993).

77. N. J. Donato *et al.*, *Blood* **101**, 690 (2003).

78. J. Wu *et al.*, *J. Natl. Cancer Inst.* **100**, 926 (2008).

79. C. L. Sawyers, *N. Engl. J. Med.* **340**, 1330 (1999).

80. S. Faderl *et al.*, *N. Engl. J. Med.* **341**, 164 (1999).

81. S. Danhauser-Riedl, M. Warmuth, B. J. Druker, B. Emmerich, M. Hallek, *Cancer Res.* **56**, 3589 (1996).

82. J. M. Lionberger, M. B. Wilson, T. E. Smithgall, *J. Biol. Chem.* **275**, 18581 (2000).

83. A. Klejman *et al.*, *EMBO J.* **21**, 5766 (2002).

84. M. A. Meyn, III *et al.*, *J. Biol. Chem.* **281**, 30907 (2006).

85. B. J. Druker *et al.*, *N. Engl. J. Med.* **344**, 1031 (2001).

86. N. P. Shah *et al.*, *Cancer Cell* **2**, 117 (2002).

87. M. E. Gorre *et al.*, *Science* **293**, 876 (2001).

88. N. P. Shah *et al.*, *Science* **305**, 399 (2004).

89. O. T. Fackler, A. S. Baur, *Immunity.* **16**, 493 (2002).

90. K. Saksela, G. Cheng, D. Baltimore, *EMBO J.* **14**, 484 (1995).

91. K. Saksela, *Front. Biosci.* **2**, D606 (1997).

92. R. G. Herna, K. Saksela, *Front Biosci.* **5**, D268 (2000).

93. Z. Hanna *et al.*, *Cell* **95**, 163 (1998).

94. F. Kirchhoff, T. C. Greenough, D. B. Brettler, J. L. Sullivan, R. C. Desrosiers, *N. Engl. J. Med.* **332**, 228 (1995).

95. R. Mariani *et al.*, *J. Virol.* **70**, 7752 (1996).

96. R. P. Trible, L. Emert-Sedlak, T. E. Smithgall, *J. Biol. Chem.* **281**, 27029 (2006).

97. Z. Hanna *et al.*, *J. Virol.* **75**, 9378 (2001).

98. C.-H. Lee *et al.*, *EMBO J.* **14**, 5006 (1995).

99. C.-H. Lee, K. Saksela, U. A. Mirza, B. T. Chait, J. Kuriyan, *Cell* **85**, 931 (1996).

100. M. D. Schaller *et al.*, *Proc. Natl. Acad. Sci. U. S. A* **89**, 5192 (1992).

101. Y. Furuta *et al.*, *Oncogene* **11**, 1989 (1995).

102. L. A. Cary, R. A. Klinghoffer, C. Sachsenmaier, J. A. Cooper, *Mol. Cell Biol.* **22**, 2427 (2002).

103. D. Lietha *et al.*, *Cell* **129**, 1177 (2007).

104. I. Hayashi, K. Vuori, R. C. Liddington, *Nat. Struct. Biol.* **9**, 101 (2002).

105. D. F. Ceccarelli, H. K. Song, F. Poy, M. D. Schaller, M. J. Eck, *J. Biol. Chem.* **281**, 252 (2006).

106. M. D. Schaller *et al.*, *Mol. Cell Biol.* **14**, 1680 (1994).

107. T. R. Polte, S. K. Hanks, *Proc. Natl. Acad. Sci. USA* **92**, 10678 (1995).

108. G. Liu, C. D. Guibao, J. Zheng, *Mol. Cell Biol.* **22**, 2751 (2002).

109. G. Gao *et al.*, *J. Biol. Chem.* **279**, 8441 (2004).

110. L. A. Cooper, T. L. Shen, J. L. Guan, *Mol. Cell Biol.* **23**, 8030 (2003).

111. S. K. Mitra, D. A. Hanson, D. D. Schlaepfer, *Nat. Rev. Mol. Cell Biol.* **6**, 56 (2005).

112. K. A. DeMali, K. Wennerberg, K. Burridge, *Curr. Opin. Cell Biol.* **15**, 572 (2003).

113. M. B. Calalb, X. Zhang, T. R. Polte, S. K. Hanks, *Biochem. Biophys. Res. Commun.* **228**, 662 (1996).

114. M. B. Calalb, T. R. Polte, S. K. Hanks, *Mol. Cell Biol.* **15**, 954 (1995).

115. D. D. Schlaepfer, T. Hunter, *Mol. Cell. Biol.* **16**, 5623 (1996).

116. D. D. Schlaepfer, S. K. Hanks, T. Hunter, P. van der Geer, *Nature* **372**, 786 (1994).

117. L. A. Cary, D. C. Han, T. R. Polte, S. K. Hanks, J. L. Guan, *J. Cell Biol.* **140**, 211 (1998).

118. X. Zhao, J. L. Guan, *Adv. Drug Deliv. Rev.* **63**, 610 (2011).

119. A. J. Ridley *et al.*, *Science* **302**, 1704 (2003).

120. V. J. Fincham, M. C. Frame, *EMBO J.* **17**, 81 (1998).

121. D. Ilic *et al.*, *Nature* **377**, 539 (1995).

122. A. S. Yap, W. M. Brieher, B. M. Gumbiner, *Annu. Rev. Cell Dev. Biol.* **13**, 119 (1997).

123. C. Jamora, E. Fuchs, *Nat. Cell Biol.* **4**, E101 (2002).

124. J. M. Daniel, A. B. Reynolds, *BioEssays* **19**, 883 (1997).

125. M. Bergman, V. Joukov, I. Virtanen, K. Alitalo, *Mol. Cell Biol.* **15**, 711 (1995).

126. L. Tremblay *et al.*, *Int. J. Cancer* **68**, 164 (1996).

127. E. Avizienyte *et al.*, *Nat. Cell Biol.* **4**, 632 (2002).

128. C. Rivat *et al.*, *Oncogene* **23**, 3317 (2004).

129. B. J. Druker *et al.*, *N. Engl. J. Med.* **344**, 1038 (2001).

130. B. J. Druker, *Adv. Cancer Res.* **91**, 1 (2004).

131. V. Nardi, M. Azam, G. Q. Daley, *Curr. Opin. Hematol.* **11**, 35 (2004).

132. H. Kantarjian *et al.*, *N. Engl. J. Med.* **354**, 2542 (2006).

133. J. S. Tokarski *et al.*, *Cancer Res.* **66**, 5790 (2006).

134. S. Panjarian, R. E. Iacob, S. Chen, J. R. Engen, T. E. Smithgall, *J Biol Chem.* **288**, 5443 (2013).

135. B. Nagar *et al.*, *Cancer Res.* **62**, 4236 (2002).

136. Y. Liu, N. S. Gray, *Nat. Chem. Biol.* **2**, 358 (2006).

137. L. K. Gavrin, E. Saiah, *Medicinal Chemistry Communications* **4**, 41 (2012).

138. T. Schindler *et al.*, *Science* **289**, 1938 (2000).

139. ClinicalTrials.gov. Dasatinib in Treating Patients With Previously Treated Metastatic Colorectal Cancer. 7-1-2013.
Ref Type: Online Source

140. ClinicalTrials.gov. Dasatinib in Treating Patients With Recurrent or Metastatic Head and Neck Cancer. 4-22-2013.
Ref Type: Online Source

141. ClinicalTrials.gov. Dasatinib or Placebo, Radiation Therapy, and Temozolomide in Treating Patients With Newly Diagnosed Glioblastoma Multiforme. 2-17-2013.
Ref Type: Online Source

142. ClinicalTrials.gov. Personalized Treatment Selection for Metastatic Breast Cancer. 6-10-2013.
Ref Type: Online Source

143. L. F. Hennequin *et al.*, *J. Med. Chem.* **49**, 6465 (2006).

144. ClinicalTrials.gov. Phase I Study in Patients with Solid Tumors. 9-21-2010.
Ref Type: Online Source

145. ClinicalTrials.gov. Phase I/Ib Study of Paclitaxel in Combination With VS-6063 in Patients With Advanced Ovarian Cancer. 9-9-2013.
Ref Type: Online Source

146. ClinicalTrials.gov. Phase II Study of VS-6063 in Patients With KRAS Mutant Non-Small Cell Lung Cancer. 9-27-2013.
Ref Type: Online Source

147. ClinicalTrials.gov. Study Of PF-00562271, Including Patients With Pancreatic, Head And Neck, Prostatic Neoplasms. 3-14-0013.
Ref Type: Online Source

148. C. M. Bagi *et al.*, *Cancer Biol. Ther.* **8**, 856 (2009).

149. J. R. Infante *et al.*, *J. Clin. Oncol.* **30**, 1527 (2012).

150. W. G. Roberts *et al.*, *Cancer Res.* **68**, 1935 (2008).

151. S. J. Parsons, J. T. Parsons, *Oncogene* **23**, 7906 (2004).

152. M. D. Resh, *Biochim. Biophys. Acta* **1451**, 1 (1999).

153. T. J. Boggon, M. J. Eck, *Oncogene* **23**, 7918 (2004).

154. Y. P. Chong, K. K. Ia, T. D. Mulhern, H. C. Cheng, *Biochim. Biophys. Acta* **1754**, 210 (2005).

155. W. Xu, S. C. Harrison, M. J. Eck, *Nature* **385**, 595 (1997).

156. M. T. Brown, J. A. Cooper, *Biochim. Biophys. Acta* **1287**, 121 (1996).

157. I. Moarefi *et al.*, *Nature* **385**, 650 (1997).

158. S. D. Briggs, M. Sharkey, M. Stevenson, T. E. Smithgall, *J. Biol. Chem.* **272**, 17899 (1997).

159. M. A. Meyn, III, T. E. Smithgall, *Sci. Signal.* **2**, ra64 (2009).

160. X. Zhang, M. A. Meyn, III, T. E. Smithgall, *ACS Chem. Biol.* (2013).

161. C. Anneren, C. A. Cowan, D. A. Melton, *J. Biol. Chem.* **279**, 31590 (2004).

162. F. Sancier *et al.*, *PLoS. One.* **6**, e17237 (2011).

163. M. LaFevre-Bernt *et al.*, *Journal of Biological Chemistry* **273**, 32129 (1998).

164. M. A. Seeliger *et al.*, *Protein Sci.* **14**, 3135 (2005).

165. R. E. Iacob *et al.*, *Proc. Natl. Acad. Sci. U. S. A* **106**, 1386 (2009).

166. R. J. Rickles *et al.*, *Proc. Natl. Acad. Sci. U. S. A.* **92**, 10909 (1995).

167. N. W. Charter, L. Kauffman, R. Singh, R. M. Eglen, *J. Biomol. Screen.* **11**, 390 (2006).

168. K. S. Lam, J. Wu, Q. Lou, *Int. J. Pept. Protein Res.* **45**, 587 (1995).

169. R. J. Boerner *et al.*, *Biochemistry* **35**, 9519 (1996).

170. R. S. Plumb *et al.*, *Rapid Commun. Mass Spectrom.* **20**, 1989 (2006).

171. E. C. Lerner *et al.*, *J. Biol. Chem.* **280**, 40832 (2005).

172. M. Porter, T. Schindler, J. Kuriyan, W. T. Miller, *J. Biol. Chem.* **275**, 2721 (2000).

173. S. D. Briggs, E. C. Lerner, T. E. Smithgall, *Biochemistry* **39**, 489 (2000).

174. O. Hantschel, G. Superti-Furga, *Nat. Rev. Mol. Cell Biol.* **5**, 33 (2004).

175. S. Panjarian *et al.*, *J Biol Chem.* **288**, 6116 (2013).

176. S. K. Mitra, D. D. Schlaepfer, *Curr. Opin. Cell Biol* **18**, 516 (2006).

177. A. V. Wang, P. R. Scholl, R. S. Geha, *J. Exp. Med.* **180**, 1165 (1994).

178. K. Kedzierska, N. J. Vardaxis, A. Jaworowski, S. M. Crowe, *J. Leukoc. Biol.* **70**, 322 (2001).

179. D. L. Durden, H. M. Kim, B. Calore, Y. Liu, *J. Immunol.* **154**, 4039 (1995).

180. A. Bhattacharjee, S. Pal, G. M. Feldman, M. K. Cathcart, *J. Biol. Chem.* **286**, 36709 (2011).

181. Y. P. Chong *et al.*, *J. Biol. Chem.* **281**, 32988 (2006).

182. D. Wang, W. J. Esselman, P. A. Cole, *J. Biol. Chem.* **277**, 40428 (2002).

183. T. Nakamoto, R. Sakai, K. Ozawa, Y. Yazaki, H. Harai, *J. Biol. Chem.* **271**, 8959 (1996).

184. S. T. Arold, M. K. Hoellerer, M. E. Noble, *Structure.* **10**, 319 (2002).

185. Y. Lim *et al.*, *J. Biol. Chem.* **279**, 29060 (2004).

186. P. L. Judson, X. He, W. G. Cance, L. L. Van, *Cancer* **86**, 1551 (1999).

187. L. J. Kornberg, *Head Neck* **20**, 745 (1998).

188. L. J. Kornberg, *Head Neck* **20**, 634 (1998).

189. L. V. Owens *et al.*, *Cancer Res.* **55**, 2752 (1995).

190. A. L. Lark *et al.*, *Mod. Pathol.* **18**, 1289 (2005).

191. A. L. Lark *et al.*, *Clin. Cancer Res.* **9**, 215 (2003).

192. J. Zhao, J. L. Guan, *Cancer Metastasis Rev.* **28**, 35 (2009).

193. P. M. Siesser, S. K. Hanks, *Clin. Cancer Res.* **12**, 3233 (2006).

194. L. C. Kim, L. Song, E. B. Haura, *Nat. Rev. Clin. Oncol.* **6**, 587 (2009).

195. S. Zhang, D. Yu, *Trends Pharmacol. Sci.* **33**, 122 (2012).

196. G. W. McLean *et al.*, *Nat. Rev. Cancer* **5**, 505 (2005).

197. C. Lieu, S. Kopetz, *Clin. Colorectal Cancer* **9**, 89 (2010).

198. L. N. Puls, M. Eadens, W. Messersmith, *Oncologist.* **16**, 566 (2011).

199. S. Hellwig *et al.*, *Chem. Biol.* **19**, 529 (2012).

200. S. M. Rodems *et al.*, *Assay. Drug Dev. Technol.* **1**, 9 (2002).

201. L. Emert-Sedlak *et al.*, *ACS Chem. Biol.* **4**, 939 (2009).

202. M. J. Eck, S. E. Shoelson, S. C. Harrison, *Nature* **362**, 87 (1993).

203. R. J. Boerner, S. C. Barker, W. B. Knight, *Biochemistry* **34**, 16419 (1995).

204. S. C. Barker *et al.*, *Biochemistry* **34**, 14843 (1995).

205. Z. A. Knight, K. M. Shokat, *Chem. Biol.* **12**, 621 (2005).

206. D. K. Treiber, N. P. Shah, *Chem. Biol.* **20**, 745 (2013).

207. M. A. Seeliger *et al.*, *Structure.* **15**, 299 (2007).

208. M. D. Jacobs, P. R. Caron, B. J. Hare, *Proteins* **70**, 1451 (2008).

209. D. R. Koes, M. P. Baumgartner, C. J. Camacho, *J. Chem. Inf. Model.* **53**, 1893 (2013).

210. T. E. Wales, J. R. Engen, *Mass Spectrom. Rev.* **25**, 158 (2006).